Protease-activated receptor 4-deficiency reduces inflammation-associated neutrophil-platelet aggregation

Inaugural-Dissertation

zur Erlangung des Doktorgrades
der Mathematisch-Naturwissenschaftlichen Fakultät
der Heinrich-Heine-Universität Düsseldorf

vorgelegt von

Kristin Plesser
aus Duisburg

Düsseldorf, Mai 2017

1.1 Declaration

Ich versichere an Eides Statt, dass die Dissertation von mir selbständig und ohne unzulässige fremde Hilfe unter Beachtung der „Grundsätze zur Sicherung guter wissenschaftlicher Praxis an der Heinrich-Heine-Universität Düsseldorf“ erstellt worden ist.

Düsseldorf, den 17. Mai 2017

TABLE OF CONTENTS

2 Summary

Neutrophil-platelet aggregations (NPAs) are important regulators of inflammatory responses. During inflammation, platelets are essential for endothelial cell adhesion and the recruitment of neutrophils to the site of inflammation. Protease-activated receptors (PARs) belong to the G-protein coupled receptors, which are expressed in all tissues. Pathophysiological mechanisms including vascular injury cause the release of proteases that mediate the activation of PARs. In the present study, we aim to understand the role of the PAR4/cathepsin G (catG) pathway in platelets and NPA and its implication in the progression of diseases of vascular inflammation, such as leukocytoclastic vasculitis (LcV).

Using flow cytometry and a catG acticitv assay we evaluated increased formation of NPAs and elevated levels of catG in patients with LcV compared to healthy volunteers. *In vitro*, we stimulated platelets with catG and revealed an enhanced ability of platelets to form aggregates with neutrophils co-incubation. This effect is in part mediated by PAR_4, as blocking of PAR_4 with an antagonist significantly decreased NPA induction by catG. In an *in viv*o model of vasculitis, the reverse passive Arthus reaction (RPA), we confirmed the human findings and revealed a significant increase in NPA counts and a trend towards elevated catG levels in the whole blood of RPA mice compared to untreated mice. *Par4*$^{-/-}$ mice showed severely downregulated formation of NPAs in the circulation, while plasma catG levels were significantly increased. Furthermore, we measured increased neutrophil tissue invasion (myeloperoxidase [MPO] tissue levels) and edema formation (weight of biopsy) as measures of inflammation in RPA mice. Histologically, we confirmed the massive infiltration of neutrophils, whereas low levels of macrophages and no T cells were detected. Differential blood count analysis revealed increased abundance of circulating neutrophils and monocytes in the whole blood of RPA mice compared to control mice, while lymphocyte numbers were decreased. Additionally, we analysed the surface expression profile of murine platelets after stimulation with different concentrations of catG. Stimulation of murine platelets revealed a dose-dependent increased surface expression of P-selectin, GP1bα, GPIIIβ, GPIIIbIIa, and GPVI, whereas a low catG concentration decreased the expression of GP1bα and a high concentration decreased that of GPIIIβ.

Taken together, we identified the formation of NPAs and increased plasma catG levels as important markers for vasculitis *ex vivo* in patients as well as in our *in vivo mouse* model. Furthermore, we also investigated the crucial role of the catG/PAR_4 pathway in the induction of NPA *in vitro* and *in vivo*. We further confirmed an important function of catG as a mediator of inflammation and hemostasis, as detected after investigating platelet surface expression after stimulation with catG.

3 Zusammenfassung

Neutrophilen-Thrombozyten Aggregate (NTAs) spielen eine wichtige Rolle bei der Regulierung von Entzündungsreaktionen. Während einer Entzündung sind Thrombozyten essentziell für einerseits die Interaktion von Neutrophilen mit dem Endothelium and andererseits für die Rekrutierung von Neutrophilen zum Entzündungsherd. Protease-aktivierte Rezeptoren gehören zu den G-Protein-gekoppelten Rezeptoren, die in allen Gewebearten exprimiert werden. Pahtophysiologische Mechanismen, wie Gefäßverletzungen oder akute Entzündungen führen zur Freisetzung verschiedener Proteasen, die PARs aktivieren. Ziel unserer Untersuchungen ist das Verständnis der Rolle von PAR_4 und Cathepsin G (CatG) in Thrombozyten und NTAs sowie ihre Auswirkungen im Fortschreiten vaskulärer Entzündungen, wie die Leukozytoklastische Vaskulitis (LcV).

Mittels Durchflusszytometrie und eines CatG Aktvitätstest haben wir vermehrte Formationen von NTAs und erhöhte CatG-Werte in LcV Patienten im Vergleich zu gesunden Probanden gemessen. *In vitro*, konnten wir vermehrte NTA Formationen nach Stimulation von Thrombozyten mit CatG detektieren. Dieser Effekt ist teilweise durch PAR_4 reguliert, da die Blockierung des Rezeptors mit einem spezifischen Antagonisten die Bildung von NTAs signifikant verringerte. Mittels unseres *in vivo* Model der Vaskulitis, der reverse passiven Arthusreaktion (RPA), konnten wir unsere Humandaten validieren und haben vermehrte NTA Formation sowie einen Trend zu erhöhten CatG-Plasma-Spiegel in Wildtyp RPA im Vergleich zu den unbehandelten Mäusen gemessen. *Par4*$^{-/-}$ Mäuse zeigten eine massive Verminderung der Aggregate in der Zirkulation, während der CatG-Spiegel deutlich erhöht ist. Gewebeinfiltration von Neutrophilen (MPO Spiegel im Gewebe) und die Ödembildung (Gewicht der Biopsie) waren deutlich sowohl in Wildtyp als auch *Par4*$^{-/-}$ Mäusen starkt erhoht. Histologischen Untersuchungen bezeugten die massive Infiltration von Neutrophilen im entzündeten Gewebe, wohingegen nur geringe Anzahlen von Makrophagen und keine T-Zellen detektiert wurden. Mittels eines Differntialblutbildes konnte wir ein erhöhtes Auftreten von Granulocyten und Monozyten im Blut der RPA Mäuse feststellen, während die Zahl der Lymphozyten vermindert war. Außerdem haben wir die Oberflächen Expression von murinen Thrombozyten nach Stimulierung mit verschiedenen Konzentrationen von CatG analysiert. Stimulierung von murinene Thrombozyten zeigte eine Dosisabhängig erhöhte

Expression von P-selectin, GP1bα, GPIIIβ, GPIIIbIIa und GPVI, wobei eine niedriege Konzentration von CatG die Expression von GP1bα verringert und eine hohe die von GPIIIβ.

Zusammenfassend haben wir eine vermehrte Bildung von NTAs sowie einen erhöhten Plasma-CatG-Spiegel als wichtige Marker für die Diagnose einer Vaskulitis ermittelt. Eine entscheidende Rolle der CatG/PAR_4-Achse wurde auch bei der Formation von NTAs *in vitro* und *in vivo* festgestellt. Durch unsere Analyse der Thrombozyten Oberflächen Expression nach CatG-Stimulation haben wir eine wichtige Rolle von CatG als Mediator von Entzündung und Blutstillung validiert.

4 Introduction

4.1 Neutrophil-platelet aggregation

Neutrophils are important players in the acute phase of inflammation due to their degranulation response and respiratory burst [1, 2]. Tissue damage and inflammation cause the invasion of pathogens and other antigens, which induce the secretion of proinflammatory cytokines [3]. These cytokines activate and recruit circulating neutrophils to the site of inflammation, following a distinct recruitment pattern along the endothelium called the leukocyte-adhesion cascade [3, 4] (Figure 4-1). During this recruitment cascade, activated platelets play an essential proinflammatory role. On the one hand, they are required for the recruitment of neutrophils to the inflammatory tissue, while, on the other hand, they activate neutrophils for their efficient adhesion to the vascular endothelium [5-7].

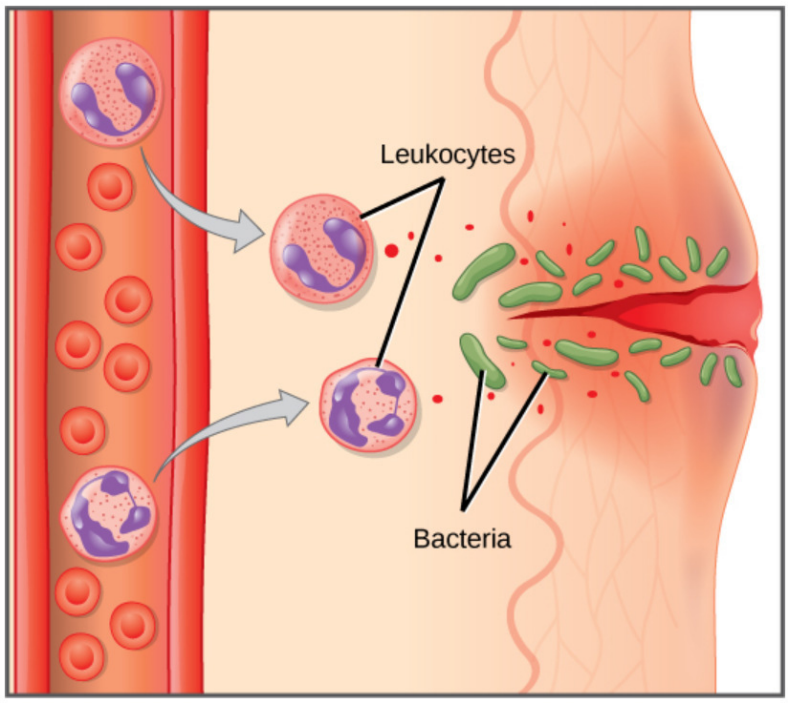

Figure 4-1 Innate immune response [8] Traumatic injuries and inflammation cause the invasion of pathogens or antigens, which induce the release of proinflammatory cytokines. These cytokines activate neutrophils to migrate along the endothelium to the site of inflammation. During this process, platelets are known to have a putative function. On the one hand, they favour the recruitment of neutrophils to the inflammatory tissue, while, on the other hand, they activate neutrophils for their efficient adhesion to the vascular endothelium

Source: www.boundless.com, 2016

4.1.1 The formation of neutrophil-platelet aggregations (NPAs)

The maintenance of vascular integrity requires an intact and functional endothelium and platelets that circulate in the quiescent state [9]. Certain pathogenic circumstances that lead to tissue and vascular injuries, including the presence of pathogens (bacteria and viruses), proinflammatory cytokines (interleukin-1 (IL-1) and tumor necrosis factor (TNF)), and physical and oxidative stress, are capable of activating endothelial cells [9]. When activated, endothelial cells lose their vascular integrity, causing the efflux of fluids from the intravascular lumen [9]. Furthermore, endothelial cells upregulate the expression of leukocyte adhesion molecules, including E-selectin, P-selectin, intercellular adhesion molecule 1, and vascular cell adhesion protein 1, and produce pro-coagulant mediators e.g. tissue factor and pro-inflammatory cytokines, IL-6, IL-8 (CXCL8), and monocyte chemoattractant protein-1 (CCL2) [9, 10]. All of these changes lead to the activation of both platelets and neutrophils [7, 11].

Once activated, platelets change their shape, degranulate, and upregulate the expression of several adhesion molecules such as glycoprotein Ibα (GP1bα), glycoprotein IIbIIIa (GPIIbIIIa, αIIbβ3), and P-selectin. Increased secretion of proinflammatory cytokines, including IL-1, CCL5 (RANTES), platelet-derived growth factor (PDGF), transforming growth factor-β (TGF- β), epidermal growth factor (EGF), and the chemokines, CXCL4, CXCL8, and CCL2, is also associated with the activation of platelets and, in turn, causes further activation of endothelial cells and neutrophils [12-15].

Activated neutrophils migrate along the vessel wall in a multistep process. Here, the interaction between the neutrophil and the endothelium is crucial for mediating the migration of neutrophils to the site of inflammation. The binding of neutrophils from the free flow directly to the endothelium is called primary capture [16]. Under shear stress, more efficient and firm adhesion between neutrophils and the endothelium is mediated by activated platelets. This mechanism, called secondary capture, requires immobilized platelets on the endothelium that promote adhesion of the neutrophils to the endothelium [17]. Based on this finding, platelets are important mediators of the neutrophil-endothelial interaction and are therefore crucial for the initiation of acute inflammatory responses [7, 17, 18].

4.1.2 Ligand-receptor interactions of NPAs

The heterotypic interaction between neutrophils and platelets is regulated by several surface receptors [18]. Platelet P-selectin and neutrophil P-selectin glycoprotein ligand 1 (PSGL-1) are required for the initial interaction between both cell types. P-selectin is produced by platelets and is stored in their α-granules until it is released upon platelet activation [6, 19-22]. PSGL-1 on neutrophils is needed for the binding to P- and E-selectin on endothelial cells and mediates neutrophil recruitment to the endothelial sheet, neutrophil rolling and tethering [23]. Mice, expressing high plasma levels of soluble P-selectin, display an increase in pro-coagulant microparticles. In turn, blocking PSGL-1 severely reduces procoagulant activity in these mice, hinting toward an essential role of the PSGL-1/P-selectin interaction for the formation of thrombi [24]. Consequently, P-selectin deficiency prevents neutrophils from adhering to platelet thrombi at the site of arteriolar injury [25]. In loss-of-function studies, deficiencies in either PSGL-1 or P-selectin also lead to irregularities in the initial phase of neutrophil rolling along the endothelial layer and subsequent diapedesis [20, 26-37].

The initial interaction between platelets and neutrophils and the subsequent activation of intracellular signaling of both cell types is abolished by deletion of PSGL-1 and P-selectin or by blocking antibodies against them [6, 38, 39]. Furthermore, PSGL-1 deficiency or inhibition in neutrophils prevents the binding of platelets at the uropod [19].

The stable and firm adhesion of neutrophils and platelets is mediated via interaction between neutrophil αMβ2 and platelet GP1bα [40]. αMβ2, also called membrane-activated complex 1 (Mac-1), is important for several neutrophilic functions, including crawling, chemotaxis, and apoptosis [41-43]. GP1bα, together with GP1bβ, GPIX, and GPV, forms the receptor complex on platelets that is bound by von Willebrand factor (vWF) at the site of vascular injury. This interaction is further necessary to initiate platelet adhesion and accumulation [44]. Inhibition or deficiency of αMβ2 or GP1bα markedly reduces the heterotypic interaction between neutrophils and platelets [40, 45]. Furthermore, mice deficient in αMβ2 show an increased blood flow rate during TNFα-mediated inflammation, indicating that αMβ2-GP1bα interactions are crucial for neutrophil-platelet interactions under thromboinflammatory conditions [46]. αMβ2 is also capable of interacting with the fibrinogen receptor αIIbβ3 (GPIIbIIa) on the platelet surface [47]. αIIbβ3 is important for

platelet aggregation during thrombus formation, but it seems not to be essential for neutrophil-platelet aggregation during vascular inflammation [38, 48].

Other molecules also contribute to the heterotypic interaction between platelets and neutrophils. These include the binding of platelet JAM-3 to neutrophil αMβ2 integrin-, and the binding between CD40 and CD40L [18].

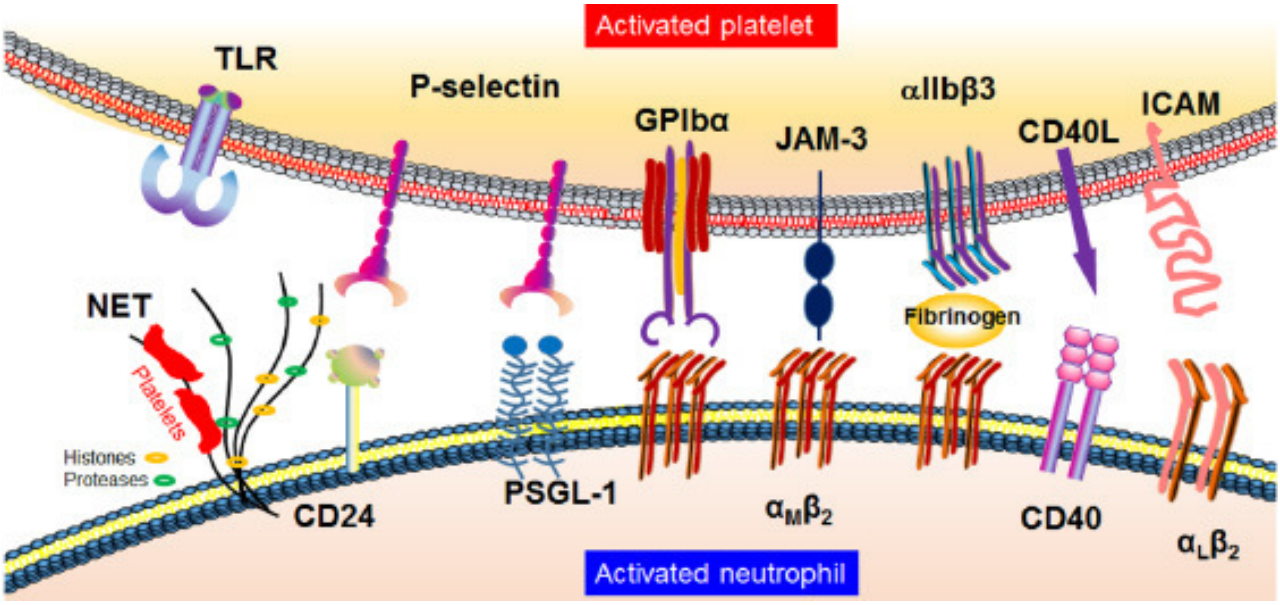

Figure 4-2 Neutrophil-platelet interaction during vascular inflammation. During the heterotypic cell-cell interaction of neutrophils and platelets different receptor-ligand pairs are involved. The most prevalent binding between neutrophils and platelets is mediated via binding of neutrophil PSGL-1 and its counterpart P-selectin, which is expressed on platelets. Firm adhesion can also be achieved by binding of αMβ2 integrin (CD11b/CD18 = Mac-1) with Glycoprotein Ibα (GPIbα) [49].

Source: Li et al., Cell Mol Life Sci, 2015

4.1.3 Interaction of neutrophils and platelets during vascular inflammation

Interactions between neutrophils and platelets play an important role in several vascular inflammatory disorders.

In sickle cell disease, increased levels of neutrophil-platelet interactions were detected in the circulation of human patients and mice, relative to their appropriate control groups. These aggregates cause vascular inflammation and pulmonary dysfunction, as inhibition of platelet P-selectin by a specific antibody abolishes the formation of NPAs and improves lung conditions [50]. In Kawasaki disease, which is another vascular injury disease, the elevated levels of NPAs in circulation are decreased after treating the patients with the

glucocorticoid prednisolone [51]. In addition, patients suffering from angina pectoris or atherosclerosis have particularly large numbers of NPAs in the peripheral blood, which promote the formation of vascular lesions [52, 53]. All together, these data validate the important role of neutrophil-platelet interactions in the progression of vascular inflammation.

In the present study, we aim to focus on a cutaneous vascular inflammation, leukocytoclastic vasculitis (LcV), that is characterized by a massive infiltration of neutrophils into the skin, subsequently leading to dermal inflammation. Based on these findings and the involvement of neutrophil-platelet interactions in the progression of multiple vascular disorders, we aim to analyze the contribution of platelets to neutrophil activation in the progression of LcV.

4.2 Leukocytoclastic vasculitis (LcV)

Leukocytoclastic vasculitis, also designated as vasculitis allergica or immune complex (IC)-mediated vasculitis, is the most common form of cutaneous vasculitis and was first described in the 19th century by Heberden (1802), Schönlein (1832), and Henoch (1868) [54]. LcV is, dependent on its exposure, classified as either systemic or cutaneous LcV, and its onset mainly manifests in adulthood between the ages of 39 and 49. Women are 2-3 times more frequently affected than men. Additionally, vasculitis can also occur during childhood, as is the case with the systemic vasculitis Henoch–Schönlein purpura [54].

4.2.1 Pathogenesis

LcV is an inflammatory disorder of the small vessels, mainly post-capillary venules, that is induced by the accumulation of immune complexes (ICs) at the vessel wall. These ICs bind to the Fc gamma receptor (FcγR) expressed on the surface of neutrophils and mediate their recruitment and infiltration to the site of inflammation [55]. The recruited neutrophils are activated for degranulation and oxidative burst and subsequently release reactive oxygen species (ROS) and degrading enzymes close to the vessel wall, a process that is proposed to phagocytose the ICs. Instead, neutrophil activation causes destruction of the endothelial wall, leading to extravasation of erythrocytes out of the intraluminal space and inflammation [56].

4.2.2 Histological characteristics

Histologically, LcV is characterized by a superficial, intramural and perivascular infiltrate consisting of inflammatory cells including lymphocytes, histiocytes, and apoptotic, fragmented neutrophil granulocytes (leukocytoclasia, karrhyorhexis) [54, 57]. Eosinophil granulocytes have also been detected to varying extents in the inflamed areas of the skin [54]. Furthermore, endothelial cells reshape to become more swollen and to reach into the vascular lumen. The emerging damage of the vessel wall is accompanied by extravasation of erythrocytes into the surrounding tissue (hemorrhage). Potential vessel occlusion is characterized by a grey discoloration in the center of the lesion, indicating incipient tissue necrosis that is determined by epidermal edema (spongiosis) and fading keratinocytes [54, 56].

4.2.3 Clinical hallmarks

The clinical hallmarks of LcV include the formation of palpable purpura caused by the inflammatory infiltrate and hemorrhage [56]. Initially, typical LcV patients complain of increased temperature, headache, exhaustion, and rheumatoid symptoms including arthralgia and arthritis. The main clinical image of LcV, the purpura, is comprised of lesions ranging from 1 mm to several centimeters in size. Depending on the stage of the disease, these petechial hemorrhages are able to expand to hemorrhagic spots (palpable purpura) and their occurrence is mainly accompanied by pruritus and stinging pain. With further progression of the disease hemorrhagic plaques, secondary pustules, blisters, as well as erosion and ulceration can occur [54]. The formation of blisters may be a result of excessive sub epidermal edema formation subsequent to vessel occlusion [56].

4.2.4 Etiology

There are many different known causes that lead to the development of LcV. These include the intake of medication such as antibiotics, especially substances of the sulfonamide, penicillin, and tetracycline classes, and non-steroidal antiphlogistics [54]. However, infections themselves caused by bacteria (e.g., streptococci, staphylococci, *Escherichia coli*), fungi (*Candida albicans*), or viruses (e.g., Hepatitis B virus (HBV) and influenza A virus subtypes) are also potential causes of LcV [54]. The occurrence of the

disease can also be due to combined modes of action of infection and medication or due to autoimmune diseases with accompanied autoantigens, including rheumatoid arthritis (RA) or systemic lupus erythematosus (SLE) [54]. Furthermore, malignancies such as lymphomas and hairy cell leukemia lead to the development of LcV. However, in up to 50% of LcV cases, a defined trigger is absent from the anamnesis and the LcV must be named idiopathic [54].

4.2.5 Diagnosis and therapeutic intervention

The diagnosis of LcV is embedded in the exclusion of persistent renal dysfunction and multiple phenotypically related clinical and histological differential diagnoses [54]. Clinical differential diagnoses include papulonecrotic tuberculid, a disease characterized by necrotic papules that are caused by a hypersensitivity to antigens of *Mycobacterium tuberculosis* [58] and autoimmune diseases such as Pityriasis lichenoides et varioliformis acuta (PLEVA), which is defined by rashes and erythemateous plaques of the skin [59]. Furthermore, the neutrophil-independent inflammatory hemorrhagic skin disease, purpura pigmentosa [60] and congestive bleeding due to chronic venous insufficiency, designated Purpura jaune d'ocre [61], also must be excluded for the certain diagnosis of LcV [54]. Erythema exsudativum multiforme, characterized by the appearance of acute exanthema, is a further differential diagnosis that must be excluded clinically as well as histologically [62]. Other histological differential diagnoses include the septic vasculitides, urticaria and vasculitis racemose [54].

Milder forms of LcV are, in general, self-limiting and undergo remission without the use of systemic medication. However, forms with severe chronic progression require therapeutic intervention [54]. Patients with predominant cutaneous symptoms are treated with glucocorticoids (e.g., prednisone) alone or in combination with immunosuppressive medications (e.g., azathioprine). Unresponsive patients can be treated with high-dose intravenous immunoglobulins [54]. Patients with severe visceral involvement may require high doses of systemic glucocorticoids (e.g., prednisone) with or without the chemotherapeutic agent cyclophosphamide [54]. Severe courses might supplementarily be treated by plasmapheresis [54]. In general, patients with LcV have a favorable prognosis that is dependent on the acuteness and the degree of the disease. Based on statistical analysis, the mortality rate is about 2-3% [54].

4.2.6 The reverse passive Arthus reaction (RPA)

The accumulation of ICs in tissues is the main inflammatory trigger responsible for tissue destruction and subsequently morbidity and mortality in diseases like RA, SLE and immune vasculitis [63]. The Arthus reaction is an *in vivo* model recapitulating the IC-mediated inflammation that was first described in 1903 by Maurice Arthus [64]. His approach implicates that intradermal injections of horse serum into (substance)-sensitized mice lead to the formation of edema, hemorrhage and neutrophil infiltration. Later, it was revealed that the formation of ICs induced an activation of the complement system via Fc receptors binding and leukocyte chemotaxis [63, 65]. Due to the ease of the procedure and its minute reproducibility, the reverse passive Arthus reaction is currently the prevailed applied experimental variant of IC-mediated inflammation *in vivo* [63].

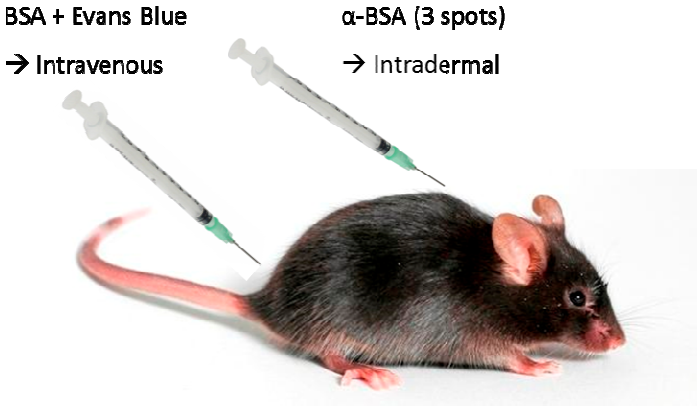

Figure 4-3 Model of the reverse passive Arthus reaction (RPA) The RPA is induced in mice by intravenous injection of BSA and Evans Blue followed by intradermal injection of anti-bovine serum albumin antibodies in the skin of the back. During 4 h of incubation, immune complexes (ICs) are formed, leading to a local inflammation characterized by neutrophil recruitment [63].

Briefly here, the RPA is induced in mice by intravenous injection of bovine serum albumin (BSA) in combination with Evans Blue and a subsequent intradermal injection of anti-BSA-antibody (anti-BSA-ab) into the skin of the back, resulting in a local formation of ICs and subsequent inflammation (Figure 4-3) [63]. Thus, Evans Blue is used as a measure for edema formation because the dye has a strong affinity for serum albumin in plasma and marks serum albumin extravasation. As early as 4 h post-IC-challenge, mice show cutaneous edema formation and neutrophil infiltration, accompanied by petechial hemorrhages in the areas surrounding the anti-BSA-ab injections.

4.3 Protease and Protease-activated receptors (PARs)

Protease-activated receptors (PARs) belong to the G-protein coupled receptors, which are expressed in virtually all tissues. Pathophysiological mechanisms, including vascular injury, acute inflammation, or allergen exposure, cause the release of several proteases that mediate the activation of PARs[16, 66].

PARs were identified in the 1990s, and four PAR family members, PAR_{1-4}, have been discovered so far. All PARs consist of seven transmembrane alpha-helices and are activated through proteolytic cleavage at the N-terminus by proteases including thrombin, trypsin, and cathepsin G (CatG) [67-72].

Proteases, also designated as peptidases and proteinases, are proteolytic enzymes that catalyse the degradation of proteins by hydrolysis of peptide bonds. Analysis of the human and murine genomes revealed that about 2% of all proteins encode for proteases [73-76]. Dependent on their mechanism of action and the amino acid sequence they target, proteases are classified as serine, cysteine, threonine, aspartic, metallo-, or glutamic proteases. Serine proteases form the most abundant group, and are named after their serine residue in the catalytic active domain. All serine proteases use a catalytic triad, consisting of three amino acids, to hydrolyze peptide bonds [76].

In their azurophilic granules, neutrophils store a specific set of different serine proteases, including neutrophil elastase (NE), proteinase 3, and cathepsin G (catG). All neutrophil serine proteases play an essential role in the defense against microorganisms by catalyzing the destruction of bacteria and the cleavage of extracellular matrix proteins [77-80]. Neutrophil-derived proteases are also capable of modulating inflammatory responses via activation of protease-activated receptors and, thereby, contribute to homeostasis or pathophysiological mechanisms [81].

4.4 Functional structure and activation of PARs

PAR_1 (*FR2*), PAR_2 (*F2RL1*) and PAR_3 (*F2RL2*) are encoded by genes that cluster on chromosome 5q 13 while the expression of the remarkably smaller PAR_4 (*F2RL3*) gene is encoded on chromosome 19p 12 [70, 71, 82]. Aside from seven transmembrane regions, PARs consists of an extracellular N-terminal domain comprising the protease cleavage site and an intracellular carboxy terminal domain. Compared to the other members of the *PAR*

family, the sequences of the intra- and extracellular domains of *PAR₄* are only slightly comparable with those of other *PARs*. The tethered ligand binding site of *PAR₄* only contains three amino acids (ITT**CHD**V) of the consensus sequence that is conserved in all other known *PARs* [71]. Furthermore, all receptors feature three intra- and three extracellular loops [83].

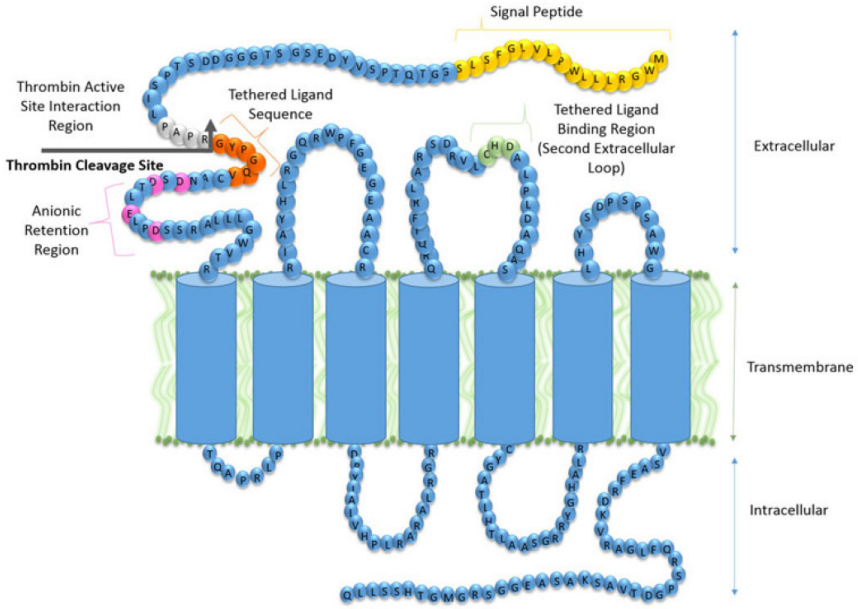

Figure 4-4 Structure of PAR₄ Similar to the other PAR members, PAR_4 consists of seven transmembrane regions. PARs further contain an extracellular N-terminal domain that contains the protease cleavage site and an intracellular carboxyl terminal domain. The sequence of the carboxy and amino domains of PAR_4 differ from those of other PARs. The tethered ligand binding site of PAR_4 only contains three amino acids (ITT**CHD**V) of the consensus sequence that is conserved in all other known PARs. All PARs have three intra- and three extracellular loops [84].

Source: French et. Al, Br J Pharmacol, 2016

PARs are activated by proteolytic cleavage at a particular site of the extracellular domain. This leads to the irreversible elimination of the original amino terminal and unmasks the cryptic amino terminal sequence, which is designated as the “tethered ligand” [67, 83]. The tethered ligand sequence interacts intramolecular with the conserved tethered binding site located on the second extracellular loop, and causes receptor activation. Asa consequence, the coupled G-protein dissociates and induces physiological responses, including apoptosis, cell growth, differentiation, and inflammation [66, 83]. For thrombin binding and proteolysis, PAR_1 and PAR_3 express a hirudin-like binding domain within the amino terminus, which is absent in PAR_4. Due to the lack of a hirudin-like binding domain within the amino terminus, PAR_4 has only low affinity for the binding of thrombin. Instead,

the extracellular terminal of PAR_4 contains a dual proline motif, named $P^{45}APR$, and a motif of certain anionic residues (D^{57}, D^{59}, E^{62}, and D^{65}) that is required for slow dissociation of thrombin [85, 86].

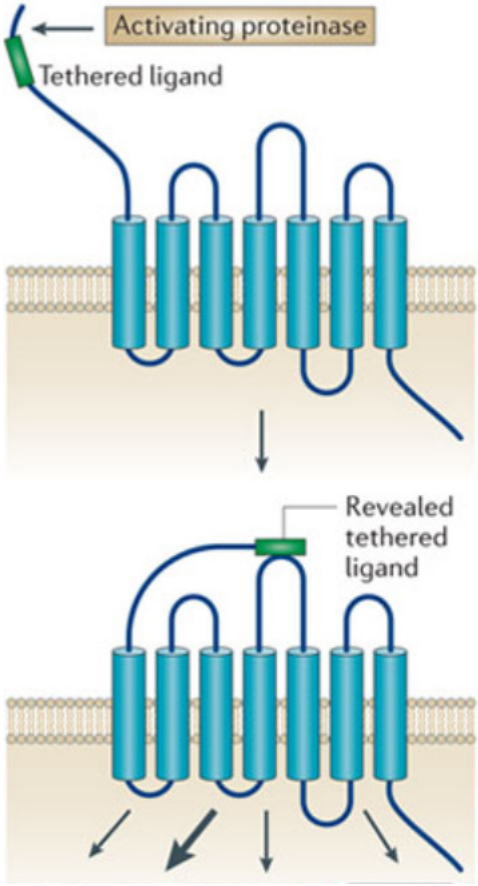

Figure 4-5 Activation of PARs Proteolytic cleavage of the amino-terminal by proteases eliminates the original amino terminal and unmasks the cryptic amino terminal sequence, which is designated as the "tethered ligand". The tethered ligand binds intramolecularly to the second extracellular loop of the receptor, the tethered ligand binding region, and leads to receptor activation [87].

Source: Ramachandran, Nat Rev Drug Discov, 2012

4.5 PAR_4

PAR_4 is the most newly discovered PAR, and was cloned in 1998. Only little is known about its physiological roles and functions [70, 71].

4.5.1 Expression and tissue distribution of PAR_4

PAR_4 expression has been detected in several cell types. The main PAR_4-expressing cell types include human platelets [70, 71, 88], leukocytes [89], endothelial cells [90], smooth muscle cell (SMCs) [91] and dorsal root ganglia (DRG) neurons [92]. Under certain

conditions, increased expression of the receptor has been detected. Upregulated PAR_4 expression and enhanced receptor responsiveness to thrombin is reported in SMCs following high-glucose stimulation, which might be implicated in the exacerbation of vascular damage in diabetes [93]. *In vitro* studies investigating the stimulation of monocytes by the apoptosis and chemotaxis mediator sphingosine-1-phosphate revealed increased expression of PAR_4 on human monocytes. This, in turn, increases the thrombin responses of monocytes and might facilitate their migration to the site of inflammation [93]. Increased expression of PAR_4 in human coronary artery by stimulation with the proinflammatory cytokines IL-1α and TNF-α demonstrates the role of PAR_4 in vascular inflammation [91]. This has been confirmed in a study by Pavic et al., who investigated increased expression of the receptor in vessels of patients suffering from type 2 diabetes mellitus [94].

Expression of PAR_4 has also been analyzed in tissues of heart, lung, skeletal muscle, kidney, pancreas, thyroid, testis, and small intestine [70, 71]. Here, an alteration in the expression profile relates to pathogenic mechanisms. Aggressive lung adenocarcinoma and esophageal squamous cell carcinoma are associated with decreased expression of PAR_4 [95, 96].

4.5.2 Activation of PAR_4 by coagulation factors and regulators of inflammation

PAR_4 is activated by coagulation factors and regulators of inflammation. As mentioned above, PAR_4 plays a role in the coagulation cascade and, upon stimulation with high levels of thrombin, it induces platelet aggregation [70, 97]. The activation of PAR_4 by thrombin also induces the recruitment of neutrophils to the site of vascular injury in a murine endothelial injury model, indicating an important role of the receptor in mediating vascular inflammation [98]. Furthermore, coagulation factor Xa leads to activation of the PAR_4 receptor and induces increased calcium signaling in *Xenopus* oocytes [99].

In the presence of inflammatory mediators, mast cell-derived trypsin and neutrophil-derived catG are able to cause PAR_4 activation. Thereby, trypsin stimulation induces TNF-α secretion, as shown in a human leukemic mast cell line, and has been shown to increase calcium signaling in *Xenopus* oocytes[70, 100]. CatG stimulation of PAR_4 triggers calcium mobilization in *PAR_4*-transfected fibroblasts, *PAR_4*-expressing *Xenopus* oocytes, and washed human platelets [72].

In addition to physiological mediators, PAR_4 can also be activated by amidated peptides (APs) that are based on the native tethered ligand sequence of the receptor. So far, there are two PAR_4-APs, GYPGKF-NH_2 and AYPGKF-NH_2, of which AYPGKF-NH2 has a higher specificity for PAR4 to induce platelet aggregations [70, 101, 102]

4.5.3 PAR_4 contributes to the development of thrombosis

Currently, thrombosis is a major cause of morbidity and mortality, and the activation of platelets by the coagulation protease thrombin is crucial for hemostasis during coagulation. PAR_1, the first PAR to be discovered, was identified as a high affinity thrombin receptor, and its expression has been detected in human endothelial cells, megakaryocytes, and platelets [67]. Because expression of PAR_1 is absent in murine platelets and rodent and rat platelets show no response to PAR_1-AP, the search for further thrombin receptors seemed necessary and revealed two additional receptors, PAR_3 and PAR_4 [69, 70, 103, 104].

PAR_3 is expressed in human bone marrow and murine megakaryocytes; however, although the receptor has a similar affinity to thrombin as PAR_1, it is not able to signal by itself via the thrombin-relevant sequence, even when overexpressed [69, 97, 105]. PAR_4, expressed in human and murine platelets and endothelial cells, is the third discovered thrombin receptor. Compared to PAR_1 and PAR_3, PAR_4 has only a low affinity to thrombin, and high concentrations of the coagulation protease are necessary for receptor activation [70, 97]. PAR_3 and PAR_4 are co-expressed in murine platelets, and the potential interaction between both receptors has been identified to activate thrombin signaling even, when only small amounts of the protease are present. In rodents, PAR_3 is activated by thrombin and acts as a cofactor for PAR_4 activation, leading to the induction of thrombin signaling [105]. Taken together, PAR_1, PAR_3, and PAR_4 are important mediators for thrombin signaling in platelets and are, therefore, critical for the understanding of thrombosis and homeostasis.

To investigate the key physiological function of PAR_4, a transgenic knockout mouse was established in 2001 by Sambrano et al. [106]. Platelets from these mice demonstrate no effect upon stimulation with PAR_4-AP, which confirms the complete loss of function of the PAR_4 receptor in the knockout mouse line. Unlike human platelets, which express PAR_1 and PAR_4, murine platelets express PAR_3 instead of PAR_1. Therefore, platelets from *Par4*$^{-/-}$ mice are completely unresponsive to thrombin and don't show platelet shape changes, calcium

mobilization, ATP secretion, or platelet aggregation after stimulation with varying concentrations of the coagulation protease [106]. In a tail-bleeding assay, a part of the tail tip of wild type and knockout mice is amputated and the bleeding time, as a measure of thrombosis, is assessed. Indeed, the bleeding time of *Par4*$^{-/-}$ mice is severely extended compared to that measured in wild type mice [106]. Furthermore, mice treated with a PAR_4 antagonist pepducin [70, 102], also show increased bleeding time and are protected against platelet activation, a phenotype that is consistent with that of *Par4*-deficient mice [107]. Taken together, these results confirm the insufficiency of Par_3 alone to induce thrombin-mediated platelet activation and the necessity of PAR_4 activation for maintaining normal platelet homeostasis.

Furthermore, the *Par4*$^{-/-}$ phenotype seems to be protected against thrombosis, since injury of mouse mesenteric arterioles by exposure to ferric chloride shows an increased latency until vessel occlusion compared to wild type mice [106]. Additional evidence for the protection against thrombosis in Par_4 deficiency has been reported by Hamilton et al., who showed increased survival after thromboplastin-induced pulmonary embolism in *Par4*$^{-/-}$ mice compared to wild type mice [108]. In addition, Par_4-deficient mice are remarkably protected against the formation of stable, platelet-rich, occlusive thrombi after electrolytic-induced vascular injury of the carotid artery [109].

4.5.4 Role of PAR_4 in neutrophil migration

Further studies have also analyzed the role of PAR_4 in the crosstalk between coagulation and diseases of systemic inflammation such as diabetes mellitus and rheumatoid arthritis.

In a streptozotocin-induced mouse model of type 1 diabetes mellitus, PAR_4-deficient mice are protected against augmented neointimal hyperplasia after carotid artery ligation [94]. In a mouse model of arthritis, extravascular inflammation is induced by hind paw application of coagulation mediators, such as recombinant soluble murine tissue factor ($sTF_{1–219}$). This causes a rapid onset of paw swelling in wild type mice, but *Par4*$^{-/-}$ mice are almost completely resistant to sTF-induced inflammation and only show slight edema, hemorrhage, and inflammation. Furthermore, fibrin deposition is markedly regulated by PAR_4, which has been demonstrated by reduced deposition measured in *Par4*$^{-/-}$ mice. Fibrin is

a proinflammatory mediator that induces the expression of adhesion molecules in endothelial and, when degraded, neutrophil chemotaxis. Further, fibrin deposition is associated with increased severity of glomerulonephritis and arthritis in human patients and analogous animal models [110].

In a mouse model of stroke, PAR_4 deficiency produces protection against reperfusion injury. Here, *Par4*$^{-/-}$ mice show reduced infarct volume, improved neurological and motor function, and less cerebral edema after occlusion of the transient middle cerebral artery. Furthermore, microvascular inflammation, including disruption of the blood-brain barrier and both platelet and leukocyte rolling and adhesion, was more efficiently attenuated in *Par4*$^{-/-}$ mice after artery occlusion when compared to wild type mice [111]. Taken together, mice deficient in PAR_4 show inhibited platelet activation and decreased vascular inflammation and, therefore, seem to be more protected against reperfusion injury than wild type mice.

In wild type mice treated with the PAR_4 antagonistic pepducin p4pal10, reduced edema formation and granulocyte recruitment were detected after 4 h of carrageenan-induced substantial edema provocation. Furthermore, treatment with a PAR_4-AP (AYPGKF-NH_2) severely increased the induction of edema and granulocyte recruitment, which are remarkably downregulated after co-administration of the tissue and plasma kallikrein inhibitors FE999024 and FE999026. Taken together, PAR_4 is an important mediator of edema formation during inflammation, acting specifically by activating granulocytes and the kallikrein-kinin system [112].

4.6 Cathepsin G

CatG belongs to the chymotrypsin family and is synthesized during the promyelocyte stage of neutrophil development [80, 113-115]. The chromosomal localization of human catG is found on chromosome 14q11.2 in a complex of genes coding for closely related serine protease [115, 116]. The murine catG gene is also located within a cluster of serine proteases on chromosome 14, and the protein shares a high homology with the human catG [116]. CatG preferentially cleaves substrates at aromatic residues at position P1 as has also been discovered for the serine endopeptidase chymotrypsin [117, 118]. As mentioned above (see 4.5.2), catG exerts its molecular action via the cleavage of the thrombin receptor PAR_4

[72]. However, little is known about the physiological function of this catG-mediated PAR_4 activation.

4.6.1 Implication of cathepsin G in coagulation

CatG has a vital mediator function in coagulation. It mediates the cleavage of several coagulation factors such as fibrinogen, prothrombin, and clotting factors (II, VII, IX, X) and activates coagulation factor V [119-123]. CatG has also been shown to inactivate tissue factor pathway inhibitor, the main inhibitor of the coagulation process, and has an effect on thrombin receptor function [124-127]. Several studies have also reported the role of catG as a potent human platelet activator [128-134]. Research by Rosa et al. revealed increased surface expression of P-selectin, fibrinogen receptor (glycoprotein IIb/IIIa), and thrombospondin receptor (glycoprotein IV), on platelets upon stimulation with catG, while the expression of the van Willebrand receptor (glycoprotein 1b) is down-regulated [133]. Further, catG induces aggregation in human platelets, as pharmacological inhibition of catG severely reduces aggregation of activated platelets in the presence of catG-containing neutrophils [135]. Mice deficient in catG or treated with a catG inhibitor show longer bleeding duration in a tail bleeding assay when compared to wild type and untreated control mice, validating the potent role of catG in coagulation [135].

4.6.2 Cathepsin G and neutrophil recruitment

Early studies dealing with neutrophil serine proteases revealed an abundance of catG and NE on the surface of neutrophils in addition to its abundance on the azurophilic granules [114, 136]. While unstimulated neutrophils only express small quantities of catG and NE on the surface, the expression is dramatically increased after stimulation with certain inflammatory mediators, including phorbol 12-myristate 13-acetate (PMA). Surface-expressed neutrophil serine proteases are thought to be protected from naturally circulating inhibitors, and a dense surface expression of proteases might be involved in chemokine processing and, therefore, neutrophil recruitment at sites of inflammation [114, 136].

In the murine model of IC-mediated inflammation, Raptis et al. investigated an efficient role of catG in the FcγR-induced interaction of neutrophils with ICs in mice deficient in NE and catG [137]. Similar results were demonstrated by Adkison et al., who detected no neutrophil accumulation in the joints of NE/catG-deficient mice using a model of antibody-

induced acute arthritis. Furthermore, this effect was accompanied by reduced production of the inflammatory cytokines TNF-α and IL-1β at the site of inflammation [138].

4.7 Aim of the project

Platelets are reported to play a crucial role in the regulation of inflammatory responses. They activate neutrophils to induce efficient adhesion to the vascular endothelium and favor their recruitment along the vessel to the site of inflammation. Therefore, the interaction of neutrophils and platelets has come more and more into focus as a marker for several inflammatory diseases, including vascular inflammation. Platelets express PAR_4 on their surface, and the activation of this receptor can be mediated by neutrophil protease catG. Both catG and PAR_4 are known to play an important role in coagulation, but, recently, an essential contribution of the catG/PAR_4-axis to inflammation has been reported. In this project, we aim to unravel the role of the catG/PAR_4-axis in platelets and the formation of NPAs. Furthermore, we sought to investigate the contributions of catG and PAR_4, as well as NPA, to the progression of vascular inflammation diseases such as LcV.

5 Material and Methods

5.1 Materials

5.1.1 Human antibodies

Antibody	Clone	Isotype	Company	Cat#	Vol/test
PE-anti-human CD41	HIP8	mIgG1-PE	Biolegend, San Diego, CA, USA	303706	5 µl
PE-Cy5 anti-human CD16	3G8	mIgG1-PE-Cy5	BD Biosciences, Franklin Lakes, NJ, USA	555408	5 µl

5.1.2 Mouse antibodies

Conjugated antibodies for flow cytometry					
Antibody	Clone	Isotype	Company	Cat#	Vol/test
Anti-Mouse Ly-6G APC	1A8	rat IgG2a	Biolegend, San Diego, CA, USA	127614	3 µl
PE-labeled rat anti-mouse GPIbα (CD42b)	Xia.G5	rat IgG2b	EMFRET analytics, Eibelstadt, Germany	M040-2	3 µl
Glycoprotein VI-FITC	JAQ1	rat IgG2a	EMFRET analytics, Eibelstadt, Germany	M011-1	3 µl
Two-Color Analysis of Mouse Platelet Activation	Wug.E9 JON/A	rat IgG2b/ IgG1	EMFRET analytics, Eibelstadt, Germany	D200	3 µl
FITC-labeled Rat Anti-Mouse Integrin β3 chain (GPIIIa, CD61)	Luc.H11	rat IgG2b	EMFRET analytics, Eibelstadt, Germany	M031-1	3 µl

Conjugated antibodies for histological examination					
Antibody			Company	Cat#	Dilution
Donkey anti-Goat IgG (H+L) Secondary Antibody, Alexa Fluor® 488 conjugate			Thermo Fisher Scientific, Waltham, MA, USA	A-11055	1:1000
Donkey anti-Rat IgG (H+L) Secondary Antibody, Alexa Fluor® 594 conjugate			Thermo Fisher Scientific, Waltham, MA, USA	A-21209	1:1000
Donkey anti-Rat IgG (H+L) Secondary Antibody, Alexa Fluor® 488 conjugate			Thermo Fisher Scientific, Waltham, MA, USA	A-21208	1:500
Donkey anti-Goat IgG (H+L) Secondary Antibody, Alexa Fluor® 568 conjugate			Thermo Fisher Scientific, Waltham, MA, USA	A-11057	1:500
Unconjugated antibodies for histological examination					
Antibody	Clone	Isotype	Company	Cat#	Dilution
LEAF™ Purified anti-mouse Ly-6G Antibody	1A8	rat IgG2a	Biolegend, San Diego, CA, USA	127620	1:100
Human/Mouse Myeloperoxidase/MPO Antibody	Poly-clonal	goat IgG	R&D systems, Minneapolis, MN, USA	AF3667	1:350
Anti-Mouse/Human Mac-2 (Galectin-3), Purified	M3/38	rat IgG2a	Cederlane, Burlingto, Canada	CL8942AP	1:200

5.1.3 Activators and antagonists

Proteases and activators	Company	Cat#	Concentration
Cathepsin G (human neutrophils), (purified)	Enzo Life Science, Farmingdale, NY, USA	BML-SE283	10 mU/ml
PAR_4 Agonist (one letter code: AYPGKF-NH_2)	Bachem Holding AG, Buldendorf, Switzerland	H-6046	100 µM
Adenosine diphosphate (ADP)	Calbiochem, Billerica, MA, USA	538925	10 µM
U46	Tocris Cookson Ltd., Bristol, United Kingdom	1932	3µM
Collagen related peptide (CRP)	Cambridge University, United Kingdom	-	5 µg/ml

Antagonists	Source	Concentration
Pepducin P4pal10	Kind gift of Rithwik Ramachandran Department of Physiology and Pharmacology Schulich School of Medicine & Dentistry University of Western Ontario London (Canada)	2 µM

5.1.4 Media, Buffers, Water

Medium	Company	Cat#
Phosphate-buffered saline (PBS)	Biochem, Berlin, Germany	L1825
Gibco® RPMI 1640 medium	Thermo Fisher Scientific, Waltham, MA, USA	61870-010
Lymphocyte separation Medium (LSM) 1077	GE Healthcare, Little Chalfont, United Kingdom	315-004
BD FACS Lysing Solution (10x concentrated)	BD Biosciences, Franklin Lakes, NJ, USA	349202
BD FACS Flow, 20 liters	BD Biosciences, Franklin Lakes, NJ, USA	342003

Rotiphorese 10x TRIS-Acetate-EDTA (TAE) Puffer	Carl Roth GmbH + Co. KG, Karlsruhe, Germany	CL86.2
Nuclease-free water	Carl Roth GmbH + Co. KG, Karlsruhe, Germany	T143.3
Demineralized water	Otto Fischar GmbH & Co. KG, Saarbrücken, Germany	18880
Water, HiPerSolv CHROMANORM® for HPLC	VWR Chemicals, Langenfeld, Germany	7732-18-5
Antibody dilution buffer	DCS Labline Innovative Diagnostik-Systeme GmbH & CO KG, Hamburg, Germany	AL120R500

5.1.5 Self-prepared buffers

Buffer	Ingredients	Company	Cat#
FACS wash buffer	500 ml PBS Dublecco	Biochem, Berlin, Germany	L1825
	1% heat-inactivated fetal bovine serum (FBS)		
Fixation Buffer	PBS Dublecco	Biochem, Berlin, Germany	L1825
	4 % paraformaldehyde (PFA)	Merck KGaA, Darmstadt, Germany	104005
Acid-citrate-dextrose anticoagulant	97 mM sodium citrate	Sigma-Aldrich, St. Louis, MO, USA	6132-04-3
	65 mM citric acid anhydrous	Sigma-Aldrich, St. Louis, MO, USA	77-92-9
	75 mM D-glucose	Sigma-Aldrich, St. Louis, MO, USA	50-99-7
	dissolved in 250 ml „Demineralisiertes Wasser“	Otto Fischar GmbH & Co. KG, Saarbrücken, Germany	18880
Tyrode’s buffer	136.5 mM sodium chloride	Sigma-Aldrich, St. Louis, MO, USA	3014
	2.68 mM potassium chloride	Merck KGaA, Darmstadt, Germany	104936
	11.9 mM sodium bicarbo-nate	Carl Roth GmbH + Co. KG, Karlsruhe, Germany	9105
	0.4 mM disodium hydrogen	Carl Roth GmbH + Co. KG,	T876

	phosphate	Karlsruhe, Germany	
	25 mM 4-(2-hydroxyethyl)-1-piperazineethanesulfonic acid (HEPES)	Carl Roth GmbH + Co. KG, Karlsruhe, Germany	9105
	1 mM magnesium chloride	Carl Roth GmbH + Co. KG, Karlsruhe, Germany	KK36
	2 mM calcium chloride (as required)	Sigma-Aldrich, St. Louis, MO, USA	A7646
	1% glucose	Carl Roth GmbH + Co. KG, Karlsruhe, Germany	HN06
	0.02 U/ml Apyrase (as required)	Sigma-Aldrich, St. Louis, MO, USA	A7646
	0.5 µM Prostaglandin I_2 (as required)	Calbiochem, Billerica, MA, USA	538925
Potassium Phosphate Buffer	1 M Potassium dihydrogen phosphate (pH 4) (Buffer A)	Merck KGaA, Darmstadt, Germany	104877
	1 M di-Potassium hydrogen phosphate trihydrate → to adjust pH 6 (Buffer A)	Merck KGaA, Darmstadt, Germany	105099

5.1.6 Kits

Kits	**Company**	**Cat#**
KAPA Mouse Genotyping Kit	KAPA Biosystems, Inc., Wilmington, MA, USA	KK7352
Cathepsin G Activity Assay Kit	Abcam, Cambride, United Kingdom	ab126780
Hemoglobin Mouse ELISA Kit	Abcam, Cambride, United Kingdom	ab 157715

5.2 *In vitro* experiments using purified human neutrophils and platelets

5.2.1 Isolation of neutrophils from human whole blood

Human whole blood was collected in venous blood collection tubes containing ethylenediaminetetraacetic acid (EDTA; BD Biosciences, Franklin Lakes, NJ, USA) to purify neutrophils using density gradient centrifugation. Gently, the whole blood was layered on 10 ml Lymphocyte separation Medium 1077 (LSM; GE Healthcare, Little Chalfont, United Kingdom) and centrifuged at 600 x g and 4°C without brakes for 20 min using a centrifuge (Rotanta 46 RC; Hettich, Kirchlengern, Germany). The supernatant containing lymphocytes and monocytes was discarded by gentle aspiration. The pellet containing neutrophils was washed with cold PBS (Biochem, Berlin, Germany) for 5 min at 850 x g and 4°C. Erythrocytes were lysed by hypotonic shock on ice using Millipore purified water (AG Zimmermann, Institute for Virology, Düsseldorf, Germany) and a 5 M sodium chloride solution to recover the physiological sodium concentration (145 mM). Purified neutrophils were washed for three times in 15-50 ml PBS. Neutrophils were resuspended $1*10^6$/ml in pre-warmed medium (RPMI Medium 1640; Thermo Fisher Scientific, Waltham, MA, USA) and rested for 1-2 h at 37°C and 5% CO_2 in an incubator (INCO_2; Memmert GmbH + Co.KG, Schwabach, Germany). A purity of ~95% was assessed by forward and sideward scattering using a flow cytometer (FACSCalibur; BD Biosciences).

5.2.2 Isolation of platelets from human whole blood

Human platelets were purified from whole blood collected in venous blood collection tubes containing sodium citrate anticoagulant (BD Biosciences, Franklin Lakes, NJ, USA). In brief, 3 ml of whole blood were centrifuged at 150 x g for 15 min at 24-26°C (24-26°C). The upper phase containing the platelet rich plasma was carefully transferred to a 15 ml falcon tube (BD Biosciences) and was resuspended with 1/10 volume of an acid-citrate-dextrose anticoagulant (see section 5.1.5). Platelets were pelleted by centrifugation at 900 x g for 5 min at 24-26°C and were resuspended at $20*10^6$ cells/ml in pre-warmed medium (RPMI Medium 1640; Thermo Fisher Scientific).

5.2.3 *In vitro* aggregation assay of platelets and neutrophils

20*106 platelets in 1 ml medium (RPMI Medium 1640; Thermo Fisher Scientific) were pre-treated with 2 µM of the PAR4 antagonist pepducin, P4pal10 (a kind gift from Rithwik Ramachandran, Department of Physiology and Pharmacology, Schulich School of Medicine & Dentistry, University of Western Ontario, London, Canada) or remained untreated for 30 min at 37°C and 5% CO_2 in an incubator (INCO_2; Memmert GmbH + Co.KG,). Thereafter, the platelets were stimulated with 10 mU/mL of purified human neutrophil-derived CatG (Enzo Life Science, Farmingdale, NY, USA) or remained unstimulated for 2 min at 37°C and 5% CO_2. According to the physiological ratio in human whole blood (1:20), $1*10^6$ neutrophils were co-incubated with $20*10^6$ platelets of each condition for 5 min at 37°C and 5% CO_2. The reaction was stopped by adding 1:1 fixation buffer, containing 4 % PFA (Merck KGaA; see section 5.1.5) for 15 min on ice. PFA-fixed NPAs were centrifuged for 5 min at 1200 rpm using a Rotixa/RP centrifuge (Modell 4200; Hettich, Kirchlengern, Germany) and were resuspended in 125 µl of FACS wash buffer. Next, aggregates were stained in a 1:20 antibody dilution for neutrophil marker, PE-Cy5 anti-human CD16, clone 3G8 (RUO), (BD Biosciences) and platelet marker, PE anti-human CD41, clone HIP8 derived from Biolegend (San Diego, CA, USA). The appropriate isotype controls PE-Cy5 mouse IgG1 κ IC (1:200, clone MOPC-21 (RUO) (BD Biosciences) and mouse IgG1 K isotype control PE (1:20, clone P3.6.2.8.1; eBiosciences, San Diego, CA, USA) were added in the same concentration. The staining was performed for 30 min at 4°C in the dark and cells were washed in 2 ml FACS wash buffer (see section 5.1.5) at 1200 rpm using a Rotixa/RP centrifuge (Modell 4200; Hettich). Cells were resuspended in the same buffer for flow cytometric analysis with FACSCalibur (BD Biosciences) and aggregation of neutrophils and platelets was assessed using double-staining for CD16 and CD41 and given as percentages.

5.3 *Ex vivo* human blood analysis

5.3.1 Human subjects

Blood samples were obtained from consenting adult patients diagnosed with leukocytoclastic vasculitis and from healthy control subjects at the Department of Dermatology of the Heinrich-Heine University Hospital in Düsseldorf. All patients and healthy

subjects were free of any anti-platelet, antibiotics, and corticosteroid treatments for at least two weeks before blood collection. The human protocol was approved by the ethics committee of the medical faculty of the Heinrich-Heine-University in Düsseldorf (Germany; study number: 4372; Role of Neutrophil Proteases and Protease-activated Receptors for the Regulation of Leukocyte-Endothelial Cell Interactions).

5.3.2 Assessment of NPAs in human whole blood

Human whole blood from healthy volunteers and patients with LcV was collected in venous blood collection tubes containing EDTA derived from BD Biosciences. 100 µl of whole blood were stained for the neutrophil marker PE-Cy5 anti-human CD16, clone 3G8 (RUO) (BD Biosciences) and the platelet marker PE anti-human CD41, clone HIP8 (1:20) derived from Biolegend (both applied in 1:20 dilutions) in disposable polystyrene Falcon round-bottom tubes (BD Biosciences). Unspecific staining was excluded by the appropriate isotype controls PE-Cy5 Mouse IgG1 κ IC (1:200, clone MOPC-21 (RUO); BD Biosciences) and Mouse IgG1 K Isotype Control PE (1:20, clone P3.6.2.8.1; eBiosciences). Staining was performed for 20 min at 24-26°C in the dark, followed by the addition of 2 ml of BD Pharm Lyse™ lysing solution (BD Biosciences) diluted in water (HiPerSolv CHROMANORM; VWR Chemicals, Langenfeld, Germany) for 10 min to fix cells and to lyse the erythrocytes. Thereafter, the cells were washed two times with 2 ml of FACS wash buffer for 5 min at 1200 rpm using a Rotixa/RP centrifuge (Modell 4200; Hettich). Percentages of NPA formation were determined using a flow cytometer (FACSCalibur; BD Biosciences) and the single cell analysing software FlowJo (FlowJo LLC, Ashland, OR, USA).

5.3.3 Analysis of catG activity in human plasma

Whole blood of human patients and healthy control subjects was collected in EDTA anticoagulant-containing tubes (BD Biosciences). Plasma was generated by centrifugation of the whole blood for 10 min at 1300 x g using a centrifuge (Rotanta 46 RC; Hettich). Aliquots of the plasma were stored in cryogenic vials (Corning Inc., Corning, NY, USA) at -20°C until further processing. CatG activity was assessed according to the manufacturer's instructions for the Cathepsin G Activity Assay Kit (Abcam, Cambridge, United Kingdom; see section 5.1.6). In brief, 50 µl of plasma samples were incubated for 10 min at 37°C and 5% CO_2 in an incubator (INCO_2; Memmert GmbH + Co. KG) with either 10 µl of the supplied Assay buffer

(S) or 10 µl of the 1:50 diluted Cathepsin G Inhibitor, which served as a background control (B). The prepared samples were then diluted with 40 µl of Substrate Solution and the optical density (OD) was evaluated at 405 nm in an Infinite microplate reader (M200 PRO; TECAN, Männedorf, Switzerland). The OD was first measured at timepoint 0 (T_1) and at a second time point (T_2) after incubation for 60 min at 37°C in the dark. The OD generated by the catalyzation of the substrate by catharpin G is calculated as follows:

$$A\Delta = (AS_{T2} - AS_{T1}) - (AB_{T2} - AB_{T1})$$

5.4 Mouse experiments

5.4.1 Mice

Wild type C57BL/6 mice were obtained from the internal breeding of the Zentrale Einrichtung für Tierforschung und Tierschutzaufgaben (ZETT) at the Heinrich-Heine University in Düsseldorf, Germany. *Par4*$^{-/-}$ mice were a kind gift from the working group of Professor Fischer at the institute for Pharmacology and Clinical Pharmacology of the Heinrich-Heine University in Düsseldorf, Germany. All mice were healthy, fertile and did not display evidence of infection or disease. Wild type and *Par4*$^{-/-}$ mice were used at the age of 6 to 12 weeks and were housed in pathogen-free conditions in the ZETT. All animal experiments were approved by the „Landesamt für Natur, Umwelt und Verbraucherschutz Nordrhein-Westfalen“ (Germany; Az.84-02.04.2012.A401; „Proteinase-aktivierter Rezeptor 1 und 2 ($PAR_{1/2}$): Regulation von Leukozyten-Endothel Interactionen in der Vaskulitis“).

5.4.2 Genotyping

5.4.2.1 Genotyping of *Par4*$^{-/-}$ mice

Approximately 1 mm of the tail of each *Par4*$^{-/-}$ mice was amputated and lysed in 50 µl of nuclease-free water (Carl Roth GmbH + Co. KG, Karlsruhe, Germany), comprising 1:10 10x KAPA Express Extract Buffer and 1 U/ml KAPA Express Enzyme, both supplied in the mouse genotyping Kit (KAPA Biosystems, Inc., Wilmington, MA, USA; see section 5.1.6). Lysis was performed for 10 min at 75°C followed by enzyme inactivation for 5 min at 95°C. Lysate mixtures were gently centrifuged using a centrifuge (5415 R; Eppendorf, Hamburg, Germany). 0.5 µl of the undiluted DNA were added to 15 µl of the KAPA-Mix and 0.5 µM

each of mPAR4 reverse primer, mPAR4 forward primer, and mPAR4 lacZ r diluted in nuclease-free water (Carl Roth GmbH + Co. KG). Polymerase chain reaction (PCR) was performed according to the following cycling protocol: the initial denaturation was done for 3 min at 95°C, followed by 35 cycles of denaturation for 15 s ecah at 95°C, annealing for 15 s at 50°C, and extension for 30 s at 72°C. The final extension was performed for 1 minute at 72°C.

2 g peqGOLD Universal Agarose (Peqlab Biotechnology GmbH, Erlangen, Germany) were diluted in 100 ml of 10-times diluted Rotiphorese 10x TAE Puffer (Carl Roth GmbH + Co. KG) and were boiled in a microwave (Micromat; AEG, Frankfurt am Main, Germany), until the agarose powder was dissolved. The mixture was then cooled to approximately 50°C, and 5 µl of Red Safe Nucleic Acid Staining Solution (20000x; Intron Biotechnology, Sangdaewon Seongnam, South Korea) were added. Agarose liquid was poured into a gel chamber (Bio-Rad Laboratories, Inc., Hercules, CA, USA), pockets were inserted by using a pocket crest, and gel was allowed to harden at 24-26°C. 13 µl of each amplified sample were added to the gel pockets and were electrophoresed for approximately 30 min at 90 V in a Mini Sub Cell GT (Bio-Rad Laboratories, Inc.) using a microprocessor (Model 200/2.0 power; Bio-Rad Laboratories, Inc.). Wild type and knockout DNA sequences were visualized under UV light after staining with Red Safe staining. The Gene Ruler 100 bp DNA ladder (Thermo Fisher Scientific) was used as a size marker for estimating the wild type (600 bp) and *Par4*$^{-/-}$ knockout (350 bp) fragment sizes.

Primer

Oligoname	**Sequence (5' → 3')**	**Primer Type**	**Company**
GT mPar4 r	AGCACATGCTGCCAGGATCAG	Wild type Reverse	Eurofins Genomics, Luxemburg, Luxemburg
GT mPar4 f	GGGGATGTTGTGGAGATTTG	Wild type Forward	Eurofins Genomics, Luxemburg, Luxemburg
GT mPar4 lacZ r	ATTCAGGCTGCGCAACTGTTGG	Mutant	Eurofins Genomics, Luxemburg, Luxemburg

5.4.3 The reverse passive Arthus reaction

5.4.3.1 Induction of the reverse passive Arthus reaction (RPA)

The RPA is induced by intravenous administration of 1 % Bovine Serum Albumin (BSA; Sigma-Aldrich, St. Louis, MO, USA) in combination with 0.5 % Evans blue (Sigma-Aldrich) to wild type and knockout mice using a needle (27-gauge; Terumo, Hatagaya, Japan) attached to a 1 ml syringe (Braun, Melsungen, Germany). The hair on the dorsal skin of each mouse was removed by a clipper (Isis Cordless Animal Clipper; Pioneer, Canterbury, United Kingdom) and 20 µl of 1.5 mg/ml anti-BSA (MP Biomedicals, Santa Ana, CA, USA) was injected intradermally three times to the shaved area using a needle (26-gauge; BD Biosciences).

Reagents and products for *in vivo* experiments

Product	Company	Cat#
Isis Cordless Animal Clipper	Pioneer, Canterbury, United Kingdom	C420
BD Plastipak 1 ml Sub-Q	BD Biosciences, Franklin Lakes, NJ, USA	305501
Omnifix F, 1 ml	B. Braun, Melsungen, Germany	9161406V
Neolus Cannula, 27G x 3/4, 0.4 x 20	Terumo, Hatagaya, Japan	NH-2719R
Hematocrit-capillaries, Na-Hep	Hirschmann Laborgeräte, Eberstadt, Germany	9100260
Biopsy Punch (8 mm)	pfm medical, Cologne, Germany	48801

Reagent	Company	Cat#
Albumin from bovine serum (BSA)	Sigma-Aldrich, St. Louis, MO, USA	A4503-50G
Evans Blue	Sigma-Aldrich, St. Louis, MO, USA	E2129-10G
Rabbit IgG Fraction to Bovine Albumin	MP Biomedicals	855275
Histamine	Sigma-Aldrich, St. Louis, MO, USA	H7125
Hexadecyltrimethylammonium bromide (HTAB)	Sigma-Aldrich, St. Louis, MO, USA	H9151-25G
3,3’,5,5’-Tetramethylbenzidine (TMB) Liquid Substrate System for ELISA	Sigma-Aldrich, St. Louis, MO, USA	T0440-100ML

After 4 h of RPA-challenge, murine whole blood was collected in either 20 U/ml heparin-sodium 25.000 (Ratiopharm, Ulm, Germany; see section 5.4.7) or sodium citrate (see section 5.4.6) using a 1 cm sodium/heparin coated hematocrit capillary tube (Hirschmann Laborgeräte, Eberstadt, Germany). The reaction was then stopped, and tissue biopsies (of healthy and inflamed skin) were harvested from the prepared back skin of all treated mice using 8 mm punches (pfm medical ag, Cologne, Germany). Biopsies were harvested in either PBS (Biochem) for myeloperoxidase (MPO) quantification (see section 5.4.4), formalin for immunohistochemistry (see section 5.4.8.1, 5.4.8.2), or Tissue-Tek O.C.T. Compound (Sakura, Alphen aan den Rijn, Netherlands) for cryosectioning (see sections 5.4.8.4, 5.4.8.5, 5.4.8.6).

5.4.3.2 Vascular permeability induced by histamine

Vascular permeability was assessed by injection of histamine (Sigma-Aldrich, St. Louis, MO, USA) to the skin of the back of wild type and *Par4*$^{-/-}$ mice. For this, the hair on the dorsal skin of each mouse was removed as described in section 5.4.3.1, and 20 µl of 1 mM histamine (Sigma-Aldrich) was injected intradermally twice to the shaved area using a needle (26-gauge; BD Biosciences). Additionally, 20 µl PBS (Biochem) was injected twice in the dorsal skin, serving as control. Further, all mice were injected systemically with 0.5 % Evans blue (Sigma-Aldrich). Mice were killed 4 h after induction, and 8 mm punches were harvested from the prepared back skin as described in 5.4.3.1 for further investigation of MPO activity (see section 5.4.4).

5.4.4 Determination of neutrophil myeloperoxidase (MPO) activity

After 4 h of RPA, representative pictures of the inner surface of the prepared dorsal skin of wild type and *Par4*$^{-/-}$ mice were taken with a photo camera (EOS 1100D; Canon, Tokio, Japan). Skin samples 8 mm punches (pfm medical ag) were collected for biopsy from inflamed and healthy areas of the murine dorsal skin, and mouse weight was measured using a scale (PCB 100-3; Kern & Sohn GmbH, Balingen, Germany). Subsequently, skin samples were shred in PBS using a polytron (PT 2500E; Kinematica AG, Lucerne, Switzerland) for at most 10 s. Hashed tissues were pelleted for 10 min at 15,700 x g (5417R centrifuge; Eppendorf) and were digested in freshly prepared potassium phosphate buffer (see section 5.1.5) supplemented with 1 % hexadecyltrimethyl-ammonium bromide (Sigma-Aldrich) for

15 min at 24-26°C. The hashed tissues were pelleted once more at 15,700 x g, and aliquots of 10 µl of the supernatant were added to 3,3’,5,5’-tetramethylbenzidine (TMB; Sigma-Aldrich), a liquid substrate that is catalysed by MPO. After adding the substrate, the enzymatic reaction was assessed at 620 nm for 20 min using a microplate reader (Infinite M200 PRO; TECAN, Männedorf, Switzerland).

5.4.5 Quantification of hemoglobin in murine tissue

Tissue hemoglobin levels were assessed with the Hemoglobin Mouse ELISA kit (Abcam; see section 5.1.6) according to the manufacturer’s instructions. In brief, skin biopsies (8 mm) of healthy and inflamed skin of RPA-challenged mice were shred for at most 10 s in 1 ml of PBS (Biochem) using a polytron. Hashed tissues were pelleted for 5 min at 5000 x g. For the quantification of hemoglobin, samples were diluted 1:4000 1X diluent included in the kit. Duplicates of 100 µl of each sample, as well as a standard curve (0–400 ng/mL) using the Mouse Hemoglobin Calibrator supplied in the kit, were added to the Mouse Hemoglobin ELISA Microplate and incubated for 60 min at 24-26°C. Next, the contents of the wells in the Mouse Hemoglobin ELISA Microplate were aspirated, and the wells were filled with 1X wash buffer, diluted in water (HiPerSolv CHROMANORM® for HPLC; VWR Chemicals). The buffer was aspirated and the wells were washed with 1X Wash buffer three times to wash away any unbound proteins. Next, 100 µl of 1X horseradish peroxidase-labelled secondary antibodies in 1X diluent were added to each well and incubated for 30 min at 24-26°C for detection of hemoglobin bound to the primary antibody pre-coated on the microplate. After incubation, the wells were again washed four times with 1X wash buffer to remove unbound secondary antibodies. 100 µl of the TMB Substrate Solution included in the Hemoglobin Mouse ELISA kit were added for 10 min in the dark, and the enzymatic reaction was stopped by adding 100 µl of the Kit Stop Solution. The absorbance was determined at 450 nM using an Infinite M200 PRO microplate reader (TECAN).

5.4.6 Analysis of catG activity in murine plasma

Murine whole blood was collected via puncture of the retro-orbital route using sodium/heparin-coated glass capillaries (Hirschmann Laborgeräte) loaded with citrate solution containing 95 mM sodium citrate and 23 mM citric acid (BD Biosciences). For murine plasma generation, whole blood was centrifuged for 10 min at 650 x g using a 5415 R

centrifuge (Eppendorf). The supernatant containing the plasma was aliquoted and stored at -20°C. CatG activity was assessed by the Cathepsin G Activity Assay Kit (Abcam) according to the manufacturer's instructions and is briefly described under section 5.3.3.

5.4.7 Assessment of NPAs in murine whole blood

Murine whole blood was collected via puncture of the retro-orbital route using sodium/heparin coated glass capillaries (Hirschmann Laborgeräte). Collected blood was diluted in 300 µl of 20 U/ml heparin-sodium 25.000 (Ratiopharm) and kept at 37°C. First, a blood count analysis was done using a hematology analyzer (Vet abc Plus^{+} Hematology Analyzer; scil animal care company GmbH, Viernheim, Germany). 500 µl of pre-warmed Tyrode's buffer were added and blood was centrifuged for 5 min at 650 x g. The supernatant was removed, and the blood was washed twice with 500 µl of pre-warmed Tyrode's buffer (see section 5.1.5) with a 5 min pause at 37°C between every washing step to prevent spontaneous platelet aggregation. Finally, 50-100 µl of pre-warmed Tyrode's buffer were added, and the blood rested for another 10 min at 37°C. For the quantification of murine NPAs, 25µl of the prepared blood were stained for 10 min at 24-26°C with 3 µl of platelet marker PE-labeled rat anti-mouse GPIbα (CD42b), clone Xia.G5 (EMFRET Analytics GmbH & Co. KG, Eibelstadt, Germany) and an additional 3 µl of neutrophil marker anti-mouse Ly-6G APC, clone 1A8 (Biolegend). Heterotypic aggregations were measured using a flow cytometer (FACS Calibur; BD Biosciences), and absolute numbers were normalized to $9*10^5$ events per collected sample.

5.4.8 Analysis of tissue infiltration of inflammatory cells

5.4.8.1 Paraffin sections

One piece of bisected 8 mm punches of control and inflamed skin were each embedded in formaldehyde and stored at 24-26°C. Punches were processed in a tissue processor from Tissue Tek, Sakura (Model: VIP^{R} Vacuum Infiltration Processor Floor) and embedded in paraffin using The Tissue-Tek Tissue Embedding Console System (Sakura; Typ: 12100).

5.4.8.2 Hemoatoxylin and eosin staining

Three to four 3 µm sections (see section 5.4.8.1) were placed on each microscope slide. Hematoxylin and eosin (H&E) staining was performed according to the standard protocol of the histology department of the clinic of dermatology. For this, object slides were placed twice in xylol followed by incubation in 99%, 96%, and 70% isopropanol. Slides were washed in water and subsequently submerged in hemalum five times. Slides were again washed in water, HCL-alcohol, water, scotspuffer, water, and then distilled water. Next, slides were stained with eosin and rinsed two times each in 96% and 99% isopropanol and two times in xylol. The incubation times for each step of the staining protocol took about 40 s in a plastic cuvette at 24-26°C. Finally, object slides were covered with a cover slip using the Tissue Tek coverslipper (Sakura; Model: SCA-4765 Film Coverslipper).

5.4.8.3 Cryostat sections

One piece each of bisected 8 mm punches of control and inflamed skin were embedded in Tissue Teck O.C.T. Compound (Sakura) and stored at -80°C in a Hera Freeze HFU B Series (Thermo Fisher Scientific) until further processing. For cryostat sectioning, samples were slowly thawed in a -20°C freezer and three to four 4 µm sections were placed on each microscope slide. Up to 10 microscope slides were prepared and stored at -80°C until immunofluorescent staining was performed as described in sections 5.4.8.4, 5.4.8.5, and 5.4.8.6. For histological examination of neutrophils and T cells, all antibodies were diluted in an antibody dilution buffer (DCS Labline; Innovative Diagnostik-Systeme GmbH & Co KG, Hamburg, Germany (see sections 5.4.8.4 and 5.4.8.6). Antibodies for the staining of macrophages were diluted in PBS supplemented with 1% BSA (see section 5.4.8.5).

5.4.8.4 Histological examination of neutrophil tissue infiltration

Sections of inflamed and control skin (see 5.4.8.3) were dried at 24-26°C for approximately 30–40 min and were washed with PBS (Biochem) to remove the embedding medium. Edges were dried using facial tissues, and a closed water-repelling circle was drawn around every sample using a grease pen (Dako, Hamburg, Germany). Microscope slides were then washed three times in PBS for 5 min each. All sections were blocked for 45 min 24-26°C in a moist chamber with 50 µl of 10% donkey serum (Merck KGaA, Darmstadt, Germany) diluted in PBS. Directly after blocking, the primary antibody, Human/Mouse-MPO Antibody,

clone 392105 (R&D systems, Minneapolis, MN, USA) was diluted 1:350. 50 µl of the suspension were applied to each section, except keeping one unstained control section where the pure antibody dilution buffer was subjected. The 1st antibody was incubated for 90 min at 24-26°C in a moist chamber. Before adding the 2nd antibody, all slides were washed three times in PBS for 5 min. The donkey anti-Goat IgG (H+L) secondary antibody (Thermo Fisher Scientific) was conjugated to Alexa Fluor 488 and diluted 1:1000. 50 µl/section were added and incubated for 60 min at 24-26°C in a moist chamber. Microscope slides were again washed three times for 5 min in PBS in the dark and were stained for another 1st antibody, LEAF™ Purified anti-mouse Ly-6G, clone 1A8 (Biolegend). The antibody was applied in a 1:100 dilution and 50 µl/section were added. This antibody was not added to the control sections, where pure antibody dilution buffer was used instead. Antibody staining was performed for 90 min at 24-26°C in a moist chamber. Microscope slides were again washed three times for 5 min in PBS, followed by staining with the 2nd antibody in combination with 4',6-diamidino-2-phenylindole (DAPI), (Sigma-Aldrich). Donkey anti-Rat IgG (H+L) secondary antibody (Thermo Fisher Scientific) was conjugated to Alexa Fluor 594 and diluted 1:1000. Additionally, 2 µg/ml DAPI was added to the mixture and 50 µl per section were added and incubated for 60 min at 24-26°C in a moist chamber. Finally, microscope slides were again washed three times in PBS in the dark, the edges were dried, and all slides were mounted with Fluoromount-G (Sothern Biotech, Birmingham, AL, USA) and cover-slipped. After drying overnight at 4°C, immunofluorescent staining was assessed utilizing an AxioImager.Z2 (Carl Zeiss, Jena, Germany) using 10× (numerical aperture 0.3) and 40× (numerical aperture 0.75) Plan-Neofluar magnification objectives. Examination of the staining was performed using AxioVision software (Version 4.8; Carl Zeiss)

5.4.8.5 Histological examination of macrophage tissue infiltration

Sections of inflamed and control skin (see section 5.4.8.3) were dried at 24-26°C for approximately 30-40 min and were fixed with in acetone (Roth, Karlsruhe) at 4°C in a glass cuvette for 15 min. Fixed slides, were washed for four times in PBS for each 3-4 min. PBS was removed and slides were blocked for 1 h at 24-26°C with 10 % Tris-buffer saline, 10 % FCS and 1 % BSA dissolved in distilled water in the same cuvette. Edges surrounding each section were dried using facial tissues and a water repelling circle was drawn around every slide using a grease pen. The 1st antibody, Human/Mouse-MPO Antibody, clone 392105,

supplied by R&D systems was diluted 1:300 in PBS supplemented with 1% BSA and 30-50 µl were added to each section except for the isotype control. The first antibody was incubated over night at 4° C in a moist chamber. The next day, slides were washed in PBS four time each 3-4 minutes. The second antibody Donkey anti-Goat IgG (H+L) Secondary Antibody, Alexa Fluor® 568 conjugate (Thermo Fisher Scientific) was diluted 1:500 in PBS and 30-50 µl were added per section for 1 h at 24-26°C in the dark. Slides were again washed for four time each 3-4 min and another first antibody was added. Anti-Mouse/Human Mac-2 (Galectin-3), Purified (Clone M3/38) (rat IgG2a) supplied by Cederlane, Burlingto, Canada was diluted 1:200 and 30-50 µl per section, while keeping one unstained control section. The 1st antibody was incubated for 1 h at 24-26°C in the moist chamber. Before adding the 2nd antibody all slides were washed four times in PBS for 3-4 min each. Next, the Donkey anti-Rat IgG (H+L) Secondary Antibody, conjugated to Alexa Fluor 488 (Thermo Fisher Scientific) was diluted 1:500 and 30-50 µl per section were added to each section for 1 h at 24-26°C in the moist chamber. Last, the slides were washed for additional four time in PBS each 3-4 min. Sections were mount with Roti®-Mount FluorCare DAPI, supplied by Roth, Karlsruhe, Germany and were covered with an object-glass. Slides were dried for 4 h at 24-26°C in the dark and at 4°C over night. immunofluorescent staining was assessed utilizing an AxioImager.Z2 (Carl Zeiss, Jena, Germany) using 10× (numerical aperture 0.3) and 40× (numerical aperture 0.75) Plan-Neofluar magnification objectives. Examination of the staining was performed by means AxioVision Version 4.8.

5.4.8.6 Histological examination of T lymphocyte tissue infiltration

Sections of inflamed and control skin (see section 5.4.8.3) were dried at 24-26°C for approximately 30-40 min and were fixed with -20°C acetone (Carl Roth) in a glass cuvette for 10 min at -20°C. Next, slides were washed in PBS (Biochem) for 10 min at 24-26°C and the edges were dried using facial tissues. A water-repelling circle was drawn around every slide using a grease pen (Dako). Slides were then washed once more in PBS for 10 min at 24-26°C. All sections were blocked with 100 µl of 2% BSA (GE Healthcare), diluted in PBS, for 45 min at 24-26°C in a moist chamber. Purified anti-mouse CD8a Antibody, clone 5H10-1 (Biolegend) was diluted 1:100 and 50 µl were added per section, while one section remained unstained, serving as a control. The 1st antibody was incubated overnight at 4°C in a moist chamber. After incubation, slides were washed three times in PBS for 5 min and the 2nd antibody was

added. For this, 50 µl of donkey anti-rat antibodies conjugated to Alexa Fluor 488 (Thermo Fisher Scientific) were added in a 1:1000 dilution and incubated for 60 min at 24-26°C in a moist chamber. After this, the slides were manually washed three times with PBS in the dark. A Biotin Blocking System (Dako) containing 0.1% avidin and 0.01% biotin was then used to prevent nonspecific staining of endogenous biotin by the previously used avidin-based immunohistochemistry reagents. First, 50 µl of the avidin solution were added per section for 10 min, then sections were washed, dry-rinsed, and re-subjected to 50 µl/section of a biotin solution for another 10 min at 24-26°C in a moist chamber. Biotin anti-mouse CD4 Antibody, clone RM4-5 (Biolegend) was diluted 1:100 in the antibody dilution buffer (DCS Labline; Innovative Diagnostik-Systeme GmbH & CO KG). As before, 50 µl of antibody-containing buffer per section were added, with the exception of the control section where only buffer was applied, and sections were incubated for 60 min at 24-26°C in a moist chamber. Before adding the 2nd antibody in combination with DAPI, microscope slides were washed three times in PBS in the dark. PE Streptavidin (Biolegend) was used at a dilution of 1:2000, and 2 µg/ml DAPI were applied to the antibody mixture. Incubation was performed for 120 min at 24-26°C in the dark and the washed microscope slides were mount and immunofluorescent staining was assessed as described in section 5.4.8.4.

5.4.9 Activation of murine platelets

5.4.9.1 Isolation of platelets from murine whole blood

Whole blood from healthy, untreated mice was collected in a 1.5 ml tube (Eppendorf) containing 300 µl of 20 U/ml heparin-sodium 25.000 (Ratiopharm) and kept at 37°C until further processing. Blood was centrifuged for 5 min at 250 x g using a centrifuge (5415 R; Eppendorf). The supernatant and a minor part of the erythrocyte phase were collected in a fresh 1.5 ml tube (Eppendorf) and centrifuged for 6 min at 60 x g. The supernatant was transferred to another 1.5 ml tube (Eppendorf) and 0.02 U/ml apyrase (Sigma-Aldrich) and 0.5 µM prostaglandin I_2 (Calbiochem, Billerica, MA, USA) were added to the collected supernatant. 200 µl of 37°C Tyrode's buffer (see section 5.1.5) were added to the pellet followed by centrifugation for 6 min at 60 x g. The supernatant was collected and added to the previously collected supernatant. Platelets were pelleted for 5 min at 650 x g. The supernatant was discarded, and 1 ml of 37°C Tyrode's buffer containing 0.02 U apyrase and

0.5 µM prostaglandin I_2 was added. Platelets were pelleted again for 5 min at 650 x g in 200 µl of 37°C Tyrode's buffer containing 2 mM calcium chloride (Sigma-Aldrich). 10 µl of platelets were resuspended in 90 µl PBS and counted using hematology analyzer (KX-21N™ Automated Hematology Analyzer; Sysmex Coperation, Kobe, Japan). $1*10^5$ platelets were used for each assay.

5.4.9.2 CatG-dependent platelet activation

Stimulation of 1*105 platelets in 20 µl in 10 µM adenosine diphosphate (ADP)] alone or in combination with either U46 (Tocris Cookson Ltd., Bristol, United Kingdom) or 5 µg/ml collagen-related peptide (CRP) (Cambridge University, Cambridge, United Kingdom) for 7 min at 37°C served as positive controls for platelet activation. The same amount of platelets was stimulated dose-dependently using 0.01 U/ml, 0.1 U/ml, or 1 U/ml CatG (Enzo Life Science). PAR4-AP (Bachem Holding AG, Buldendorf, Switzerland) was assed at a concentration of either 50 µM or 100 µM. Stimulation with catG and PAR4-AP was performed for 30 min at 37°C. An unstimulated sample of resting platelets served as control. Following this, three antibody cocktails were prepared for staining of platelet surface molecules. I. The Two-Color Analysis of Mouse Platelet Activation (Emfret Analytics, Eibelstadt, Germany), containing PE-labeled JON/A antibody as well as FITC-Labeled Wug.E9 antibody. JON/A binds with a high affinity to the activated mouse integrin $\alpha IIb\beta 3_1$ (synonyms GPIIb/IIIa, CD41/CD61), the platelet receptor for fibrinogen, vWF, fibronectin, and vitronectin, and mediator of platelet adhesion and aggregation. Wug.E9 reacts with mouse adhesion molecule, P-selectin (CD62P) that is stored in the α-granula of platelets and translocated to the surface upon platelet stimulation; II: An antibody mix supplemented with PE-labeled rat anti-mouse GPIbα (CD42b) and FITC-labeled Rat Anti-Mouse Integrin β3 chain (GPIIIa, CD61) both supplied by Emfret Analytics, Eibelstadt, Germany. GPIb is part of the GPIb-V-IX complex, the platelet receptor for vWF. Here, the Anti-Mouse Integrin β3 chain binds to the surface expressed, also inactivated, form of the integrin; and III: An antibody cocktail only containing Glycoprotein VI-FITC. GPVI is a platelet/megakaryocyte-specific type I transmembrane glycoprotein that serves as an activating collagen receptor. All antibody mixtures (I, II, and III) were added in a volume of 3 µl to each stimulation condition and were incubated for 10 min at room temperature in the dark. The antibody binding was stopped by adding 400 µl of PBS (Biochem). Expression of surface molecules on platelets was assessed

by flow cytometry using the FACS Calibur (BD Biosciences), and statistics were analysed using PRISM 6 software (GraphPad, San Diego, CA, USA).

6 Results

6.1 Patients with LcV show a massive cutaneous infiltration of neutrophils accompanied by leakage of erythrocytes into the inflamed skin

The LcV is an IC-mediated inflammatory disorder that is characterized by a massive cutaneous infiltration of neutrophils and other inflammatory cells, including lymphocytes and tissue macrophages [54, 57]. Due to the vast accumulation of ICs at the vessel wall, neutrophils are recruited and release ROS and degrading enzymes in a purpose to phagocytose the ICs [54, 57]. However, instead of degrading ICs, the release of ROS and degrading enzymes leads to the destruction of the endothelial wall leading to the extravasation of red blood cells into the perivascular dermis [54, 57]. The resulting petechial bleeding, also called purpura, (Figure 6-1 A, blue arrows), is the main clinical symptom of the LcV. More severe progression of the LcV is characterized by hemorrhagic plaques (Figure 6-1 A, white bracket), accompanied by blisters (yellow arrow) and necrotic ulcerations (Figure 6-1 A, white arrows), as seen on the ankle of a representative patient, suffering from extensive LcV.

Hematoxylin and eosin staining of skin biopsies of patients with LcV demonstrated a massive inflammatory infiltrate dominated by neutrophils (Figure 6-1 B, black arrows) and eosinophils (Figure 6-1 B, light blue arrows). The neutrophils are responsible for the destruction and interspersion of the vessel walls which is caused by their transmigration and nuclear dust because of neutrophil destruction (red arrow) [54, 57]. The increased permeability of the damaged vessel walls leads to extravasation of red blood cells (green arrows) in the inflamed area in the dermis. In the area surrounding the blood vessel a massive fibroid degeneration can be detected as well.

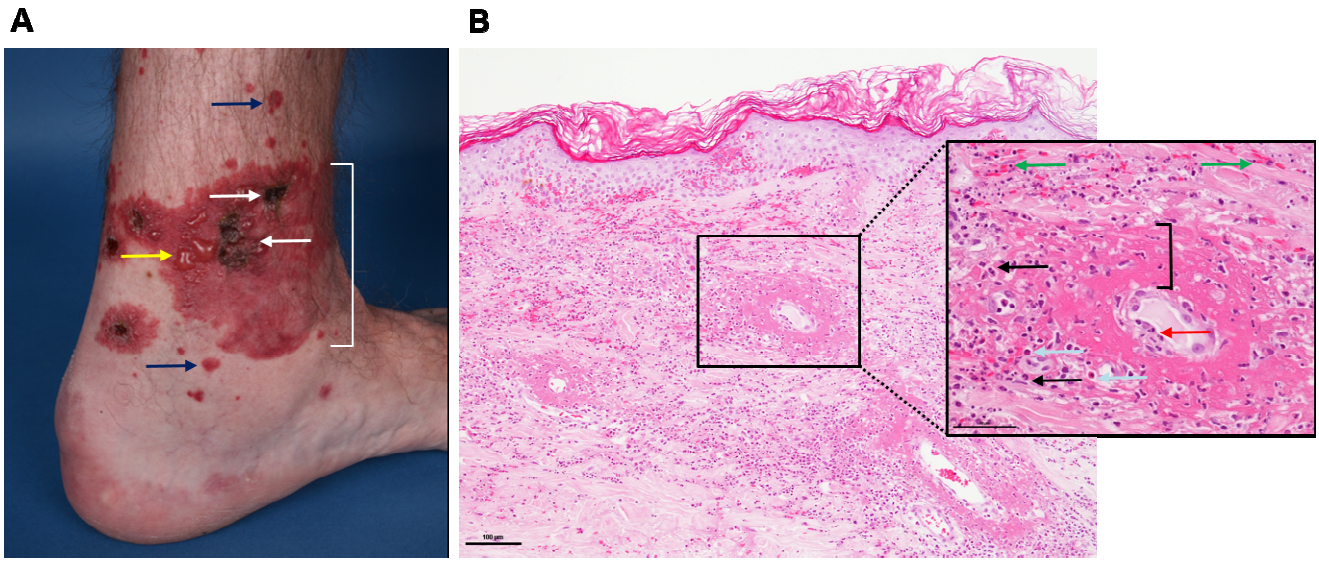

Figure 6-1 Patients with LcV show a massive cutaneous infiltration of neutrophils accompanied by leakage of erythrocytes into the inflamed skin (purpura) (A) Representative picture of the ankle of a patient suffering from LcV. The release of neutrophil-derived ROS and destructive enzymes causes endothelial wall destruction and subsequent extravasation of red blood cells into the dermis. This results into the main clinical symptom of LcV, the pupura (blue arrow) that can develop into more severe hemorrhagic plaques (white bracket), accompanied by blisters (yellow arrow) and necrotic ulcerations (white arrows). (B) Hematoxylin and eosin staining of lesional skin presenting the infiltration of inflammatory cells. The inflammatory infiltrate dominated by neutrophils (black arrows) and eosinophils (light blue arrows) is characteristic for LcV. Neutrophils that transmigrate through the vessel wall (red arrow) cause destruction and interspersion of the vessels which results in an increased vascular permeability, accompanied by the extravasation of red blood cells (green arrows).

6.2 Circulating NPAs and plasma levels of catG are severely increased in patients with LcV

During the multistep cascade of neutrophil migration, a potent role for platelets has already been reported in the activation of neutrophils. Platelets are required for neutrophil recruitment to the site of inflammation and for the efficient adhesion of neutrophils to the vascular endothelium [5, 6]. Many vascular diseases, including sickle cell disease, the Kawasaki syndrome, angina pectoris and atherosclerosis are associated with increased numbers of circulating NPAs [50-53]. To clarify a putative involvement of neutrophil-platelet interaction in IC-mediated inflammation, we initially studied the abundance of NPAs in the whole blood of healthy volunteers and patients that were clinically and histologically diagnosed with LcV. Therefore, whole blood of healthy volunteers and affected patients was collected and fluorescent stained for neutrophils (CD16) and platelets (CD41) (Figure 6-1 A). Neutrophils alone or in aggregation with platelets were gated according to their granularity,

size and expression of CD16 and revealed about 90% purity by means of flow cytometry. Collected events, that were positive for CD16 and platelet marker CD41, were supposed to be NPAs as described previously [139]. Analysis of 20 LcV patients and 16 healthy donors revealed a significant and more than 2-fold increase in the percentage of NPAs in the patient's blood compared to the healthy control ($p < 0.03$). Hereby, healthy volunteers showed 3.3 ± 0.5 % while patients with LcV revealed 7.5 ± 1.7 % of circulating NPAs (Figure 6-2 A, B). Thus, in accordance with other studies, analyzing the role of NPAs in vascular inflammation, we assume an important contribution of NPA formation also in the progression of LcV [50-53]. Notably, patients that suffer from petechial skin diseases without the involvement of neutrophils, like the purpura pigmentosa progressiva (PPP), show a percentage of NPAs in the circulation, as seen in the control group (Figure 6-2 B) [60]. Compared to healthy donors, that form 3.3 ± 0.5 % of circulating aggregates, patients with PPP show 3.7 ± 0.4 % NPAs in their whole blood. Thus, the formation of NPAs seems not to be a specific marker for all vascular inflammatory disorders, but may indicate neutrophil-dependent vascular inflammatory diseases, such as LcV. Furthermore, the formation of NPAs is not important for the development of petechial bleeding per se, since cutaneous bleeding occurs also in the absent of neutrophils or NPAs.

CatG is a protease that is stored in the azurophilic granula of neutrophils and is released upon degranulation. Besides its crucial contribution to coagulation and degradation of microorganisms, catG is also an important mediator in inflammation [137]. Previous studies demonstrate that catG is especially important for the FcγR-induced interaction of neutrophils with ICs in *neutrophil elastase*- and *catG*-deficient mice during the RPA [137]. To further estimate the effect of catG on the progression of IC-mediated inflammation, we aimed to quantify catG activity in the circulation of the LcV patient cohort and the healthy control group. Therefore, plasma was generated from human whole blood of LcV patients and healthy volunteers and was further analysed for catG protein levels using a Cathepsin G Activity Assay Kit. As a result, we detected a 5.5-fold elevated catG protein level in the plasma of LcV patients compared to the healthy control. In patients suffering from LcV, we detected 0.1 ± 0.03 mU/ml active catG, while healthy propands show 0.02 ± 0.01 mU/ml catG in their plasma (Figure 6-2 C). According to these results, we assumed an important contribution of the neutrophil-derived serine protease, catG, in IC-mediated vascular

inflammation. However, the specific effect of the protease has still to be elucidated. As a next step, we therefore aimed to analyze a potential effect of catG on the activation of platelets and subsequently their ability to form aggregates with neutrophils. Further, we speculate that catG-induced activation of platelets is mediated via PAR_4 on platelets. In the following, we treated platelets with either the PAR_4 antagonist, P4pal10, or DMSO control and stimulated them with or without platelets. The subsequent co-incubation with neutrophils was analysed for the ability of activated and non-activated platelets to form heterotypic aggregates with neutrophils, and whether PAR_4 is involved in the formation of these aggregates.

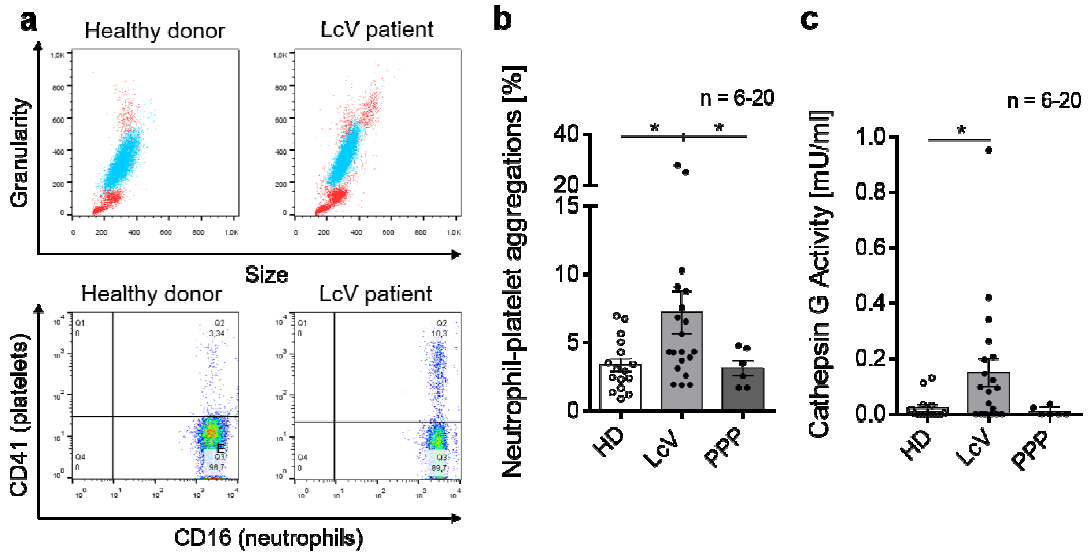

Figure 6-2 Circulating NPAs and plasma catG levels in LcV patients are dramatically increased compared to healthy controls (A) Flow cytometric analysis of human whole blood of a representative healthy volunteer and LcV patient was stained for neutrophils (CD16) and platelets (CD41) to analyze their heterotypic cell interactions. (B) *Ex vivo*, the abundance of NPAs in the whole blood was analysed in healthy volunteers (n = 16), patients with LcV (n = 20), and patients with petechial skin diseases without neutrophil involvement (n = 6; Purpura pigmentosa progressiva). (C) Plasma levels of catG measured in healthy control and patients that were clinically and histopathologically diagnosed as LcV (C). Mann-Whitney U test was performed to evaluate significant differences (*p<0.05, **p<0.01). Results are presented as mean values ± SEM. HD, healthy donor; LcV, leukocytoclastic vasculitis; PPP, purpura pigmentosa progressive.

6.3 CatG-mediated PAR4 activation causes increased formation of NPAs *in vitro*

Our clinical findings revealed significantly increased numbers of circulating NPAs as well as elevated plasma levels of catG protein in patients with LcV compared to healthy donors. On their surface, platelets express the thrombin receptor PAR_4, that is also a target

receptor for catG. Since there is only little understanding about the catG-mediated activation of PAR_4 on platelets, we aimed to evaluate the effect of the catG/PAR_4-axis on the regulation and formation of NPAs. Therefore, isolated platelets obtained from the whole blood of human healthy donors were pre-treated for 30 minutes with either DMSO or PAR_4 antagonist, P4pal10, and were subsequently stimulated briefly with 10 mU/ml of catG or remained unstimulated. Next, stimulated and unstimulated platelets were co-incubation with isolated human neutrophils for a short period. Finally, the reactions were fixed and cell mixtures were stained for neutrophils (CD16) and platelets (CD41) and analyzed for their heterotypic aggregation. Neutrophils were identified according to their granularity, size and their surface expression of CD16 and revealed about 90 % purity by means of flow cytometry. Aggregations of neutrophils with platelets were determined by double-positive staining for CD16 (neutrophils) and CD41 (platelets) (Figure 6-3 A, B).

Upon stimulation of DMSO-treated platelets with catG, we detected an increased ability of platelets to form aggregates with neutrophils compared to unstimulated platelets (Figure 6-3 A). In the representative samples as depicted in Figure 6-3 A, we measured 4.9 % of NPAs in the absence of catG and 33.3 % of heterotypic interactions with catG-stimulated platelets. For in total n = 5 donors we measured 5.3 ± 0.5 % of heterotypic aggregates with unstimulated platelets, while the addition of catG to platelets increases the NPA formation by 8-fold, up to 41.2 ± 11.1 % (Figure 6-3 C). These data clearly indicate an important impact of catG on platelets to get activated and consequently interact with healthy unstimulated neutrophils *in vitro*. Next, we hypothesized that the inhibition of PAR_4 by the P4pal10 antagonist abolishes the catG-mediated interaction of platelets with neutrophils. Upon stimulation of P4pal10-treated platelets with catG, we only detected a trend of platelets to form aggregates. Quantification of NPAs after P4pal10 treatment as depicted in Figure 6-3 B revealed 6.2 % of NPAs with non-stimulated platelets, while the addition of catG to platelets showed 20.1 % of aggregates. In total for n = 5 donors after P4pal10 treatment, we detected 8.2 % ± 1.6 of NPAs with unstimulated platelets, whereas the addition of catG to platelets revealed 17.6 % ± 5.2 of NPAs on average (Figure 6-3 C). These data clarify that pharmacologic inhibition of PAR_4 for 30 minutes does not abolish the formation of NPAs completely. However, as expected, inhibition of the PAR_4 receptor on platelets severely down-regulates the increase in NPAs observed with DMSO-treated platelets after catG

stimulation. Here, we detected 33 % heterotypic aggregations in the absence of P4pal10, while in the presence of the antagonist only 20.1 % of NPAs were measured (Figure 6-3 B, C). In total for all tested donors, stimulation with catG showed a 2-fold decreased ability of P4pal10-treated platelets to form aggregates with neutrophils compared to DMSO-treated platelets (Figure 6-3 C). P4pal10 treatment of platelets showed 17.6 % ± 5.2 of NPAs after catG stimulation, while the control platelets revealed 41.2 % ± 11.1 of heterotypic cell interactions (Figure 6-3 C). Herein, we described for the first time, that the ligand-receptor interaction between catG and the PAR_4 receptor plays a crucial role in the heterotypic interaction between human platelets and neutrophils *in vitro*. Since, NPAs are identified in several vascular inflammatory diseases, our data might indicate an important contribution of the catG/PAR_4-axis in NPA-associated vascular inflammation, such as LcV [50-53]. To test this hypothesis, we sought to analyze edema formation and neutrophil tissue infiltration using an *in vivo*-model of IC-mediated vasculitis in wild type mice as well as mice deficient for PAR_4, 4 h post IC-challenge.

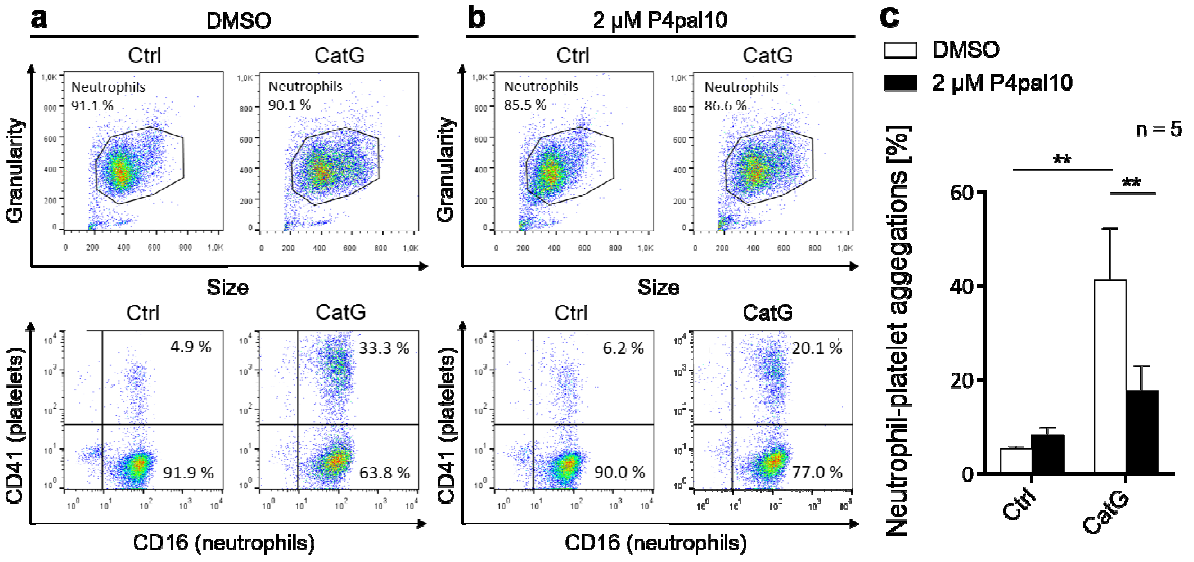

Figure 6-3 CatG-mediated PAR_4 activation increases the formation of NPAs *in vitro*. Flow cytometric analysis of heterotypic aggregations between (A) DMSO- or (B) PAR_4 antagonist (P4pal10)-treated platelets (CD41) with neutrophils (CD16). The ability of platelets to form aggregates was analysed upon stimulation with or without catG. (C) Abundance of NPAs after co-incubation of human neutrophils with non- or catG-stimulated platelets in the presence or absence of a PAR4 antagonist (P4pal10) for in total n = 5 donors. For statistical analysis Mann-Whitney U test and 2^{way} ANOVA was used (*p<0.05, **p<0.01). Results are presented as mean values ± SEM of n = 5 tested healthy donors. DMSO, Dimethyl sulfoxide; Crtl, control; catG, cathepsin G.

6.4 Role of PARs in cutaneous IC-mediated inflammation

6.4.1 IC-mediated inflammation causes cutaneous hemorrhage in the area of inflammation in *Par4*$^{-/-}$ mice

The IC-mediated inflammation is characterized by increased neutrophil infiltration and edema formation in the area of cutaneous inflammation in wild type mice [139, 140]. Previous results already confirmed an important role of the platelet PAR_4 in the formation of human NPAs *in vitro* (Figure 6-3), indicating an important pro-inflammatory function of this receptor in the activation of neutrophils. Furthermore, the thrombin-mediated activation of PAR_4 has been shown to induce the recruitment of neutrophils to the site of vascular injury in a murine endothelial injury model [98]. Furthermore, mice deficient for PAR_4 display attenuated microvascular inflammation, including both platelet and leukocyte rolling and adhesion in a murine model of stroke [111]. However, the contribution of PAR_4 in the cutaneous IC-mediated inflammation has not been elucidated so far. Therefore, we quantified in an *in viv*o-model of vasculitis, namely the RPA, edema formation and neutrophil infiltration within the skin of wild type mice as well as mice deficient for PAR_4, 4 h post IC-challenge. Briefly, the RPA is induced in mice by intravenous injection of BSA/Evans blue and followed by intradermal injection of anti-BSA into the back skin. To initially evaluate the IC-mediated inflammation in the skin of wild type and knockout mice, we took a picture of the inner surface of the prepared back skin 4 h after the initiation of RPA. The representative pictures of prepared back skin specimens of wild type and knockout mice, as depicted in Figure 6-4 A, indicated a massive edema formation (dotted circles), as reflected by the blue coloration due to Evans blue leakage from damaged blood vessels to skin tissue. Furthermore, petechial bleeding, the main clinical hallmark of IC-mediated vasculitis, visualized in the inflamed areas of wild type and knockout mice, indicating a comparable clinical outcome between human LcV and murine induced IC-mediated inflammation. Interestingly, *Par4*$^{-/-}$ mice additionally show a massive hemorrhage in the area of the inflammation that is more concentrated to the center of the spot around the needle puncture and that is absent in healthy skin and in wild type mice (Figure 6-4 A). These findings indicated a trend towards an excessive and prolonged bleeding of *Par4*$^{-/-}$ mice during vascular inflammation.

Hematoxylin and eosin staining of the inflamed skin biopsies of wild type and knockout mice (Figure 6-4 B), confirms the large edema formation in the wild type and knockout back skin after 4 h of RPA (Figure 6-4 A, dotted circles). Along, we detected a robust thickening of the dermis apical of the subcutaneous tissue and muscle layer (Figure 6-4 B, RPA). Furthermore, the hematoxylin and eosin stained inflamed skin sections of wild type and knockout mice represent a vast inflammatory infiltrate in the thickened dermis and beneath the muscle layer of the inflamed biopsies when compared to the healthy control skin (Figure 6-4 B, black arrows). Taken together, the cutaneous infiltration of inflammatory cells in wild type and *Par4*$^{-/-}$ mice was in line with the results obtained from affected skin biopsies of patients with LcV (Figure 6-1 B). In contrary to our expectations, histological analysis revealed an equal reflection of inflammatory cell infiltration as well as dermal thickening in wild type and *Par4*$^{-/-}$ mice, indicating no significant contribution of PAR_4 in the progression of IC-mediated cutaneous inflammation. To further characterize, whether neutrophils form the dominant cell type during cutaneous IC-mediated inflammation in mice, we performed specific immunofluorescent staining for neutrophils (histological marker: Ly6G) (Figure 6-5 C). Immunofluorescent staining for macrophages (histological marker: mac-2) (Figure 6-6 A) and T cells (histological markers: CD4, CD8) (Figure 6-6 B) were done to give further detail about the composition of the inflammatory infiltrate in the affected skin of wild type and knockout mice.

During IC-mediated inflammation neutrophils cause the destruction of the endothelium that was associated with increased permeability and subsequent extravasation of erythrocytes to the side of tissue inflammation [54, 57]. These petechial bleedings were also detected in the inflamed back skin of wild type mice (Figure 6-4 B, green arrow) 4 h post RPA. In the inflamed skin of PAR_4 deficient mice we confirmed an excessive bleeding as designated in Figure 6-4 B (yellow arrow) that was also detected in the representative picture of the inner surface of the skin of *Par4*$^{-/-}$ mice (Figure 6-4 A). The massive haemorrhage, detected in the inflamed skin of PAR_4 deficient mice, supports the hypothesis of an ineffective coagulation response leading to prolonged bleeding duration until wound occlusion after tissue destruction [106]. In a next step, we aimed to quantify the abundance of erythrocytes in the inflamed skin of wild type and PAR_4 deficient mice compared to healthy skin by depicting the tissue contents of hemoglobin (Figure 6-7 A). Furthermore, we

sought to analyze whether the defect in coagulation reported for *Par4*$^{-/-}$ mice is responsible for an enhanced endothelial permeability that causes increased neutrophil infiltration upon inflammation in *Par4*$^{-/-}$ mice. By inducing vascular leakage in wild type and knockout mice and subsequent quantification of edema formation and neutrophil infiltration we aimed to clarify this hypothesis (Figure 6-7 B, C).

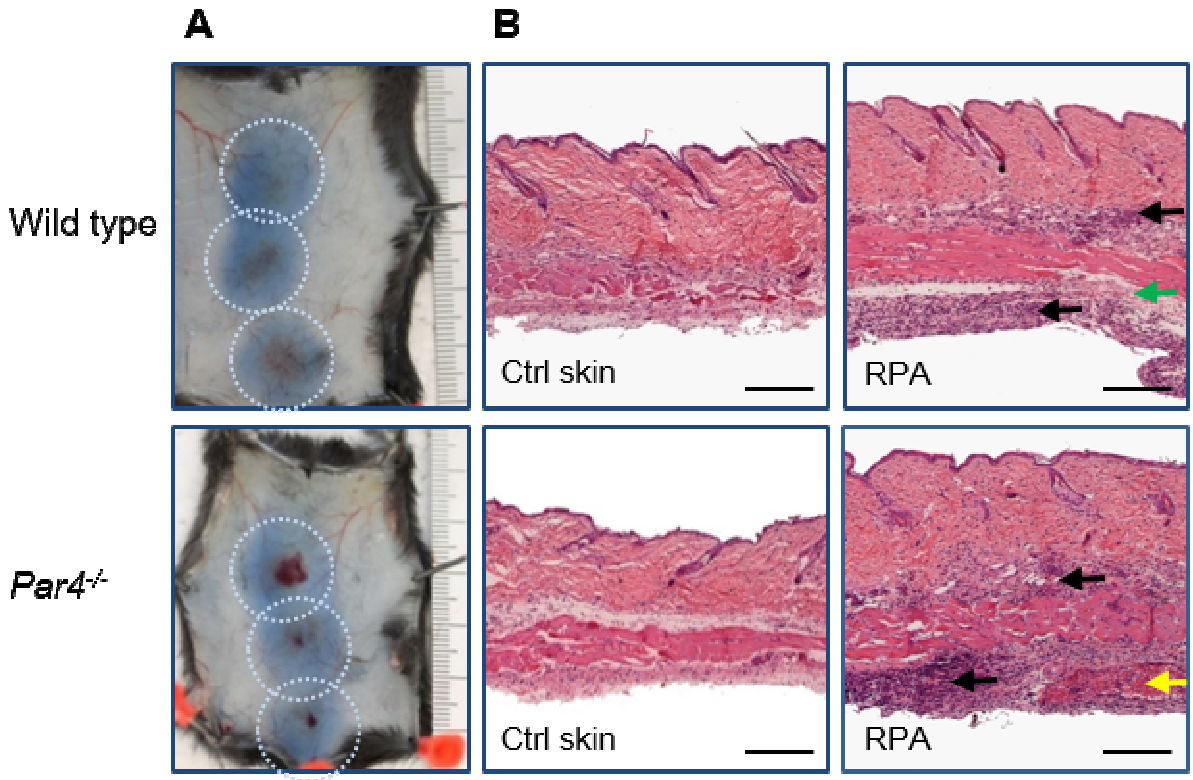

Figure 6-4 IC-mediated inflammation causes a massive cutaneous hemorrhage in the area of inflammation *Par4*$^{-/-}$ mice. (A) Representative murine back skin of wild type and knockout mice 4h after RPA induction (dotted circles). The blue color represents the Evans blue leakage as an indicator of vascular permeability in the skin. (B) H&E staining of a control and inflammatory spots of wild type and knockout mice, the latter reveals massive infiltration of inflammatory cells. Crtl, control; RPA, reverse passive Arthus reaction. Bar = 500 µm.

6.4.2 PAR_4 deficiency does not protect mice against IC-mediated inflammation

Our initial histological analysis of RPA skin biopsies of wild type and knockout mice revealed a marked increase in edema formation. Subsequently, we aimed to more specifically quantify the effect of IC-mediated vascular inflammation on edema formation by measuring the weight of 8 mm punches of inflamed and control biopsies of mice 4 h post IC-challenge. Furthermore, we sought to analyse a putative role of PAR_4 in edema formation and compared the weight of inflamed and control skin of wild type to *Par4*$^{-/-}$ mice. We confirmed that edema formation in wild type and *Par4*$^{-/-}$ mice is severely altered in the inflamed areas

(lesional skin) on the back skin (Figure 6-5 A). Compared to the healthy control skin, we detected a marked increase of the biopsy weight of wild type and *Par4*$^{-/-}$ inflamed skin, albeit no significant difference in the biopsy weight taken from wild type and knockout mice was observed (Figure 6-5 A). In wild type mice, we detected an increase of 17.1 ± 1.2 mg and in *Par4*$^{-/-}$ 18 ± 1.3 mg biopsy weight after 4 h post IC-mediated cutaneous inflammation. Based on these findings PAR_4 seems not to have a significant contribution to the formation of edema during IC-mediated vascular inflammation.

Our hematoxylin and eosin staining of the inflamed murine skin biopsies of wild type and *Par4*$^{-/-}$ mice revealed a massive infiltration of inflammatory cells, that was absent in the healthy vehicle-treated skin. Since the IC-mediated inflammation is mainly characterized by a vast infiltration of neutrophils into the skin, we next proceeded to quantify neutrophil abundance in RPA skin biopsies by quantifying the abundance of myeloperoxidase (MPO), an intracellular leukocyte marker. Moreover, we sought to investigate whether PAR_4 has a significant contribution in neutrophil tissue infiltration during IC-mediated inflammation. Therefore, collected inflamed and control skin biopsies of wild type and *Par4*$^{-/-}$ mice were homogenized, digested and subsequently MPO activity was quantified as a measure of TMB breakdown. As shown in Figure 6-5 B, we detected robust MPO signals in the inflamed skin of wild type and *Par4*$^{-/-}$ mice that lacked regulation when the experimental groups were compared. MPO signals were about 2.1 ± 0.3 mU in wild type and 2.0 ± 0.2 mU in *Par4*$^{-/-}$ mice inflamed skin after 4 h of IC-mediated inflammation. According to these data, we assumed that PAR_4 does not contribute to neutrophil infiltration, characterized by MPO release, during cutaneous IC-mediated inflammation.

In a next step, we aimed to validate the prevalence of neutrophils as the dominant inflammatory cell type in the inflamed skin of wild type and *Par4*$^{-/-}$ mice 4 h post RPA. Therefore, sections of inflamed and control skin of both experimental mice groups were immunofluorescently stained for the neutrophil marker, Ly6G in addition to MPO. Histological examination revealed a massive abundance of $Ly6G^+/MPO^+$ cells in the inflamed skin of both wild type and *Par4*$^{-/-}$ mice (Figure 6-5 C). In contrast, $Ly6G^+/MPO^+$ staining was absent in the control skin of wild type and knockout mice (Figure 6-5 C). Thus, in accordance with our expectations and as designated in skin biopsies of LcV patients (Figure 6-1 B), we confirmed MPO-releasing neutrophils as the main inflammatory cell type in the inflamed

skin of wild type and *Par4*$^{-/-}$ mice after 4 h of IC-mediated inflammation. However, the abundance of Ly6G^{+}/MPO^{+} neutrophils did not significantly differ between the inflamed tissues of wild type and *Par4*$^{-/-}$ mice, as it has already been detected by measuring the MPO activity in tissue biopsies of both experimental groups. These findings suggest that PAR_4 deficiency does not protect mice against neutrophil tissue infiltration and degranulation during IC-mediated vascular inflammation. Hence, other receptors rather than PAR_4 might be responsible for neutrophil transmigration during IC-mediated vascular inflammation at least in mice. In the following, we further aimed to specify the inflammatory infiltrate in the skin of wild type and *Par4*$^{-/-}$ mice and analyzed the inflamed and control skin biopsies for their abundance of mac-2^{+}/MPO^{+} macrophages and CD4^{+}CD8^{+} T cells.

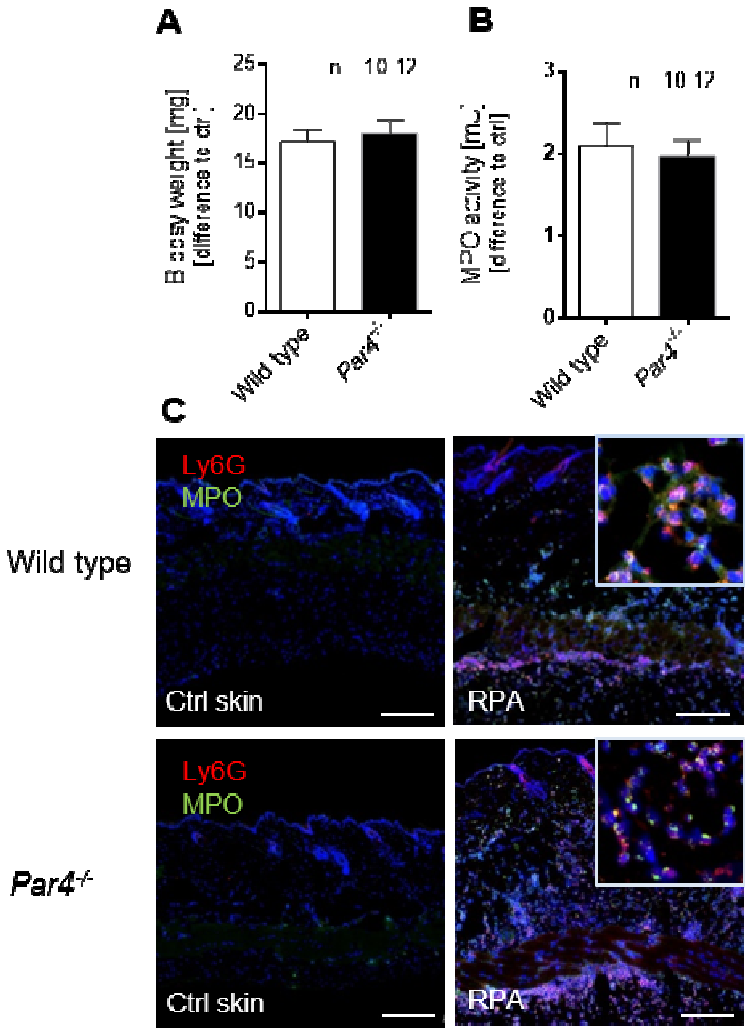

Figure 6-5 Mice with a PAR_4 deficiency are not protected against IC-mediated cutaneous inflammation. Edema formation (A, biopsy weight) and neutrophil infiltration (B, MPO activity) during 4 h of IC-mediated inflammation. Mann-Whitney U test was performed to evaluate significant differences (*p<0.05, **p<0.01). Data are presented as mean values ± SEM of relative increase to healthy control skin (n = 3-9 mice per group. Representative images of murine skin biopsies of wild type and knockout mice immunofluorescent stained for Ly6G (red) and MPO (green) (C). Crtl, control; RPA, reverse passive Arthus reaction. Bar = 200 µm.

6.4.3 IC-mediated cutaneous inflammation induces low MPO^+ macrophages tissue infiltration in wild type and *Par4*$^{-/-}$ mice

As reported above, RPA skin biopsies, especially those of wild type and *Par4*$^{-/-}$ mice, contain increased levels of MPO. Additional immunofluorescence analysis demonstrated a vast infiltration MPO-positive neutrophils into the sites of the inflamed skin. In IC-mediated cutaneous inflammation, neutrophils are known to act as the central players, mediating the progression of cutaneous inflammation [54, 57]. Besides neutrophils, a putative role for

macrophages as well as T cells has been reported for several inflammatory skin diseases, including psoriasis and atopic dermatitis [141-145]. Psoriasis is a chronic T_H17-driven inflammation that is characterized by epidermal hyperproliferation in combination with cellular infiltration, while atopic dermatitis is a chronic T_H2-dominated inflammatory skin disease associated with pruritus [141-145]. In both skin diseases, increased numbers of macrophages as well as $CD4^+$ and $CD8^+$ T cells were detected in the lesional skin, and are known to play an important function in the progression of the inflammation [146-151]. Here, we aimed to analyze whether macrophages and T cells might have a pro-inflammatory role in vasculitis and whether their recruitment to the site of cutaneous inflammation was regulated by PAR_4. In a first step, we investigated the abundance of macrophages (histological marker: mac-2) and T cells (histological markers: CD4/CD8) utilizing immunofluorescence techniques on skin samples from wild type and knockout mice that were challenged for 4 h with ICs. Additional staining for MPO was performed in a double-immunofluorescence procedure in combination with mac-2, since MPO is an enzyme that is, besides neutrophils, also stored in macrophages.

Histological examination revealed a low abundance of mac-2^+/MPO^+ cells (Figure 6-6 A, yellow arrows) in the inflamed skin of wild type and *Par4*$^{-/-}$ mice, albeit no difference between both experimental groups was detected. However, control sections of both wild type and *Par4*$^{-/-}$ mice were completely absent of mac-2^+/MPO^+ cells (Figure 6-6 A). These findings indicate a low contribution of mac-2^+/MPO^+ macrophages in the progression of IC-mediated inflammation in mice and suggest that PAR_4 has no significant contribution to macrophage tissue infiltration during IC-mediated vascular inflammation.

Immunofluorescent staining for CD4 and CD8 revealed no T cell infiltration in the control as well as the inflamed skin of wild type and *Par4*$^{-/-}$ mice (Figure 6-6 B). As expected $CD4^+CD8^+$ T cells seem not to contribute to tissue inflammation during IC-mediated vascular disorders.

In summary, we confirmed a low implication of mac-2^+/MPO^+ macrophages accompanied by the dominant contribution of infiltrated neutrophils as a key mediator in the progression of IC-mediated inflammation. However, the infiltration of both cell types is not regulated by PAR_4 activity, indicating no contribution of the receptor in either neutrophil

nor magrophage recruitment during IC-mediated vascular inflammation at least in the murine system (Figure 6-5 B; Figure 6-6).

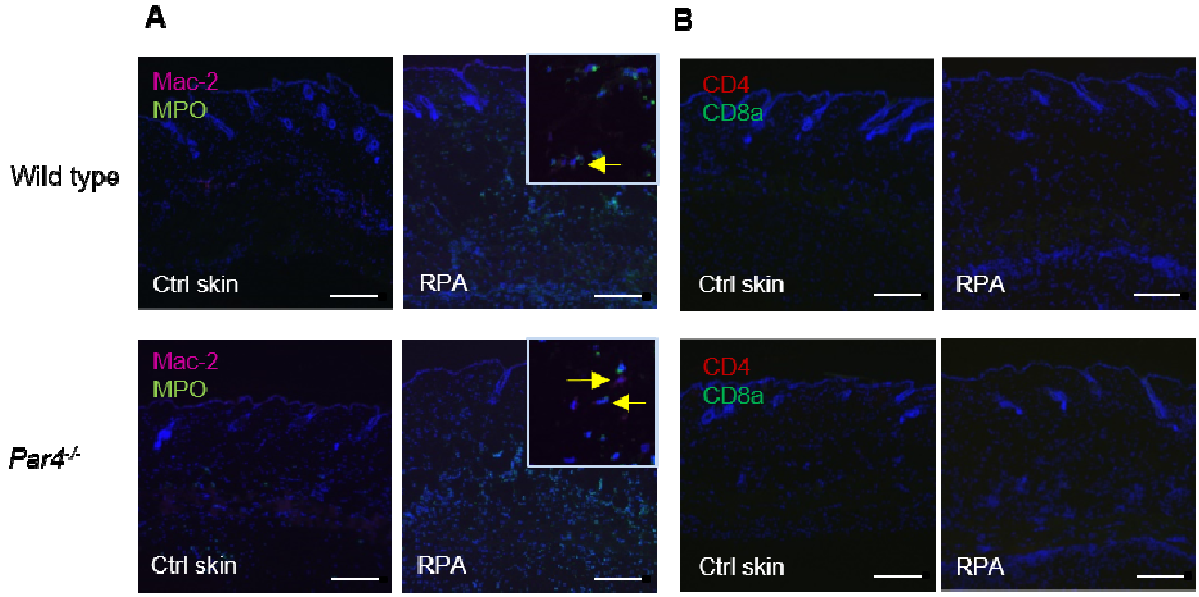

Figure 6-6 IC-mediated cutaneous inflammation induces low MPO$^+$ macrophages tissue infiltration in wild type and *Par4*$^{-/-}$ mice. Representative images of wild type and knockout skin biopsies that were stained using immunofluorescence for (A) Mac-2 (magenta) and MPO (green) positive macrophages and (B) CD4 (red) and CD8 (green) positive T cells. Crtl, control; RPA, reverse passive Arthus reaction. Bar = 200 µm.

6.4.4 Bleeding phenotype of *Par4*$^{-/-}$ mice causes no passive infiltration of neutrophils

Compared to human platelets, murine platelets only express PAR_4 to mediate thrombin responses and lack the PAR_1 receptor [104]. Consequently, platelets of *Par4*$^{-/-}$ mice showed no response to thrombin signaling, which dramatically affects their coagulation response [70, 103, 104]. In a tail bleeding assay, PAR_4 deficient mice displayed a six-fold increased bleeding duration when compared to wild type mice, supporting the hypothesis of an ineffective coagulation response that results in a prolonged time until wound occlusion after tissue traumata occurs [106]. In accordance with this hypothesis, our *in vivo* model of IC-mediated inflammation, revealed an increased cutaneous bleeding into the skin of *Par4*$^{-/-}$ mice (Figure 6-4 A). In a next step, we aim to quantify the detected cutaneous bleeding in RPA-treated tissue samples obtained from wild type and *Par4*$^{-/-}$ mice, by depicting the content of hemoglobin that transferred from blood to skin (Figure 6-7 A). Therefore,

collected biopsies of the inflamed and control skin were homogenized and the supernatant was analyzed for hemoglobin levels using a Hemoglobin Mouse ELISA kit.

As a result, we demonstrated that hemoglobin levels are significantly altered in the inflamed skin of wild type and *Par4*$^{-/-}$ mice 4 h post IC-initiated inflammation compared to the healthy control skin. For n = 6 wild type mice we detected 306.2 ± 36.2 µg/ml of hemoglobin protein in the inflamed tissue, compared to 99 ± 13.4 µg/ml that were found in the control skin (Figure 6-7 A). In addition, we measured 823.7 ± 194.2 µg/ml of hemoglobin protein in the inflamed skin of n = 5 *Par4*$^{-/-}$ mice, while the control skin contained only 87 ± 16.7 µg/ml of protein (Figure 6-7 A). Taken together, these data confirm the ability of IC-mediated inflammation to induce petechial bleeding in the skin of both wild type and *Par4*$^{-/-}$ mice, the main clinical hallmark that is also detected in the affected skin areas of LcV patients, (Figure 6-1 A, B).

Our previous results revealed a massive hemorrhage in the area on cutaneous inflammation in *Par4*$^{-/-}$ mice (Figure 6-4 A, B). This excessive bleeding is completely absent in wild type mice and healthy control skin (Figure 6-4 A, B), indicating an increased trend towards excessive and prolonged bleeding in *Par4*$^{-/-}$ mice during vascular inflammation. Herein, we investigated 2.7-fold increased protein levels of hemoglobin in the inflamed skin *Par4*$^{-/-}$ compared to wild type mice (wild type: 306.2 ± 36.2 µg/ml; *Par4*$^{-/-}$: 823.7 ± 194.2 µg/ml) 4 h post IC-challenge (Figure 6-7 A). These data clearly confirm the ability of IC-mediated inflammation to induce a more intensified bleeding response in the inflamed skin of *Par4*$^{-/-}$ compared to wild type mice.

It could be speculated that the defect in coagulation reported for *Par4*$^{-/-}$ mice, might already be responsible for an increased vascular permeability that subsequently could facilitate neutrophil diffusion into the skin of *Par4*$^{-/-}$ mice. To test this hypothesis, vascular leakage was induced in *Par4*$^{-/-}$ mice and wild type mice by intradermal injection of the vasodilator, histamine. As a negative control, the solvent PBS was injected into the back skin and *in vivo* application of Evans blue allowed visualization of the vascular leakage. Intradermal injection of neither histamine (Figure 6-7 B, dotted red circles) nor PBS (Figure 6-7 B, dotted blue circles) revealed a prominent erythrocyte extravasation into the skin of wild type or *Par4*$^{-/-}$ mice as depicted in the representative picture in Figure 6-7 B. This outcome indicated that needle trauma (PBS) as well as vascular permeability (histamine)

were not sufficient to induce petechial bleeding in wild type, but also in mice with a coagulation defect, like *Par4*$^{-/-}$ mice.

To quantify whereas this *in vivo*-model induces any inflammatory response including edema formation and neutrophil tissue infiltration, we measured the weight of 8 mm biopsies and the MPO tissue activity, respectively, in the affected skin areas of wild type and *Par4*$^{-/-}$ mice as described before in section 6.4.1. As a result, we detected that compared to PBS injection, injection of histamine triggered a slight increase in edema formation in both groups, albeit no significant difference in the biopsy weight taken from wild type and knockout mice was observed (Figure 6-7 C). In total for n = 7 wild type mice, we measured a biopsy weight of 17.9 ± 1.2 mg in the PBS control, while application of histamine increases edema formation only up to 21.2 ± 1.2 mg (Figure 6-7 C). In n = 4 *Par4*$^{-/-}$ mice, we investigated a biopsy weight of 16.3 ± 2.6 mg in the PBS control, whereas histamine injection revealed edema formation of 19.0 ± 3.2 mg (Figure 6-7 C). These data confirm that histamine induces a less intensive edema formation in both wild type and *Par4*$^{-/-}$ mice, compared to IC-challenge as depicted in (Figure 6-5 A). Upon histamine injection, we detected an increase in edema formation of 3.3 mg in both experimental groups, while treatment of wild type and *Par4*$^{-/-}$ mice with ICs induces an increase of 17 mg and 18 mg, respectively (Figure 6-5 A).

Next, we sought to investigate whereas the induction of a needle trauma or vascular permeability causes a passive efflux of neutrophils into the skin of wild type and *Par4*$^{-/-}$ mice (Figure 6-7 D). Infiltration of neutrophils, assayed by MPO activity, was almost absent in the histamine and PBS treated spots of both groups. In n = 7 wild type mice, we detected 0.14 ± 0.03 mU of MPO in the skin after induction of vascular permeability, while 0.22 ± 0.08 mU of the protein were detected in the control skin (Figure 6-7 D). A similar outcome was detected in *Par4*$^{-/-}$ mice (n = 5) and revealed 0.15 ± 0.09 mU of MPO in the histamine and 0.13 ± 0.05 mU of the protein in the PBS treated spots (Figure 6-7 D). However, IC-induced cutaneous inflammation causes massive infiltration of neutrophils into the skin of wild type and *Par4*$^{-/-}$ mice as already reported before and as depicted in Figure 6-4 D. For n = 6 wild type mice, we detected 0.59 mU ± 0.03 of MPO in the control skin, while application of IC induced 2.26 ± 0.21 mU of MPO release at the site of inflammation. In *Par4*$^{-/-}$ mice (n = 5), we detected an increased MPO release from 0.58 ± 0.27 mU up to 2.47 ± 0.24 mU in the inflamed area of the skin. Altogether, these data display a massive neutrophil infiltration in both wild type and

Par4$^{-/-}$ mice 4 h post IC-challenge, but not after induction of vascular leakage or tissue trauma.

In summary, in accordance to our data neither histamine-induced vascular permeability nor the application of a needle trauma by PBS injection, caused edema formation and the influx of neutrophils into the skin of wild type and *Par4*$^{-/-}$ mice. This indicates that neutrophil migration out of the vessel wall into the tissue, accompanied by edema formation is more an active process, which requires inflammatory triggers to get activated, rather than a passive effect only caused by diffusion due to damage in the vessel wall. Nevertheless, the increased bleeding phenotype in IC-mediated inflammation in PAR_4-deficient mice may account for changes in the inflammatory infiltrate; mice are potentially not the best model to study the role of PAR_4 *in vivo*.

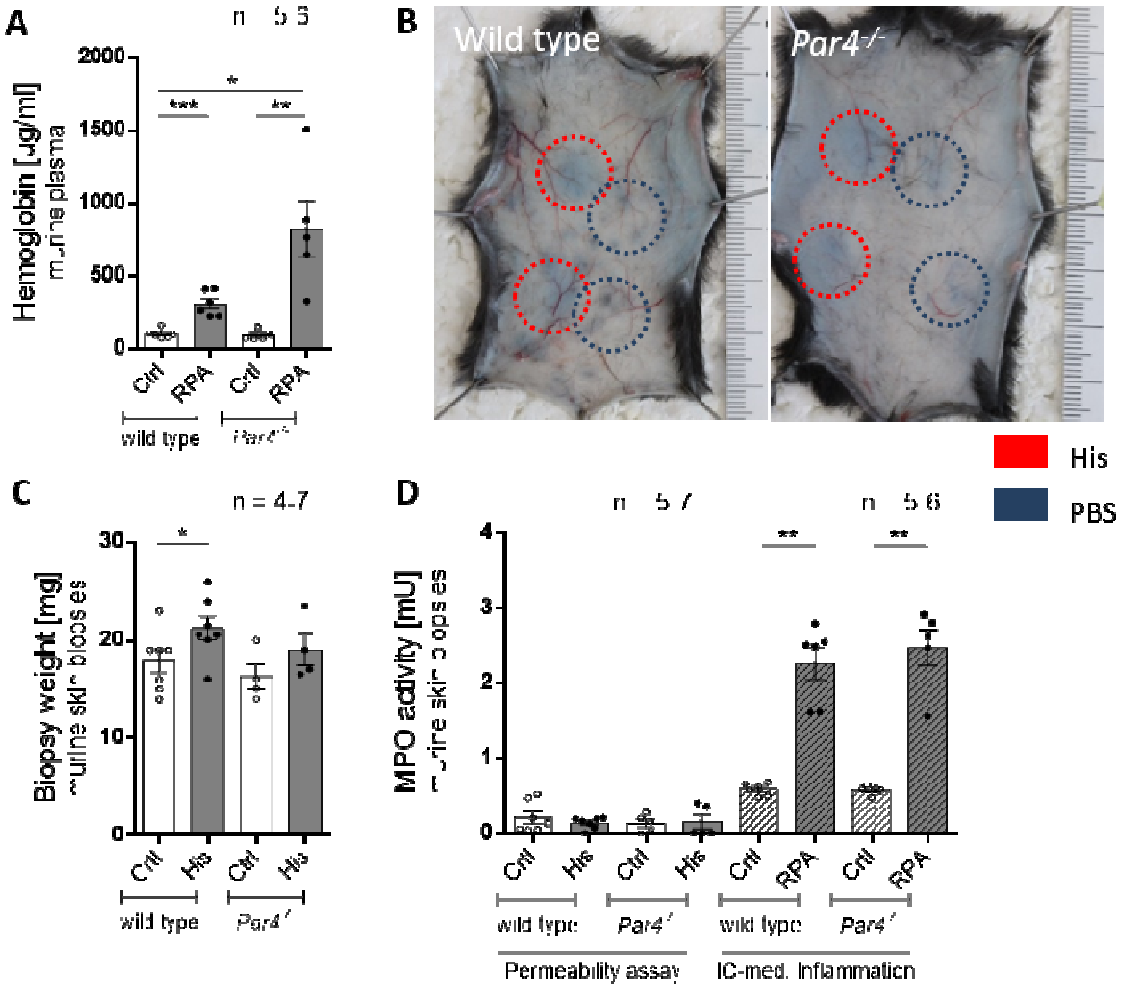

Figure 6-7 Cutaneous MPO activity in *Par4*$^{-/-}$ mice is not caused by passive neutrophil extravasation due to *Par4*$^{-/-}$ bleeding phenotype. (A) Quantitative measurement of hemoglobin in inflamed and control skin biopsies of wild type and *Par4*$^{-/-}$ mice. (B) Representative picture of wild type and *Par4*$^{-/-}$ mice after application of a needle trauma, by intradermal PBS injection (blue spot) and induction of vascular leakage, by intradermal histamine injection (white spots) compared to α-BSA/BSA administration, representing the IC-mediated inflammation. Investigation of (C) Edema formation (biopsy weight, 8 mm) and (D) neutrophil tissue infiltration (MPO activity) in wild type and *Par4*$^{-/-}$ mice 4 h post treatment. Mann-Whitney U test was performed to evaluate significant differences (*p > 0.05, **p > 0.01). Results are presented as mean values ± SEM. Crtl, control; RPA, reverse passive Arthus reaction.

6.4.5 PAR_4 deficiency reduces numbers of circulating NPA and increases plasma CatG levels in IC-mediated inflammation

As reported, interactions of neutrophils and platelets play an important role in many inflammatory vascular diseases, including sickle cell disease, the Kawasaki syndrome, angina pectoris and atherosclerosis [50-53]. All of these diseases are characterized by increased numbers of heterotypic interactions between neutrophils and platelets, a formation that is

required for efficient recruitment of the neutrophil to the site of inflammation and its firm adhesion to the vascular endothelium [5, 6]. In line with the literature, we detected a marked increase in circulating NPAs among our investigated cohort of 19 LcV patients, when compared to the healthy control group (Figure 6-8 B). To further examine whether circulating platelets are involved in the interaction with neutrophils during IC-mediated inflammation in vivo, NPAs from circulating blood of wild type and PAR4 knockout mice were analysed by flow cytometry, utilizing markers for neutrophils (Ly6G) and platelets (GP1b-α). Absolute numbers of neutrophils positive for the platelet-specific marker GP1b-α were measured in control and RPA wild type and Par4-/- mice and state events of neutrophil-platelet interaction.

As depicted in Figure 6-8 A, formation of NPAs was significantly increased by 2-fold 4 h post RPA-challenge in blood samples obtained from wild type mice when compared to the control group. In n = 9 IC-challenged wild type mice, we detected on average 213.2 ± 27.4 heterotypic interactions, while n = 13 control mice contained only 99.4 ± 11.2 NPAs (Figure 6-8 A). However, in *Par4*$^{-/-}$ mice no significant increase of circulating NPAs following IC-mediated inflammation was detected. *Par4*$^{-/-}$ mice (n = 9), that were challenged with ICs show on average 121.7 ± 10.0 NPAs, while the appropriate control group (n = 9) revealed 103.1 ± 16.1 aggregates (Figure 6-8 A). When comparing formation of NPAs in wild type and *Par4*$^{-/-}$ mice 4 h post IC-challenge, we detected a severe downregulation of NPAs by 1.7-fold in the knockout group, indicating a deficiency of *Par4*$^{-/-}$ mice to form aggregates of neutrophils and platelets. These data clearly confirm that IC-mediated inflammation is able to induce the formation of NPAs also in wild type mice after 4 h of RPA. In line with our patient's data, revealing increased formation of NPAs in LcV patients (Figure 6-2 A, B), these data indicate a crucial effect of neutrophil platelet interactions in the progression of IC-mediated vascular inflammation. Notably, aggregations of neutrophils with platelets were severely downregulated in *Par4*$^{-/-}$ mice after IC-mediated inflammation. This is in accordance with our *in vitro* data, that demonstrated an important contribution of PAR_4 in the catG-induced formation of NPAs (Figure 6-3 B, C). Therefore, this implies an important role of the receptor in the heterotypic interaction between neutrophils and platelets also in inflammation *in* vivo. In the following, we sought to analyze the contribution of catG in the progression of vasculitis *in vivo* in wild type and knockout mice.

Recent studies already reported an important role for catG in mediating inflammatory processes, including integrin clustering on neutrophils during IC-mediated inflammation [137]. In line with this data, we detected severely increased plasma levels of catG in the whole blood of patients with LcV compared to healthy volunteers (Figure 6-2 C), indicating an important role for the protease in the progression of IC-mediated inflammation. Here, we aimed to analyze whether catG concentrations were also increased in the *in vivo* model of IC-mediated vascular inflammation and whether a deficiency of PAR_4 might alter catG values during inflammation compared to wild type mice. Therefore, murine plasma of inflamed and control wild type and knockout mice was generated, and subsequently the protein levels of catG were determined using a Cathepsin G Activity Assay Kit.

As a result, plasma catG levels were increased in wild type mice by tendency, whereas *Par4*$^{-/-}$ mice show significantly increased plasma levels of the protease (Figure 6-8 B). In wild type mice (n = 9), we measured 0.005 ± 0.003 mU/ml of catG in control mice, while abundance of the protein was increased to 0.008 ± 0.004 mU/ml in mice 4 h post IC-challenge (Figure 6-8 B). In comparison, in untreated *Par4*$^{-/-}$ mice baseline catG levels of 0.0002 ± 0.0002 mU/ml were detected, which were significantly elevated up to 0.014 ± 0.007 mU/ml, after 4 h of RPA (Figure 6-8 B). Interestingly, IC-mediated inflammation induces a rise in plasma catG levels more strongly in knockout mice, compared to wild type (wild type: 0.008 ± 0.004 mU/ml; *Par4*$^{-/-}$ mice: 0.014 ± 0.007 mU/ml) Figure 6-8 B), which implies a crucial role of PAR_4 in the regulation of catG from neutrophils.

In line with our *ex vivo*-findings in patients with LcV, which revealed increased interaction between neutrophils and platelets as well as elevated plasma catG levels (Figure 6-2), we validated the formation of NPAs and increased plasma levels of catG as important markers during the progression of IC-mediated vasculitis also *in vivo*. Furthermore, we confirmed an essential role of PAR_4 in the formation of NPAs, since deficiency severely downregulated the heterotypic interaction *in vivo*. In accordance with that, we detected less catG-induced formation of aggregates, after blockage of the receptor *in vitro*, indicating that PAR_4 activation on platelets is important to induce interaction with neutrophils *in vivo* and *in vitro*. Additionally, the ability of IC-mediated inflammation to induce catG release more efficiently in *Par4*$^{-/-}$ compared to wild type mice, suggests an important contribution of PAR_4

in the regulation of catG release in the circulation. Now, the next step would be to investigate whether there was a direct effect of catG on the formation of NPAs in IC-mediated inflammation as well.

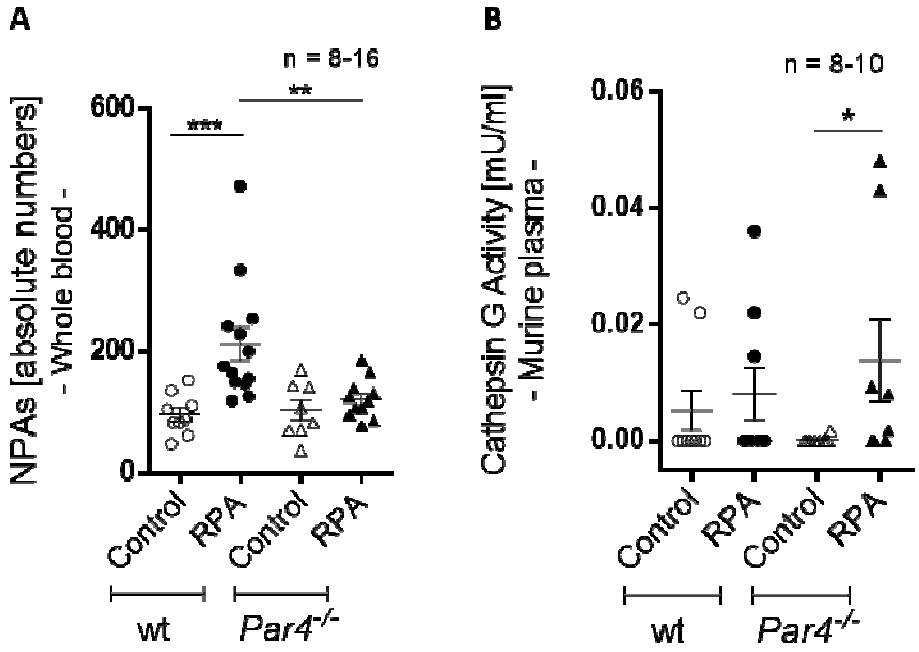

Figure 6-8 PAR_4 deficiency severely reduces numbers of circulating NPAs and increases the plasma CatG levels in a mouse model of IC-mediated inflammation. Murine whole blood of healthy control and mice with a RPA was collected and (A) stained for neutrophils (Ly6G) and platelets (GP1b-α) to investigate the number of NPAs or (B) analysed for plasma CatG activity. Mann-Whitney U test was performed to evaluate significant differences (*p<0.05, **p<0.01). Results are presented as mean values ± SEM. Crtl, control; RPA, reverse passive Arthus reaction.

6.4.6 IC-mediated vasculitis causes an increase of circulating granulocytes and monocytes whereas lymphocytes in wild type and PAR_4 knockout mice are dramatically decreased

Because the frequency of NPAs is increased in the circulation of LcV patients (Figure 6-2 A, B) and mice that were challenged with ICs (Figure 6-8 A), we analyzed the regulation of the abundance of inflammatory cell types in our *in vivo* model of vasculitis. We further, revealed less formation of NPAs in *Par4*$^{-/-}$ mice 4 h post IC-challenge and therefore sought to investigate potential differences in the distribution of inflammatory cells in the blood of wild type and *Par4*$^{-/-}$ mice. Therefore, murine whole blood of control mice and mice after RPA-challenge were analyzed for the total abundance of inflammatory cells, including granulocytes, monocytes and lymphocytes.

As depicted in Figure 6-9 A differential blood count analysis revealed an increased percentage of granulocytes by 2.4-fold in wild type and 1.9-fold in *Par4*$^{-/-}$ mice compared to baseline abundance that were about 12.9 ± 0.9 % of leukocytes in wild type mice, while the percentage increases upon the inflammatory trigger up to 31.4 ± 1.6 % (Figure 6-9 A). In comparison, untreated knockout mice show 19.6 % ± 1.4 granulocytes, whereas 4 h post IC-challenge percentage was raised up to 37.1 ± 3.1 % (Figure 6-9 A). In addition, the abundance of monocytes was severely elevated post IC-challenge in both experimental groups (Figure 6-9 B). Here, monocytes were increased by 2.1-fold in wild type mice, while knockout mice show 1.7-fold elevated percentages of circulating monocytes after 4 h of RPA-challenge. For wild type mice, we measured a baseline abundance of 3.0 ± 0.2 % monocytes and 6.4 ± 0.5 %after 4 h of IC-mediated inflammation (Figure 6-9 B). Untreated knockout mice showed 4.2 ± 0.5 % monocytes and 7.2 ± 0.4 % 4 h post IC-challenge (Figure 6-9 B). However, lymphocytes, especially T cells that form the most abundance inflammatory white blood cell in murine whole blood, were dramatically down-regulated during IC-mediated inflammation *in vivo* (Figure 6-9 C). Wild type mice that contain under normal homeostasis 84.1 ± 1.0 %lymphocytes show only 62.1 ± 1.8 % 4 h post IC-challenge (Figure 6-9 C). In *Par4*$^{-/-}$ mice baseline abundance of lymphocytes was about 76.2 ± 1.8 %, whereas 59.0 ± 1.7 % lymphocytes were detected in knockout mice after 4h of RPA-challenge (Figure 6-9 C).

Taken together, these findings confirm an important contribution of granulocytes and monocytes in IC-mediated inflammation in wild type and *Par4*$^{-/-}$ mice. In accordance with this outcome, our histological analysis of inflamed skin sections of wild type and *Par4*$^{-/-}$ mice revealed a massive infiltration of neutrophils accompanied by single macrophages. However, no T lymphocytes were abundant in the affected skin of both experimental groups. These observations suggest that inflammatory responses during IC-mediated vascular inflammations are mainly mediated by inflammatory cells of the innate immune system, rather than lymphocytes that are major cellular component of the adaptive immune response [152].

Interestingly, we detected remarkable differences between the baseline abundance of inflammatory cells between wild type and *Par4*$^{-/-}$ mice. In untreated *Par4*$^{-/-}$ mice the levels of granulocyte were significantly increased by +1.5-fold ($p < 0.01$) (Figure 6-9 A) and of monocyte by +1.4-fold ($p < 0.03$) (Figure 6-9 B), whereas lymphocyte levels were decreased

by -0.9-fold ($p < 0.01$) (Figure 6-9 C) compared to untreated wild type mice. Based on these data, we assume a defect for *Par4*$^{-/-}$ mice to regulate leukocyte abundance under normal homeostatic condition. However, it is unknown to what extent this defect leads to an increased incidence of disease so far.

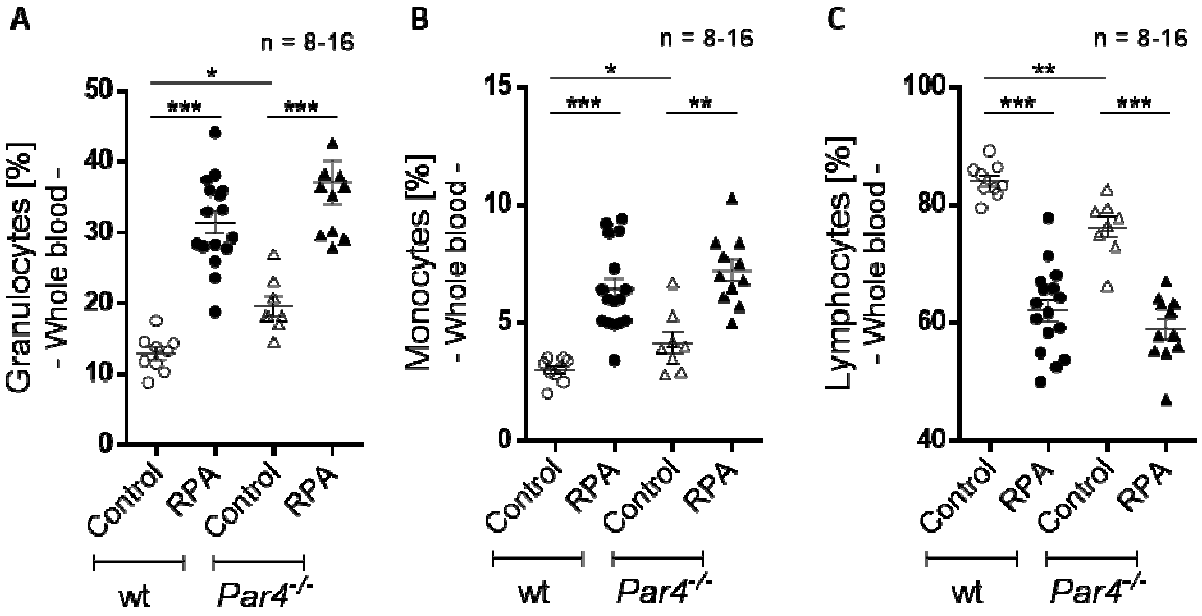

Figure 6-9 IC-mediated inflammation causes increased abundance of granulocytes and monocytes, while lymphocytes were severely decreased in wild type and *Par4*$^{-/-}$ mice. Percentage of (A) granulocytes, (B) monocytes and (C) lymphocytes in wild type and *Par4*$^{-/-}$ mice before and 4 h post IC-challenge. Mann-Whitney U test was performed to evaluate statistical differences (*$p > 0.05$, **$p > 0.01$). Results are presented as mean values ± SEM of n = 8-16 mice per group from at least three independent experiments. Crtl, control; RPA, reverse passive Arthus reaction.

6.5 CatG induces elevated surface expression of platelet P-selectin, GPIIIbIIa, GPVI, GPIII-β and GP1bα, independently from PAR_4 activation

In line with our previous results, we could demonstrate an activating effect of catG on freshly isolated human platelets *in vitro*. CatG-activated platelets immediately formed aggregates with freshly isolated neutrophils from the same donor (Figure 6-3 A, B). We therefore aimed to analyze the effect of catG on the activation status of isolated murine platelets as well as potential alteration in the expression of surface adhesion molecules on platelets. Platelets, that were activated are known to upregulate the surface expression of several adhesion molecules, including neutrophil PSGL-1 binding partner, P-selectin; Glycoprotein-1bα (GP1bα), a component of the von Willebrand receptor; and Glycoprotein-

IIbIIIa (GPIIbIIIa), the active form of the fibrinogen receptor. Surface molecules that are present persistently on platelets imply the collagen receptor Glycoprotein-VI (GPVI) and the inactive form of the fibrinogen receptor, Glycoprotein-III-β (GPIII-β), which is expressed on unstimulated platelets [153-156].

To investigate a potential effect of catG on platelet surface expression, murine platelets were stimulated dose-dependently with 0.01, 0.1 or 1 U/ml catG, respectively. Stimulation with 5 µM adenosine diphosphate (ADP) with or without U46, and 5 µg/ml collagen related peptide (CRP) served as positive controls, while unstimulated cells were used as a negative control. Because of the involvement of PAR_4 in NPA formation, we further aimed to investigate the receptors' role on the regulation of platelet surface adhesion molecule expression. In contrast to catG, only a single concentration of PAR_4 agonist (100 µM, AYPGKF-NH_2) was utilized. Post stimulation, platelets were stained for the appropriate surface molecules, which, by means of flow cytometry, were each specified as mean fluorescent intensity (MFI).

While sole ADP stimulation had no regulative effect on the MFI values of most platelet surface marker, namely P-selectin, GPVI, GP1bα, and, GPIIIβ, (Figure 6-10 A, B, C and E), GPIIbIIIa expression was markedly increased (Figure 6-10 D). In platelets we measured a low MFI of P-selectin both in resting and ADP-stimulated platelets, which were about 6.7 ± 1.1 and 6.6 ± 0.5, respectively (Figure 6-10 A). GPVI reached a higher MFI already in resting platelets of about 59.2 ± 2.7, but was almost unaltered after ADP stimulation (MFI: 60.7 ± 2.5) (Figure 6-10 E). Based on the MFI values, GP1bα and GPIIIβ were frequently expressed already on untreated platelets. GPIIIβ in untreated platelets reached an MFI of 122 ± 18.7 and in ADP-treated 160 ± 13.5, while GP1bα in unstimulated platelets even showed a higher MFI of 338 ± 33.2 that was nearly the same in ADP-stimulated platelets (MFI: 305 ± 22.13) (Figure 6-10 B, C). In contrast, upon ADP stimulation we detected increased expression of GPIIbIIIa in platelets and measured a MFI of 68.7 ± 7.8, compared to the low baseline expression of 13.6 ± 1.4 (Figure 6-10 D). According to these findings we identified that ADP alone is not able to increase expression of all tested surface molecules, expect for GPIIbIIIa. Therefore, we sought to induce surface expression more intensively by using a U46 in combination with ADP as well as CRP as positive controls.

ADP in combination with U46 as well as CRP upregulated surface adhesion molecules on platelets more profoundly than ADP alone, especially P-selectin, GPIIbIIIa and GPIIIβ displayed markedly increased MFI values when compared to the unstimulated control (Figure 6-10 A, C, D). For P-selectin expression we measured an increase of 51.7 after ADP in combination with U46 stimulation, while the MFI after CRP treated was even increased by 98.5 (Figure 6-10 A). Compared to this outcome, the expression of GPIIbIIIa and GPIIIβ was even more abundant after stimulation with both positive controls. Here, GPIIbIIIa was increased by a MFI of +273.1 after stimulation with ADP in combination with U46 and +237.7 after CRP treatment (Figure 6-10 D). Stimulation of platelets with ADP in combination with U46 showed increased GPIIIβ expression by an MFI of +104, while CRP elevated the expression by +231 (Figure 6-10 C). In contrast, the stimulation with both ADP plus U46 and CRP led to a massive downregulation of GP1bα expression on platelets. Here, stimulation of platelets with ADP in combination with U46 decreased GP1bα expression by a MFI of -141, whereas CRP stimulation reduced expression by -194.7 (Figure 6-10 B). Interestingly, GPVI expression remained unaffected upon stimulation with ADP in combination with U46 and CRP compared to unstimulated platelets (MFI: 59.2 ± 2.7) and reached MFIs of 61.2 ± 1.3 and 54.3 ± 1.1 (Figure 6-10 E).

Taken together, these data validate that activated platelets were able to upregulate surface expression of P-selectin, GPIIbIIIa and GPIIIβ, indicating an important function of these surface molecules in platelet function. However, expression of GP1bα was decreased and expression of GPVI was unaffected after stimulation with ADP in combination with U46 and CRP, indicating that both stimulators are not able to activate platelets in this way. Here, it remains elusive whether both ADP plus U46 and CRP are able to cause increased expression of other platelet surface molecules to promote platelet activation. In the following we aimed to elucidate, whether the neutrophil-derived protease, catG may increase platelet surface expression and thereby ensures platelet activation. Therefore, platelets were stimulated dose-dependently with three different concentrations (0.01, 0.1 and 1 U/ml) of catG.

CatG stimulation of murine platelets clearly increased expression of all tested surface molecules. After catG stimulation we detected the strongest effect for surface expression of P-selectin, which was increased dose-dependently upon stimulation (Figure 6-10 A). P-

selectin expression was increased by +4.7-fold (MFI: 31.6 ± 3.7) after stimulation of platelets with 0.01 U/ml catG, by +56-fold (MFI: 378.0 ± 124.9) with 0.1 U/ml and even by +136.8-fold (MFI: 916.7 ± 276.5) after platelet stimulation with the highest catG concentration compared to untreated platelets (MFI: 6.7 ± 1.1) (Figure 6-10 A). Regarding the expression of GPIII-β and GPIIbIIIa, we detected a dose-dependent increase after stimulation with 0.01 and 0.1 U/ml catG, while the MFIs were declined after stimulation with the highest concentration (Figure 6-10 C, D). Here, the MFI of GPIII-β was elevated by +3.3-fold (MFI: 410.0 ± 13.0) after 0.01 U/ml catG, by +4-fold after 0.1 U/ml (513.5 ± 40.1) and by +2-fold after stimulation of platelets with 1 U/ml catG compared to resting platelets (MFI: 122 ± 18.7) (Figure 6-10 C). Concentration of 0.01 U/ml and 0.1 U/ml catG induced an increased expression of GPIIbIIIa by +4.1-fold (MFI: 56.8 ± 4.2) and +7.1-fold (MFI: 97.2 ± 13.5), respectively, while 1 U/ml of catG showed elevated expression of GPIIbIIIa by +6.1-fold (MFI: 83.2 ± 49.2), compared to untreated platelets (MFI: 13.6 ± 1.4) (Figure 6-10 D). Interestingly, the expression GPVI was unaffected after stimulation of platelets with the lowest catG concentration (Figure 6-10 E). Compared to the MFI of 59.2 ± 2.7 in resting platelets, we detected a MFI of 63.3 ± 7.2 for GPVI in platelets stimulated with the lowest catG concentration. We further measured a dose-dependent increase after stimulation with 0.1 and 1 U/ml catG. Here, the expression of GPVI in platelets was increased by +9.9-fold (MFI: 581.3 ± 204.4) after 0.1 U/ml and severely elevated by +16.4-fold (MFI: 973.0 ± 13.0) after stimulation with 1 U/ml catG (Figure 6-10 E). Regarding the expression of GP1bα, we measured a severely declined expression after platelet stimulation with the lowest catG concentration (Figure 6-10 B). Here, the MFI of GP1bα was about 18.7 ± 1.7 upon stimulation with 0.01 U/ml catG, compared to 338.0 ± 33.2 that were measured in resting platelets. As seen for GPVI expression, the expression of GP1bα dramatically increases after stimulation of platelets with 0.1 U/ml catG only by +1.7-fold (MFI: 565.8 ± 187.0), while 1 U/ml catG increased GP1bα expression by +3.2-fold (MFI: 1066.0 ± 412.5) (Figure 6-10 B).

Altogether, we investigated an increased ability of platelets to express P-selectin, GPIIIbIIa, GPVI, GPIII-β and GP1bα more frequently upon stimulation with different concentrations of catG. Here, we detected that a concentration of 0.1 U/ml catG revealed the most profound effect on platelet surface expression. Using the highest concentration of catG had no significant outcome, because of the low number of performed experiments (n =

2-3). We further investigated that surface expression of P-selectin was most effectively increased upon stimulation with catG, indicating that P-selectin is an essential marker for platelet activation by catG. In the following, we sought to investigate a putative function of PAR_4 in the activation of platelets and its contribution in the regulation of platelet surface expression. Therefore, we stimulated platelets with AYPGKF-NH_2, a specific PAR_4 agonist.

Upon stimulation of platelets with the PAR_4 agonist, we measured elevated expression levels of P-selectin, GPIII-β and GPIIIbIIa (Figure 6-10 A, C, D). Regarding the expression of P-selectin we investigated an increased expression by +12.4-fold (MFI: 82.5 ± 2.8), while expression of GPIII-β reached an increased MFI by +3.6-fold (MFI: 442.0 ± 42.5) compared to resting platelets (MFI P-selectin: 6.7 ± 1.1; MFI GPIII-β: 122.0 ± 18.7) (Figure 6-10 A, C). GP1bα expression, in contrast, was marginally downregulated by -1.5-fold (MFI: 67.1 ± 3.8) upon PAR_4 activation of platelets, while GPVI expression was unaffected compared to the expression on resting platelets (MFI GP1bα: 338.0 ± 22.1; MFI GPVI: 59.2 ± 2.7) (Figure 6-10 B, E).

Altogether, PAR_4 agonist treatment of platelets increases surface expression of P-selectin, GPIII-β and GPIIIbIIa, while GP1bα expression was severely downregulated and GPVI expression was unaffected. Furthermore, compared to catG, stimulation with the PAR_4 agonist led to an altered pattern and strength of regulation of expression of platelet surface marker. Based on these findings, platelet activation as measured by elevated expression of P-selectin, GPIIIbIIa, GPVI, GPIII-β and GP1bα might not per se be mediated via the activation of PAR_4.

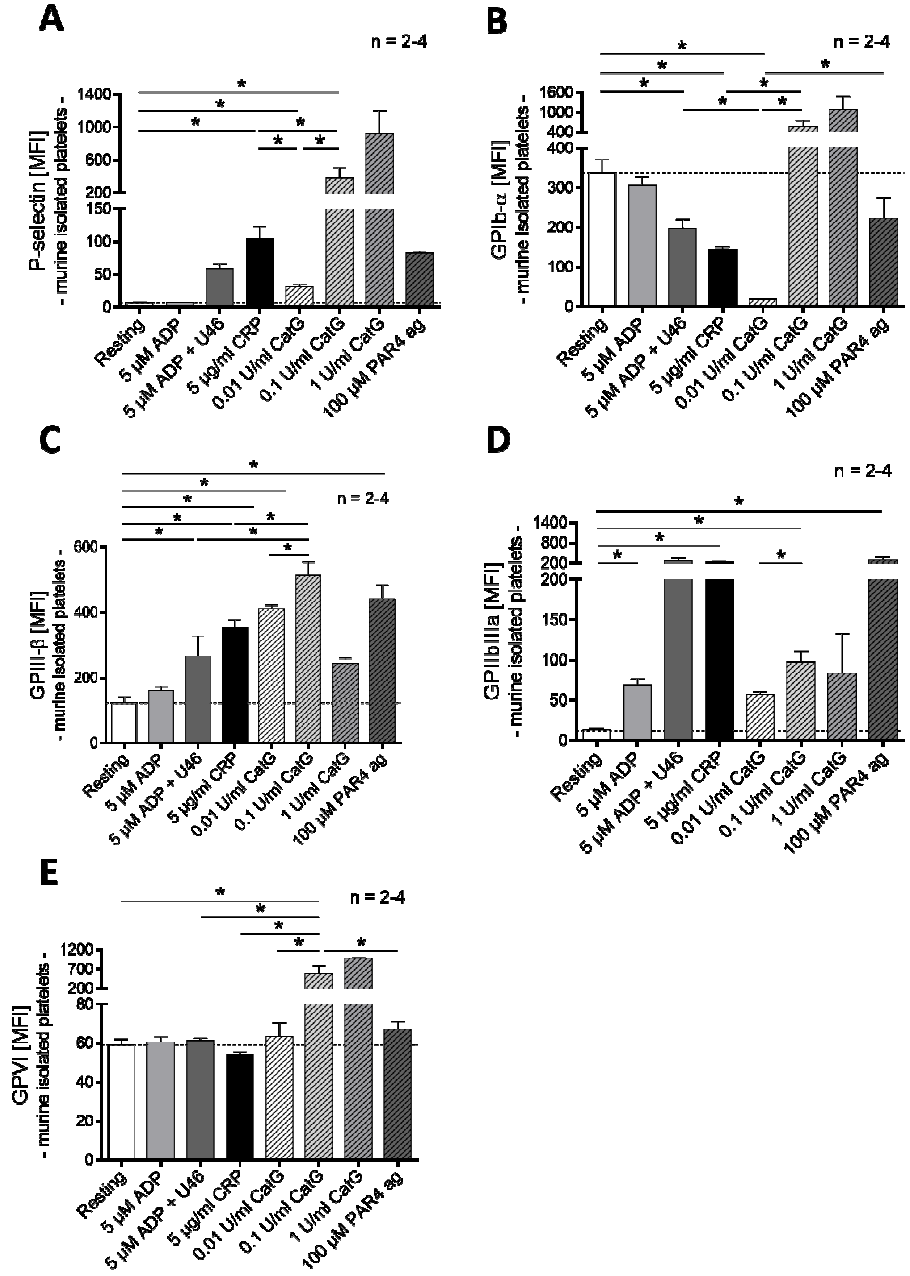

Figure 6-10 CatG induces elevated surface expression of P-selectin, GPIIIbIIa, GPVI, GPIII-β and GP1bα, independently from PAR_4 activation. Isolated murine platelets were stimulated with different catG concentrations, including 0.01 U/ml (white slash pattern column), 0.1 U/ml (light grey slash pattern column) and 1 U/ml (grey slash pattern column) or 100 µM PAR_4 agonist (dark grey slash pattern column) and fluorescent stained for (A) P-selectin, (B) GP1bα, (C) GPIIIβ, (D) GPIIIbIIa, and (E) GPVI. Unstimulated resting cells served as negative control (white column), while ADP in combination with (dark grey column) or without (light grey column) U46 as well as CRP (black column) were used as positive controls. By means of flow cytometry, the MFI was determined. Mann-Whitney U test was performed to evaluate significant differences (*p<0.05, **p<0.01). Results are presented as mean values ± SEM of n = 2-4 mice per group. GP1bα, Glycoprotein-1bα; GPIIIβ, Glycoprotein-IIIβ; GPIIIbIIa, Glycoprotein-IIIbIIa; GPVI, Glycoprotein-VI; CatG, Cathepsin G; ADP, adenosine diphyosphate; CRP, collagen relative peptide; ag, agonist; MFI, mean fluorescent intensity.

7 Discussion

In this study, we aim to unravel the role of the catG/PAR_4 axis in the formation of NPAs and its implication in the progression of vascular inflammation, such as LcV. Here, we demonstrated for the first time an increased formation of NPAs as well as elevated catG levels in the circulation of patients with LcV compared to healthy volunteers. *In vitro*, we confirmed that catG-stimulation of platelets significantly contributes to their interactions with neutrophils. This effect was in part mediated by PAR_4, since blocking of the receptor by a specific antagonist severely reduces the formation of NPAs. With our *in vivo* model of IC-mediated inflammation we validated our patient data and revealed increased formation of NPAs and elevated catG levels in the circulation of wild type mice in response to inflammation. In mice, deficient for PAR_4, we detected less formation of NPAs in the circulation during inflammation, while the catG levels were even more increased compared to wild type mice. As a measure for inflammation we detected increased neutrophil infiltration and edema formation in the inflamed skin areas of wild type and PAR_4 mice, albeit no significant differences between wild type and knockout mice were observed. Histologically, we confirmed the massive infiltration of neutrophils in the inflamed skin areas skin of wild type and PAR_4, while only single macrophages and no lymphocytes were detected. Remarkably, we investigated an enhanced bleeding property of PAR_4 mice in the skin in response to IC-mediated inflammation. In contrast, neither histamine-induced vascular permeability nor the application of a needle trauma by PBS injection, caused edema formation and the influx of neutrophils into the skin of knockout mice. Finally, we evaluated the surface expression profile of murine platelets after stimulation with catG. Here we detected a dose-dependent increased surface expression of P-selectin, GP1bα, GPIIIβ, GPIIIbIIa, and GPVI, whereas a low catG concentration decreased the expression of GP1bα and a high concentration decreased that of GPIIIβ.

The LcV is the most frequent form of cutaneous vasculitis in humans and affects about 30 cases per million people per year [157]. Patients suffering from cutaneous vasculitis experience impaired health conditions and demonstrate several clinical hallmarks, including increased temperature, headache, exhaustion and even rheumatoid complaints

including arthralgia and arthritis [54]. However, the most pronounced diagnostic hallmark is constituted by petechial hemorrhages of the skin, which compromise lesions from 1 mm up to several centimeters and predominately affect the lower distal extremities. These lesions can further develop to extensive plaques, blisters, erosions or even necrotic ulcerations that could encompass large areas of the skin and be combined with symptoms of pain, and burning rashes [54, 157]. Histologically, these cutaneous areas are characterized by a massive inflammatory infiltrate that is dominated by neutrophils that along cause a destruction of the endothelial wall leading to erythrocyte extravasation [54]. In the last decades several disease triggers, including certain medication or bacterial, fungal and viral infections, were identified to capably initiate the development of LcV [54]. However, up to now, 50 % of all LcV cases are classified as idiopathic which reflects our poor understanding of the underlying molecular mechanisms of this disease and the acute urge to extend our research efforts to unravel the mechanism of LcV initiation and progression [54].

In our study, we describe for the first time an increased formation of NPAs in the circulation of LcV patients as well as in mice that were afflicted with IC-mediated inflammation. Multiple studies reported a distinct role for platelets in NPA formation and maintenance [5, 6, 158, 159]. Platelets are famously known for their role in coagulation and vascular hemostasis as they, for example, prevent excessive bleeding during traumatic vessel injury [158, 159]. However, platelets are also increasingly recognized as key actors in inflammatory responses, by, inter alia, interacting with neutrophils, activating neutrophils and consequently recruiting this immune cell type to the side of inflammation [5, 6]. In this study, we aimed to determine a potential contribution of platelets/NPAs to IC-mediated vascular inflammation, especially, LcV. Therefore, we, in a first step, analyzed the whole blood of patients suffering from LcV and healthy volunteers for NPA occurrence. In patients, we detected severely increased formation of NPAs, suggesting that platelet binding activates neutrophils and contributes to inflammation. Taken together, the results of this study demonstrate that, beside their procoagulant role, platelets play an essential role in the progression of vascular inflammation during LcV.

The investigated healthy control group revealed already a baseline formation of NPAs of about 5 % which might be a result of the blood viscous properties during flow. In the

frame of this concept, smaller cellular components of the blood, like platelets are pushed towards the vessel wall, whereas larger neutrophils are more likely to take the central space of the vessel lumen. However, neutrophils that tile more closely to the vessel wall are therefore more proned to collide with platelets and will form temporary neutrophil-platelet complexes which disappear and form again in the absent of a stabilizing, mostly inflammatory stimulus [160, 161].

As mentioned before, the binding between platelets and neutrophils is important for inflammatory responses and can be mediated via direct cell-to-cell interaction or indirectly via platelet-derived cytokine, chemokines or microparticles [28, 162]. Inflammatory triggers increase the expression of surface molecules on platelets and the endothelium which enable their direct interaction with each other and neutrophils [162]. Activated platelets initially bind to neutrophils via the interaction of platelet P-selectin and PSGL-1 expressed on neutrophils which forms the most important binding bridge between platelets and neutrophils. Mice deficient for P-selectin or PSGL-1 demonstrate severely decreased NPAs that is associated with an impaired neutrophil recruitment, adhesion and extravasation [6, 19, 20, 28-37]. Furthermore, integrin- and glycoprotein-dependent interactions between platelets and neutrophils also contribute to neutrophil recruitment and tissue infiltration at the site of inflammation [28, 162]. Platelets, immobilized on vascular endothelial cells, elicit leukocyte rolling via GPIbIIIa and GPIb [163]. Neutrophil extravasation is also induced by the binding of Mac-1 (CD11b/CD18) to platelet P-selection and is further increased by the interaction CD40 with platelet-derived soluble CD40L [35, 164]. Platelet-induced migration of leukocytes can also be mediated indirectly via the activation of endothelial cells by platelet-derived components including serotonin which causes the expression of P-selectin and the release of neutrophil chemoattractant, IL-8 [165]. IL-8 in turn activates integrin Mac-1 on neutrophils via chemokine receptor CXCR1 signalling, that ultimately favours neutrophil adhesion and transmigration [166, 167]. In addition, platelet-derived chemokines, including CXCL4 and CXCL7, were shown to activate neutrophils and promote endothelial adhesion (CXCL4, CXCL7) [168] as well as chemotaxis and transmigration (CXCL7) [169]. Altogether, these results manifest the important role of platelets on neutrophil interaction with the endothelium from the earliest stages of recruitment through to neutrophil tissue infiltration

during inflammation. In our study, we so far confirmed that the formation of NPAs is related to inflammatory diseases and can be detected in patients suffering from LcV [50-53]. Our outcome is in accordance with several studies that already evaluated the formation of NPAs as an important marker of vascular inflammation. Increased NPAs are e.g. identified in the circulation of patients suffering from the Kawasaki syndrome, angina pectoris, sickle cell disease and atherosclerosis [50-53]. But still, the inflammatory stimuli that induce the formation of NPAs and their role during neutrophil migration and transmigration in IC-mediated inflammation are not identified.

Based on our *ex vivo* data revealing increased numbers of circulating NPAs in patients suffering from LcV, we deducted the hypothesis of increased formation of NPAs in wild type mice in a model of IC-mediated inflammation. PAR_4-deficient mice were applied to this model, because PAR_4 involvement in catG-mediated neutrophil platelet interaction has been shown *in vitro*, indicating a role of the receptor in the formation of NPAs during inflammation *in vivo.*

By means of flow cytometry, we detected a 2-fold increase in the formation of NPAs 4 h post RPA initiation in wild type mice, which is in accordance with our obtained patient data. Here, we confirmed the use of NPA as a marker for IC-mediated inflammation *ex vivo*. A study by Hara et al. reported a comparable result and detected a 9.1-fold increase of leukocyte-platelet aggregations in wild type mice after 4 h of RPA-challenge [139]. Taken together, the results demonstrate an essential role of platelets for the recruitment of neutrophils and leukocates to the skin in a murine model of IC-mediated inflammation.

The frequency of NPAs in *Par4*$^{-/-}$ mice was unaltered 4 h post RPA-challenge, but as expected, we detected a dramatic decrease in the total number of NPAs in *Par4*$^{-/-}$ mice, that was half as much as observed in wild type mice. This severe difference in the frequency of NPAs in wild type versus *Par4*$^{-/-}$ mice supports our hypothesis that PAR_4 expression on platelets might be essential for the formation of NPAs during IC-mediated inflammation. Thus, our data confirm the important role of activated platelets to stimulate neutrophils during inflammatory responses. This is validated by similar results in mice that were treated with busulfan, a cell-specific toxin that mediates platelet depletion [139]. In this model, the depletion of platelets led to a reduced frequency of NPAs in the circulation of mice 4 h post

RPA [139]. Furthermore, the frequency of aggregates was downregulated in *P-selectin*$^{-/-}$ and *PSGL-1*$^{-/-}$ mice in the following of RPA-challenge [139]. These results indicate that the RPA-induced formation of platelets-neutrophil/leukocyte aggregates can be abrogated by busulfan-treatment and is dependent on platelets' PAR_4 as well as P-selectin activity, but also on neutrophil PSGL-1 function [139, 170]. Previous studies reported that separate activation of either platelets or neutrophils induces the formation of NPAs as equal as simultaneous activation of both cell types [53, 171]. This observation points to a mechanism of platelets and neutrophils to activate each other, thereby for example influencing their secretion pattern of pro-inflammatory mediators (see introduction 4.1.1) [53, 171]. Thus, a reduced interaction of neutrophils and platelets due to PAR_4 deficiency could therefore result in a diminished or at least altered release of pro-inflammatory mediators during IC-mediated inflammation, and consequently might lead to an impaired neutrophil recruitment and adhesion to the vascular endothelium.

In previous studies, the neutrophil protease catG has been identified as a strong activator of platelets and an important mediator of coagulation [128, 135]. However, the role of catG in inflammatory processes has only been investigated in greater detail as of lately [137, 138]. In this study, we especially focussed on the role of this protease in IC-mediated inflammation and further aimed to unravel a potential role of catG in the formation of NPAs. Plasma analysis of LcV-patients revealed a severely increased level of catG when compared to the appropriate healthy control group. In accordance with our *ex vivo* data, we further demonstrated an increased plasma level of catG in IC-challenge wild type mice *in vivo*. When PAR_4 is knocked-out, catG activity is enhanced compared to the wild type situation. Based on these finding catG appears to contribute to IC-mediated inflammation and might be a potential activator of platelets in humans and mice during inflammatory responses.

Our observation aligns with studies that described a contribution of catG to vascular inflammation. Faraday et al. reported a markedly reduced formation of NPAs in murine whole blood when catG is absent [135]. Adkison et al. revealed that mice deficient for the dipeptidyl peptidase I, an enzyme required for full activation of NE and catG, as well as catG are protected against anti-collagen antibody induced arthritis [138]. Furthermore, *catG*$^{-/-}$

mice display decreased inflammation of the subcutaneous air pouch in zymosan- and IC-mediated inflammation models which was associated with a decrease of local TNF-α and IL-1β release [138]. Raptis et al. revealed that mice deficient for NE and catG show no impairment in neutrophil adhesion but CD11b clustering and cytoskeletal reorganization and cell spreading [137]. Furthermore, neutrophils of *catG/NE*$^{-/-}$ mice failed to secrete CXCL2 and to produce ROS which could be restored by exogenic administration of active catG [137]. Analyses by Ortega-Gomez et al. described a specific contribution of catG in the recruitment of neutrophils and monocytes in an arterial inflammatory disease model [172]. Using an atherosclerotic mouse model they revealed severely decreased arterial recruitment of monocytes and neutrophils in apolipoprotein E/catG-deficient mice [172]. The artery-specific recruitment pattern mediated by catG is explained by CCL5 release from platelets that is dependent on the shear forces in the blood flow of arteries. CCL5 in turn mediates catG release by neutrophils that have a higher binding affinity for arterial endothelium when compared with venular endothelium and induces enhanced integrin clustering of Mac-1 and LFA-1 on neutrophils [172]. These studies presume that catG-dependent leukocyte recruitment only occurs in arterial, but not in microvascular inflammation, that, inter alia, is the basis of lung inflammation, lung damage and emphysema [172, 173]. LcV constitutes in small vessel vasculitis, that belongs to the class of microvascular inflammation. Here, it is unexplained, whether catG also plays an essential role in leukocate, especially neutrophil recruitment. In microvasculature lung inflammation like cystic fibrosis, catG has been described to preferably rely on its proteolytic activity [174]. High concentrations of catG have been shown to degrade structural components of the extracellular matrix [174]. Furthermore, catG blockades the properties of macrophages to clear apoptotic cells, which in consequence promotes increased neutrophil necrosis and a subsequent increase in the release of proteases to the lung tissue [174]. CatG also reduces the phagocytic activity of macrophages by degrading surfactant protein A, which is required for microbial clearance [174, 175]. Recently, the proteolytic role of neutrophil-serine proteases, including catG, on endothelial cells was analysed [176]. Jerke et al. established that the endothelium is able to uptake enzymatically active neutrophil-released serine proteases that are able to cause an impaired endothelial barrier function and destruction of the endothelial actin cytoskeleton [176]. They identified neutrophils that release enzymatically active proteases when

stimulated with anti-neutrophil cytoplasmic autoantibodies (anti-proteinase 3 and anti-MPO), indicating a potent contribution of neutrophil-derived proteases, such as catG, in the proteolytic destruction of the vessel wall during neutrophil-mediated inflammatory vascular diseases [176]. These findings support the assumption that catG might also be involved in endothelial destruction in vascular inflammatory diseases including LcV. Thus, catG could be an important inducer of vessel wall permeability during vascular inflammation causing extravasation of erythrocytes out of the vessel into the surrounding tissue, a crucial hallmark of LcV.

Additionally, several studies reported an important contribution of catG in the proteolytic activation of cytokines of the IL-1 family whose members are prominently linked to acute and chronic inflammatory diseases. In psoriasis, a chronic inflammatory skin disease that is mainly mediated by neutrophils [177-180], severely elevated levels of catG are observed in the lesional skin of patients [181]. Henry et al. demonstrated an enormous capacity of catG in the activation of IL-36 that is associated with subsequent release of pro-inflammatory mediators [182-184] from skin keratinocytes, many of which are also upregulated in the lesional skin of psoriatic patients [181]. Lefrançais et al. investigated the ability of catG to activate IL-33, a pro-inflammatory mediator that is associated with several inflammatory diseases such as asthma, rheumatoid arthritis, ulcerative colitis, and cardiovascular diseases [185-188]. These studies contributed to our current understanding of an important pro-inflammatory role for catG in the progression of chronic inflammation, However, more detailed further research is needed to analyse whether catG also mediates IL-1 cytokine-induced inflammatory responses in vascular inflammation.

In this study, we demonstrate for the first time that exogenously supplemented catG suffices to mediate the interaction between human neutrophils and platelets via activation of PAR_4 on platelets *in vitro*. The ability of catG to activate PAR_4 was recently discovered, but little information exists about the effects that are activated by this pathway. However, it was reported that catG via PAR_4 results in calcium mobilization in PAR_4-transfected fibroblasts, PAR_4-expressing *Xenopus* oocytes, and human platelets [72]. In this study, we confirmed a putative role for the protease/receptor interaction in inflammation-related aggregation between neutrophils and platelets.

PAR_4 is acknowledged as a bridging receptor between coagulation and inflammation. This role was defined utilizing mice deficient for PAR_4 which are protected against augmented neointimal hyperplasia after carotid artery ligation in a streptozotocin-induced mouse model of diabetes mellitus type I, and show decreased edema formation, hemorrhage and inflammation in a sTF-induced arthritis model [94, 110]. Further in a mouse model of stroke, PAR_4-deficient mice are protected against reperfusion injury as well as microvascular inflammation, which implies the disruption of the blood brain barrier as well as platelet and leukocyte rolling and adhesion [112]. Furthermore, blockage of PAR_4 in mice intrapleurally treated with carrageenan or IL-8 inhibited neutrophil recruitment to the pleural cavity and diminished neutrophil recruitment and adhesion [189]. Besides, an important contribution of catG and other neutrophil serine proteases, including NE, in neutrophil function as well as in neutrophil recruitment and adhesion has been demonstrated [114, 136]. Here, the dense surface expression of proteases might be involved in chemokine processing and, therefore, induces neutrophil migration to the site of tissue injury [114, 136]. However, we describe for the first time a contribution of both PAR_4 and catG in the interaction of neutrophils with platelets. The PAR_4/catG axis might therefore be crucial for stimulating platelets to mediate the activation and recruitment of neutrophils to the site of inflammation. Therefore, the ligand/receptor interaction is an important inflammatory mediator, essential for multistep cascade of neutrophil adhesion to the endothelial wall.

Several studies already reported an RPA-induced increase in edema formation and neutrophil tissue migration in the back skin of wild type mice [139, 140, 190]. In this study, we aimed to analyze the specific function of PAR_4 in the cutaneous IC-mediated inflammation *in vivo*. Our previously obtained data demonstrated an important role for PAR_4 in the formation of NPAs and let one speculate of an involvement of the platelet receptor in the activation and subsequent recruitment as well as transmigration of neutrophils to the inflamed skin. Our findings of edema formation and neutrophil infiltration in *Par4*$^{-/-}$ mice align with those found in wild type mice after RPA-challenge, indicating that a deficiency in the platelet receptor does not protect mice from IC-mediated inflammation. In other inflammatory model, mice that were systemically treated with the PAR_4 antagonist p4pal10

showed reduced edema formation and granulocyte recruitment 4 h post carrageenan-induced inflammation. Additionally, the intraplantar injection of a PAR_4-Activating Peptide (AYPGKF-NH_2) to hind paw of mice severely increased inflammatory responses, characterized by increased edema formation in and granulocyte recruitment to the hind paw of the treated mice [112]. Taken together, PAR_4 might contribute to inflammatory responses and, importantly, might be involved in the regulation of such responses in different inflammatory diseases aside from IC-mediated inflammation only.

Utilizing an IC-mediated model of vascular inflammation, Hillgruber et al. revealed a severely reduced cutaneous edema formation and epidermal MPO activity in platelet-depleted mice when compared to healthy wild type mice, indicating that in vasculitis platelet-derived mediators and/or platelet-expressed receptors are responsible for the inflammation process [139]. Hara et al. identified P-selectin and PSGL-1 as crucial receptors in the recruitment and adhesion of neutrophils during IC-mediated inflammation [139, 140]. P-selectin and PSGL-1 are the main interacting partners of neutrophils and platelets, that are responsible for leukocyte rolling and interaction of leukocytes with the endothelium [21, 23, 35]. Mice, that were deficient for platelet P-selectin of PSGL-1 displayed a markedly decreased edema formation and neutrophil infiltration to skin compartments when compared to wild type mice [139]. Thus, it appears valid that PAR_4 commits a pro-inflammatory role in inflammation and is further involved in the formation of NPA, whereas neutrophil rolling and adhesion during IC-mediated inflammation seems rather to be mediated by other surface receptors or secretion products of platelets and neutrophils, including P-selecting and PSGL-1 at least.

In IC-mediated cutaneous inflammation, neutrophils are known to form the central player in the progression of the disease. Besides neutrophils, a putative role for macrophages as well as T cells has been reported in studies investigating several inflammatory skin diseases, including psoriasis and atopic dermatitis [141-145]. Psoriasis is a chronic inflammation, that is characterized by epidermal hyperproliferation of keratinocytes in combination with cutaneous immune cell infiltration, while atopic dermatitis is a chronic T_H2-dominated inflammatory skin disease associated with pruritus [141-145]. In both skin

diseases, increased numbers of macrophages and $CD4^+$ and $CD8^+$ T cells, respectively, have been detected in the lesional skin, and are known to play an important function in the progression of the inflammation, while vasculitis is dominated by neutrophil influx to the tissue [146-151]. By means of immunofluorescent staining of murine skin section of wild type and *Par4*$^{-/-}$ mice, we therefore aimed to identify the frequency of neutrophils, T cells and macrophages during IC-mediated inflammation in cutaneous specimen. In accordance to other studies, we identified neutrophils as the main inflammatory cell type that transgress to the affected tissue and there contribute to inflammation in the skin of wild type and *Par4*$^{-/-}$ mice 4 h post RPA initiation [140]. Our analysis only marked few intracutaneous macrophages, while T cells were completely absent in the inflamed skin of all experimental mouse groups. The low abundance of macrophages in the inflamed skin was already identified as a characteristic of LcV, detected in routing histological examination of lesional skin from LcV patients.

Generally, the histologically obtained results were in alignment with the results obtained by analysis of circulating leukocytes via differential blood count in wild type or *Par4*$^{-/-}$ mice under IC-mediated inflammation. Pro-inflammatory leukocytes contain granulocytes, monocytes and lymphocytes. During an inflammatory response each of them exerts a specific function which can overlap and vary during the progression of the inflammation. In the whole blood of RPA-challenged mice granulocytes, that form the first line of defense during acute inflammation, are severely increased in abundance. Under homeostatic conditions, granulocytes are stored in the bone marrow or circulate in the blood but rapidly accumulate in the affected tissue when inflammation is initiated [191]. In addition to the regulation of neutrophil frequency in IC-mediated inflammation, we further detected elevated monocyte levels in both wild type and PAR_4 knockout mice. Like granulocytes, monocytes circulate in the blood and accumulate quickly in affected tissue in response to inflammatory mediators. Monocytes, differentiated to macrophages, are mainly responsible for the uptake and breakdown of pathogens, functions that are essential for the maintenance of chronic inflammation [191]. In contrary to our results for monocytes, lymphocyte abundance was markedly decreased in wild type and *Par4*$^{-/-}$ during IC-mediated inflammation. Lymphocytes are formed in the bone marrow and thymus and provide specific adaptive immunity, which is activated only when an innate immunity is induced [152]. Taken

together, findings of the present study confirm that the LcV is an acute inflammation that is primarily induced by granulocytes, accompanied by a monocytic involvement.

Of note, we detected differences in the frequency of baseline leukocytes in vehicle-treated *Par4*$^{-/-}$ mice when compared to vehicle-treated wild type mice: *Par4*$^{-/-}$ mice demonstrate increased granulocyte and monocyte numbers, whereas lymphocyte abundance was decreased in the healthy condition only. This observation indicates that *Par4*$^{-/-}$ mice exhibit, already under homeostatic conditions, a distinct dysregulation of the immune system without displaying symptoms of inflammation. It might be possible that PAR_4 deficiency is associated with increased synthesis or release of granulocytes and monocytes by the bone marrow, thereby showing symptoms of an acute inflammation, although the mice are in a healthy condition.

Mice, that are deficient for the PAR_4 receptor possess platelets that are unresponsive to thrombin. Consequently, these mice show severely impaired coagulation, as indicated by a prolonged bleeding time in a tail-bleeding assay [57]. In our *in vivo* model of IC-mediated inflammation, we demonstrated comparable neutrophil infiltration as well as edema formation in cutaneous sites in both wild type and *Par4*$^{-/-}$ mice. Interestingly, the knockout mouse group showed more intense cutaneous bleeding that was restricted to the area of inflammation and was absent in the wild type mice, suggesting full platelets function in wildtype mice. Our results align with findings of Hillgruber *et al.* and Goerge *et al.* where cutaneous hemorrhage was more intense in thrombocytopenic mice after IC-mediated inflammation or dermatitis, respectively, and therefore dependent on full platelet function [140, 192]. Additionally, Goerge *et al.* identified an initial appearance of petechiae already 20 minutes after the induction of IC-mediated inflammation that was dramatically increased after 1 h and resulted in continuous loss of erythrocytes into the tissue after 2 h [192]. These results together with our own findings indicate an increased bleeding during inflammation in the absence of platelets or platelet dysfunction due to PAR_4 knockout. In contrast to our results obtained in *Par4*$^{-/-}$ mice, Hillgruber et al. were able to show that severely decreased edema formation as well as neutrophil infiltration in the inflamed thrombocytopenic mice is not dependent on PAR_4 [140]. As mentioned above, our results revealed no difference in edema formation and neutrophil infiltration in wild type as well as *Par4*$^{-/-}$ mice post RPA,

suggesting that both inflammatory markers are not dependent on PAR_4 function on platelets, but the abundance of functional platelets is essential [140]. The platelet receptor or receptors, responsible for edema formation and neutrophil infiltration might therefore be different from PAR_4 and need to be investigated.

We further aimed to evaluate, whether the induction of an intense vascular permeability is responsible for the increased cutaneous bleeding in *Par4*$^{-/-}$ compared to wild type mice. In accordance with thrombocytopenic mice, vascular permeability was not sufficient to induce cutaneous hemorrhage in PAR_4 knockout mice, concluding that the cutaneous inflammation, mediated by transmigrating neutrophils, might be the relevant factor to induce the massive bleeding in PAR_4 deficient mice [140]. Evidence for this assumption was further supported by Hillgruber et al. who reported that cutaneous bleeding during thrombocytopenia is dependent on neutrophil interaction with the endothelium [140]. Depletion of neutrophils or interference in the neutrophil adhesion and extravasation cascade prevents neutrophil transmigration and consequently abrogates cutaneous bleeding [140]. Recently, a study by Goerge *et al.* revealed the important role of platelet adhesion receptors in cutaneous bleeding during inflammation [192]. Deficiency of the von Willebrand receptor causes cutaneous bleeding during IC-mediated inflammation, while mice lacking P-selectin causes no tissue haemorrhage during IC-mediated inflammation [139]. In addition, the deficiency of von Willebrand factor or the collagen receptor GPVI (*FcRγ*$^{-/-}$) does not cause tissue hemorrhage after irritant contact dermatitis as well [190, 192]. This might indicate that platelet adhesion receptors, which are essential for platelet plug formation are not required for platelets to prevent skin bleeding in thrombocytopenic mice during inflammation. Boulaftali *et al.* identified an important role of immunoreceptor tyrosine-based activation motif (ITAM) that is crucial for the signalling of GPVI. Platelets that were defective in the ITAM signalling, show an impaired ability to prevent cutaneous bleeding in IC-mediated inflammation as well as LPS-induced inflammation in the lung, confirming an important role of ITAM signalling to preserve vascular integrity [193]. Taken together, these results confirm an important role of platelets and their expression of PAR_4 as well as ITAM, but not the von Willbrand factor and GPVI are crucial players to prevent massive bleeding into the skin during IC-mediated inflammation.

In this thesis, we further evaluated the role of catG on activation of isolated murine platelets and potential alteration in the expression of surface adhesion molecules on platelets. Here, we could demonstrate an activating effect of catG on freshly isolated human platelets *in vivo*. Platelets that were stimulated with catG rapidly form aggregates with freshly isolated neutrophils from the same donor (Figure 6-3 A, B). Due to this observation, we sought to analyze catG stimulation on the activation status of freshly isolated murine platelets as well as possible alteration in the surface expression profile of platelets. Activated platelets, are known to upregulate the expression of several adhesion molecules on their surfaces, including neutrophil PSGL-1 binding partner, P-selectin; Glycoprotein-1bα (GP1bα), a component of the von Willebrand receptor; and Glycoprotein-IIbIIIa (GPIIbIIIa), the active form of the fibrinogen receptor. Surface molecules that are present persistently on platelets imply the collagen receptor Glycoprotein-VI (GPVI) and the inactive form of the fibrinogen receptor, Glycoprotein-III-β (GPIII-β), which is expressed on unstimulated platelets [153-156].

Stimulation of platelets with 0.1 U/ml catG revealed the most distinct effect on platelet surface receptor profile and led to an increased expression of P-selectin, GP1bα, GPIIIβ, GPIIIbIIa and GPVI. This regulation was dose-dependent for platelet-expressed P-selectin, GPIIIbIIa and GPVI and in line with findings for catG-stimulated human platelets by Selak et al. [128]. Furthermore, we detected a down-regulation of GP1bα after stimulation with low concentration of catG. This observation is again in accordance with Selak et al, who detected down-regulation of GP1bα on human platelets following catG stimulation [128]. In addition, we demonstrated for the first time that catG induces GPIIIβ expression on murine platelets that diminished after stimulation with a high catG concentration. According to this result, high concentrations of catG might induce a negative feedback that prevents excessive expression of GPIIIβ on murine platelets, the inactive form of the fibrinogen-receptor. In contrary, we detected increased expression of GPIIIbIIa, the active form of the fibrinogen receptor, which plays a crucial role in platelet aggregation.

P-selectin is stored in the α-granules of platelets and is located to the surface upon platelet activation. P-selectin is the main interacting partner of PSGL-1, that is expressed on neutrophils, and mediates the initial binding between neutrophils and platelets [154, 155]. Studies, using blocking antibodies against P-selectin or P-selectin deficient mice revealed an

important contribution of the selectin in leukocyte rolling on post-capillary venules, and recruitment of neutrophils to the site of inflammation in several inflammatory mouse models [30, 194]. CatG stimulation of platelets might therefore play an essential role in P-selectin-dependent leukocyte rolling and recruitment along the endothelial wall and is therefore thought to be an important mediator of inflammation. Because catG is an activator of PAR_4 our findings therefore point to an important role for the catG/PAR_4 axis on platelet P-selectin interaction with neutrophil PSGL-1, thereby, mediating the formation of NPA and ultimately facilitating platelet-induced neutrophil recruitment and efficient adhesion to the endothelial wall.

Besides the multiple cascade of leukocyte recruitment, we also investigated an effect of catG on the regulation of coagulation factors that play an important role in hemostasis. GP1bα, which forms together with GP1bβ, GPIX and GPV a receptor complex on platelets that is able to bind the hemostatic glycoprotein, von Willebrand factor, is crucial for the induction of hemostasis [156]. Mutations in the GPIb gene causing a lack of function of the GPIb-IX-V complex are associated with bleeding disorders, like the Bernard-Soulier syndrome [195]. Here we show that already low concentration of catG mediate down-regulation of GP1bα, and are linked to bleeding, whereas higher concentrations of the protease might be associated with hemostasis. As reported in the beginning, GPIbα on platelets mediates the stable and firm adhesion with neutrophils via binding to the αMβ2 integrin. In contrary, to the catG-induced P-selectin expression, we detected an inhibitory effect of catG on the GPIbα expression. Taken together, catG might play an important role during vascular inflammation by on the one hand facilitating the formation of NPAs via P-selectin/PSGL-1 interaction and on the other via the down-regulation of GPIbα on platelets and the associated bleeding stop. The latter is in accordance with a study by Li et al., who revealed that mice deficient in αMβ2 show an increased blood flow rate during TNFα-mediated inflammation [46]. This indicates that αMβ2-GP1bα interactions are crucial for neutrophil-platelet interactions under thromboinflammatory conditions [46]. Besides αMβ2 is also capable of interacting with the fibrinogen receptor GPIIIbIIa on the platelet surface [47]. GPIIIbIIa is the active form of the fibrinogen receptor and plays a role in platelet aggregation during thrombus formation via the binding of fibrinogen. However, GPIIIbIIa might not be crucial for neutrophil-platelet aggregation during vascular inflammation [38, 48]. Instead,

GPIIIbIIa is involved in platelet aggregation, since patients with absent or deficiency in GPIIIbIIa are associated with Glanzmann thrombasthenia and suffer from a bleeding tendency [196]. As seen in our results, an upregulation of the GPVI receptor by catG might therefore also result in increased capacity of platelets to aggregate. Another receptor, being involved in hemostasis is GPVI, which is a collagen receptor that is only expressed on platelets [153]. Damage of the endothelium causes the exposure of collagen, that can be bound by GPVI, and subsequently causes platelet activation and adhesion [153]. GPVI has been shown to play an important role in the formation of platelet aggregates on collagen fibers, whereas mice deficient for GPVI have no severe bleeding phenotypes [153]. CatG-mediated upregulation of GPVI might therefore increase the ability of platelets to form aggregates.

Taken together, catG regulates pathophysiological mediators described in multiple diseases with bleeding phenotypes, such as leukocyte rolling and recruitment, and of coagulation, especially hemostasis, strongly indicating a role for the catG/PAR_4 axis in the induction of platelet activation and, therefore, mediating platelet aggregation and platelet-induced formation of NPAs.

In summary, we investigated for the first time that IC-mediated inflammation is associated with increased formation of NPAs *ex vivo* and *in vivo*, suggesting a high clinical relevance of these aggregates in the diagnosis of vascular inflammation. We further identified increased levels of catG in the circulation of LcV patients and IC-challenged mice. Unfortunately, a correlation between increased formation of NPAs and high levels of catG was not detected in human and mice so far. In contrast to that, we established for the first time an important role of the catG/PAR_4 on platelet activation that is associated with increased formation of NPAs *in vitro*. Hypothetically, we assume that the accumulation of ICs within the vessel walls during IC-mediated vascular inflammation causes the recruitment of neutrophils to the side of inflammation (Figure 7-1, (1)). Neutrophils express a specific receptor on their surface (CD16) that can recognize and bind to ICs which subsequently causes degranulation of neutrophils (Figure 7-1, (2)). During degranulation, neutrophils release their granular components, including serine proteases such as catG (Figure 7-1, (3)). As our *in vitro* data confirm, catG is able to activate PAR_4 on platelets surface that induces

the interaction of platelets with neutrophils (Figure 7-1, (4a)), indicating a crucial function receptor-ligand interaction on NPAs during IC-mediated inflammation. We further confirmed that neutrophils, recruited to the vessel wall start to transmigrate through the endothelium to the side of inflammation which we have seen to an equal amount in wild type and *Par4*$^{-/-}$ mice after IC-challenge (Figure 7-1, (5)). The transmigration of neutrophils to the side of inflammation is accompanied by a pronounced extravasation of erythrocytes (Figure 7-1, (5)) that was remarkably stronger in *Par4*$^{-/-}$ mice, indicating a crucial role of PAR_4 on coagulation during vascular inflammation.

Based on our findings we assume that PAR_4 and its ligands catG are indeed important mediators of NPAs during inflammation, but have no crucial effect on neutrophil migration and transmigration per se. Therefore, the *Par4*$^{-/-}$ mouse is not the ideal *in vivo* model to study the neutrophil-adhesion cascade in IC-mediated inflammation.

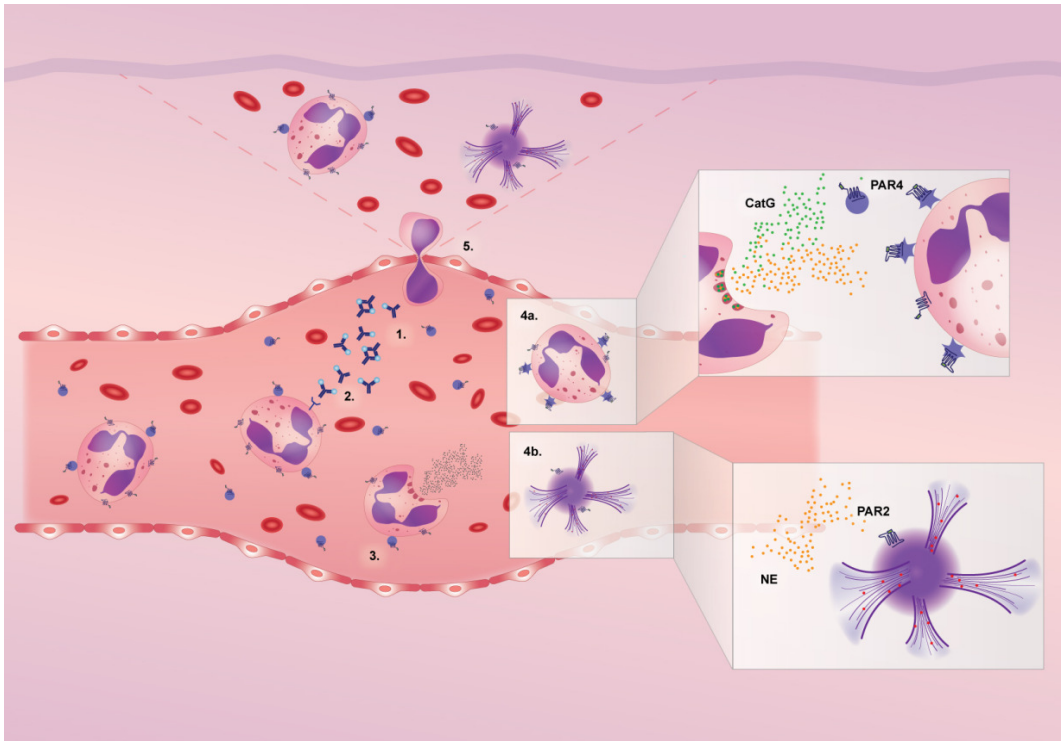

Figure 7-1 Role of Protease/PAR axis in immune complex (IC)-mediated inflammation. Accumulation of ICs within the vessel wall recruits neutrophils to the side of inflammation (1). Recognition of ICs by CD16 (FcγRIII) on neutrophil surface (2) leads to degranulation of neutrophils and the release of proteases including CatG and NE (3). Interaction of CatG with PAR_4 on platelets surface induces the formation of NPAs (4a). NE counteracts the effect of the CatG-induced PAR_4 signalling on NPA (4a) and is able to initiate the formation of neutrophil extracellular traps (NETs) (4b). Neutrophils recruited to the vessel wall transmigrate through the endothelium to the side of inflammation followed by erythrocyte extravasation (5).

8 Conclusion

In conclusion/ Taken together, our results indicate that the interaction of platelets and neutrophils is a hallmark of IC-mediated vascular inflammation *ex vivo* and *in vivo*. Furthermore, our findings suggest that neutrophil catG has a contribution to IC-mediated inflammation, as levels of the protease are increased *ex vivo* and *in vivo*. *In vitro*, we revealed increased formation of NPAs after catG-stimulation of PAR_4 on platelet. This was further confirmed in IC-challenged PAR_4-deficient mice which showed baseline circulating NPAs. Therefore, our experiments suggest that the catG/PAR_4-axis is a potential target for anti-inflammatory therapies in IC-mediated inflammation such as vasculitis. However, inhibition of catG and PAR_4 may increase bleeding risk due to their contribution in coagulation and hemostasis. Additional experiments are needed to determine the potential benefits and risks of PAR_4 and catG inhibitors in human as well as animal models of IC-mediated inflammation.

9 References

1. Kolaczkowska, E. and P. Kubes, *Neutrophil recruitment and function in health and inflammation.* Nat Rev Immunol, 2013. **13**(3): p. 159-75.
2. Kumar, V. and A. Sharma, *Neutrophils: Cinderella of innate immune system.* Int Immunopharmacol, 2010. **10**(11): p. 1325-34.
3. Newton, K. and V.M. Dixit, *Signaling in innate immunity and inflammation.* Cold Spring Harb Perspect Biol, 2012. **4**(3).
4. Ley, K., et al., *Getting to the site of inflammation: the leukocyte adhesion cascade updated.* Nat Rev Immunol, 2007. **7**(9): p. 678-89.
5. Zarbock, A., R.K. Polanowska-Grabowska, and K. Ley, *Platelet-neutrophil-interactions: linking hemostasis and inflammation.* Blood Rev, 2007. **21**(2): p. 99-111.
6. Lam, F.W., et al., *Platelets enhance neutrophil transendothelial migration via P-selectin glycoprotein ligand-1.* Am J Physiol Heart Circ Physiol, 2011. **300**(2): p. H468-75.
7. Wagner, D.D. and P.S. Frenette, *The vessel wall and its interactions.* Blood, 2008. **111**(11): p. 5271-81.
8. Resources, B. https://www.boundless.com/biology/textbooks/boundless-biology-textbook/the-immune-system-42/innate-immune-response-233/pathogen-recognition-871-12121/. 2016; 05/2017.
9. Frenette, P.S., et al., *Platelet-endothelial interactions in inflamed mesenteric venules.* Blood, 1998. **91**(4): p. 1318-24.
10. Hunt, B.J. and K.M. Jurd, *Endothelial cell activation. A central pathophysiological process.* BMJ, 1998. **316**(7141): p. 1328-9.
11. Phillipson, M. and P. Kubes, *The neutrophil in vascular inflammation.* Nat Med, 2011. **17**(11): p. 1381-90.
12. Thornton, P., et al., *Platelet interleukin-1alpha drives cerebrovascular inflammation.* Blood, 2010. **115**(17): p. 3632-9.
13. Gear, A.R. and D. Camerini, *Platelet chemokines and chemokine receptors: linking hemostasis, inflammation, and host defense.* Microcirculation, 2003. **10**(3-4): p. 335-50.
14. Semple, J.W., J.E. Italiano, Jr., and J. Freedman, *Platelets and the immune continuum.* Nat Rev Immunol, 2011. **11**(4): p. 264-74.
15. Gleissner, C.A., P. von Hundelshausen, and K. Ley, *Platelet chemokines in vascular disease.* Arterioscler Thromb Vasc Biol, 2008. **28**(11): p. 1920-7.
16. Eriksson, E.E., et al., *Importance of primary capture and L-selectin-dependent secondary capture in leukocyte accumulation in inflammation and atherosclerosis in vivo.* J Exp Med, 2001. **194**(2): p. 205-18.
17. Mine, S., et al., *Activated platelets and endothelial cell interaction with neutrophils under flow conditions.* Intern Med, 2001. **40**(11): p. 1085-92.
18. Li, J., et al., *Platelet-neutrophil interactions under thromboinflammatory conditions.* Cell Mol Life Sci, 2015. **72**(14): p. 2627-43.
19. Sreeramkumar, V., et al., *Neutrophils scan for activated platelets to initiate inflammation.* Science, 2014. **346**(6214): p. 1234-8.

20. Moore, K.L., et al., *P-selectin glycoprotein ligand-1 mediates rolling of human neutrophils on P-selectin.* J Cell Biol, 1995. **128**(4): p. 661-71.
21. Larsen, E., et al., *PADGEM protein: a receptor that mediates the interaction of activated platelets with neutrophils and monocytes.* Cell, 1989. **59**(2): p. 305-12.
22. Furie, B., B.C. Furie, and R. Flaumenhaft, *A journey with platelet P-selectin: the molecular basis of granule secretion, signalling and cell adhesion.* Thromb Haemost, 2001. **86**(1): p. 214-21.
23. Carlow, D.A., et al., *PSGL-1 function in immunity and steady state homeostasis.* Immunol Rev, 2009. **230**(1): p. 75-96.
24. Andre, P., et al., *Pro-coagulant state resulting from high levels of soluble P-selectin in blood.* Proc Natl Acad Sci U S A, 2000. **97**(25): p. 13835-40.
25. Gross, P.L., et al., *Leukocyte-versus microparticle-mediated tissue factor transfer during arteriolar thrombus development.* J Leukoc Biol, 2005. **78**(6): p. 1318-26.
26. Yang, J., et al., *Targeted gene disruption demonstrates that P-selectin glycoprotein ligand 1 (PSGL-1) is required for P-selectin-mediated but not E-selectin-mediated neutrophil rolling and migration.* J Exp Med, 1999. **190**(12): p. 1769-82.
27. Jung, U. and K. Ley, *Mice lacking two or all three selectins demonstrate overlapping and distinct functions for each selectin.* J Immunol, 1999. **162**(11): p. 6755-62.
28. Kral, J.B., et al., *Platelet Interaction with Innate Immune Cells.* Transfus Med Hemother, 2016. **43**(2): p. 78-88.
29. Kornerup, K.N., et al., *Circulating platelet-neutrophil complexes are important for subsequent neutrophil activation and migration.* J Appl Physiol (1985), 2010. **109**(3): p. 758-67.
30. Mayadas, T.N., et al., *Leukocyte rolling and extravasation are severely compromised in P selectin-deficient mice.* Cell, 1993. **74**(3): p. 541-54.
31. Patel, K.D., et al., *Neutrophils use both shared and distinct mechanisms to adhere to selectins under static and flow conditions.* J Clin Invest, 1995. **96**(4): p. 1887-96.
32. Schmidtke, D.W. and S.L. Diamond, *Direct observation of membrane tethers formed during neutrophil attachment to platelets or P-selectin under physiological flow.* J Cell Biol, 2000. **149**(3): p. 719-30.
33. Pitchford, S.C., et al., *Platelet P-selectin is required for pulmonary eosinophil and lymphocyte recruitment in a murine model of allergic inflammation.* Blood, 2005. **105**(5): p. 2074-81.
34. Sundd, P., M.K. Pospieszalska, and K. Ley, *Neutrophil rolling at high shear: flattening, catch bond behavior, tethers and slings.* Mol Immunol, 2013. **55**(1): p. 59-69.
35. Diacovo, T.G., et al., *Neutrophil rolling, arrest, and transmigration across activated, surface-adherent platelets via sequential action of P-selectin and the beta 2-integrin CD11b/CD18.* Blood, 1996. **88**(1): p. 146-57.
36. Kuligowski, M.P., A.R. Kitching, and M.J. Hickey, *Leukocyte recruitment to the inflamed glomerulus: a critical role for platelet-derived P-selectin in the absence of rolling.* J Immunol, 2006. **176**(11): p. 6991-9.
37. Stone, P.C. and G.B. Nash, *Conditions under which immobilized platelets activate as well as capture flowing neutrophils.* Br J Haematol, 1999. **105**(2): p. 514-22.
38. Caron, A., et al., *Anti-platelet effects of GPIIb/IIIa and P-selectin antagonism, platelet activation, and binding to neutrophils.* J Cardiovasc Pharmacol, 2002. **40**(2): p. 296-306.

39. Evangelista, V., et al., *Platelet/polymorphonuclear leukocyte interaction: P-selectin triggers protein-tyrosine phosphorylation-dependent CD11b/CD18 adhesion: role of PSGL-1 as a signaling molecule.* Blood, 1999. **93**(3): p. 876-85.
40. Simon, D.I., et al., *Platelet glycoprotein ibalpha is a counterreceptor for the leukocyte integrin Mac-1 (CD11b/CD18).* J Exp Med, 2000. **192**(2): p. 193-204.
41. Phillipson, M., et al., *Intraluminal crawling of neutrophils to emigration sites: a molecularly distinct process from adhesion in the recruitment cascade.* J Exp Med, 2006. **203**(12): p. 2569-75.
42. McDonald, B., et al., *Intravascular danger signals guide neutrophils to sites of sterile inflammation.* Science, 2010. **330**(6002): p. 362-6.
43. Coxon, A., et al., *A novel role for the beta 2 integrin CD11b/CD18 in neutrophil apoptosis: a homeostatic mechanism in inflammation.* Immunity, 1996. **5**(6): p. 653-66.
44. Li, R. and J. Emsley, *The organizing principle of the platelet glycoprotein Ib-IX-V complex.* J Thromb Haemost, 2013. **11**(4): p. 605-14.
45. Corken, A., et al., *Platelet glycoprotein Ib-IX as a regulator of systemic inflammation.* Arterioscler Thromb Vasc Biol, 2014. **34**(5): p. 996-1001.
46. Li, J., et al., *Neutrophil AKT2 regulates heterotypic cell-cell interactions during vascular inflammation.* J Clin Invest, 2014. **124**(4): p. 1483-96.
47. Weber, C. and T.A. Springer, *Neutrophil accumulation on activated, surface-adherent platelets in flow is mediated by interaction of Mac-1 with fibrinogen bound to alphaIIbbeta3 and stimulated by platelet-activating factor.* J Clin Invest, 1997. **100**(8): p. 2085-93.
48. Volkmann, H., et al., *[Transluminal electric catheter ablation in the treatment of drug-refractory focal ventricular tachycardias].* Z Gesamte Inn Med, 1988. **43**(14): p. 373-7.
49. Li, J., et al., *Platelet-neutrophil interactions under thromboinflammatory conditions.* Cell Mol Life Sci, 2015.
50. Polanowska-Grabowska, R., et al., *P-selectin-mediated platelet-neutrophil aggregate formation activates neutrophils in mouse and human sickle cell disease.* Arterioscler Thromb Vasc Biol, 2010. **30**(12): p. 2392-9.
51. Ueno, K., et al., *Circulating platelet-neutrophil aggregates play a significant role in Kawasaki disease.* Circ J, 2015. **79**(6): p. 1349-56.
52. Nijm, J., et al., *Circulating levels of proinflammatory cytokines and neutrophil-platelet aggregates in patients with coronary artery disease.* Am J Cardiol, 2005. **95**(4): p. 452-6.
53. Huo, Y., et al., *Circulating activated platelets exacerbate atherosclerosis in mice deficient in apolipoprotein E.* Nat Med, 2003. **9**(1): p. 61-7.
54. Professor Dr. med. P. Altmeyer, D.V.P. *Vaskulitis, leukozytoklastische (non-IgA-assoziierte), Enzyklopädie der Dermatologie, Venerologie, Allergologie und Umweltmedizin*. http://www.enzyklopaedie-dermatologie.de/artikel?id=4223; 05/2017.
55. Ravetch, J.V., *Fc receptors: rubor redux.* Cell, 1994. **78**(4): p. 553-60.
56. Sunderkotter, C., et al., *Management of leukocytoclastic vasculitis.* J Dermatolog Treat, 2005. **16**(4): p. 193-206.
57. Sunderkotter, C., et al., *Different pathways leading to cutaneous leukocytoclastic vasculitis in mice.* Exp Dermatol, 2001. **10**(6): p. 391-404.

58. Professor Dr. med. P. Altmeyer, D.V.P. *Tuberkulid, papulonekrotisches, Enzyklopädie der Dermatologie, Venerologie, Allergologie und Umweltmedizin*. http://www.enzyklopaedie-dermatologie.de/artikel?id=4058; 05/2017.
59. Professor Dr. med. P. Altmeyer, D.V.P. *Pityriasis lichenoides et varioliformis acuta, Enzyklopädie der Dermatologie, Venerologie, Allergologie und Umweltmedizin*. http://www.enzyklopaedie-dermatologie.de/artikel?id=3098; 05/2017.
60. Professor Dr. med. P. Altmeyer, D.V.P. *Purpura pigmentosa progressiva, Enzyklopädie der Dermatologie, Venerologie, Allergologie und Umweltmedizin*. http://www.enzyklopaedie-dermatologie.de/artikel?id=3406; 05/2017.
61. Professor Dr. med. P. Altmeyer, D.V.P. *Purpura jaune d'ocre, Enzyklopädie der Dermatologie, Venerologie, Allergologie und Umweltmedizin*. http://www.enzyklopaedie-dermatologie.de/artikel?id=3404; 05/2017.
62. Professor Dr. med. P. Altmeyer, D.V.P. *Erythema exsudativum multiforme, Enzyklopädie der Dermatologie, Venerologie, Allergologie und Umweltmedizin*. http://www.enzyklopaedie-dermatologie.de/artikel?id=1250.
63. Sylvestre, D.L. and J.V. Ravetch, *Fc receptors initiate the Arthus reaction: redefining the inflammatory cascade.* Science, 1994. **265**(5175): p. 1095-8.
64. Arthus, N., *Injections répétées de sérum de cheval chez le lapin.* Bull. de la Soc. de Biol., 1903.
65. Sylvestre, D.L. and J.V. Ravetch, *A dominant role for mast cell Fc receptors in the Arthus reaction.* Immunity, 1996. **5**(4): p. 387-90.
66. Steinhoff, M., et al., *Proteinase-activated receptors: transducers of proteinase-mediated signaling in inflammation and immune response.* Endocr Rev, 2005. **26**(1): p. 1-43.
67. Vu, T.K., et al., *Molecular cloning of a functional thrombin receptor reveals a novel proteolytic mechanism of receptor activation.* Cell, 1991. **64**(6): p. 1057-68.
68. Nystedt, S., et al., *Molecular cloning of a potential proteinase activated receptor.* Proc Natl Acad Sci U S A, 1994. **91**(20): p. 9208-12.
69. Ishihara, H., et al., *Protease-activated receptor 3 is a second thrombin receptor in humans.* Nature, 1997. **386**(6624): p. 502-6.
70. Kahn, M.L., et al., *A dual thrombin receptor system for platelet activation.* Nature, 1998. **394**(6694): p. 690-4.
71. Xu, W.F., et al., *Cloning and characterization of human protease-activated receptor 4.* Proc Natl Acad Sci U S A, 1998. **95**(12): p. 6642-6.
72. Sambrano, G.R., et al., *Cathepsin G activates protease-activated receptor-4 in human platelets.* J Biol Chem, 2000. **275**(10): p. 6819-23.
73. Puente, X.S., et al., *Human and mouse proteases: a comparative genomic approach.* Nat Rev Genet, 2003. **4**(7): p. 544-58.
74. Rawlings, N.D., D.P. Tolle, and A.J. Barrett, *MEROPS: the peptidase database.* Nucleic Acids Res, 2004. **32**(Database issue): p. D160-4.
75. Motyan, J.A., F. Toth, and J. Tozser, *Research applications of proteolytic enzymes in molecular biology.* Biomolecules, 2013. **3**(4): p. 923-42.
76. Polgar, L., *The catalytic triad of serine peptidases.* Cell Mol Life Sci, 2005. **62**(19-20): p. 2161-72.
77. Reeves, E.P., et al., *Killing activity of neutrophils is mediated through activation of proteases by K+ flux.* Nature, 2002. **416**(6878): p. 291-7.

78. Weinrauch, Y., et al., *Neutrophil elastase targets virulence factors of enterobacteria.* Nature, 2002. **417**(6884): p. 91-4.
79. Belaaouaj, A., K.S. Kim, and S.D. Shapiro, *Degradation of outer membrane protein A in Escherichia coli killing by neutrophil elastase.* Science, 2000. **289**(5482): p. 1185-8.
80. Gatto, B., et al., *Effective DNA inhibitors of cathepsin g by in vitro selection.* Int J Mol Sci, 2008. **9**(6): p. 1008-23.
81. Kessenbrock, K., T. Dau, and D.E. Jenne, *Tailor-made inflammation: how neutrophil serine proteases modulate the inflammatory response.* J Mol Med (Berl), 2011. **89**(1): p. 23-8.
82. Schmidt, V.A., et al., *The human thrombin receptor and proteinase activated receptor-2 genes are tightly linked on chromosome 5q13.* Br J Haematol, 1997. **97**(3): p. 523-9.
83. Adams, M.N., et al., *Structure, function and pathophysiology of protease activated receptors.* Pharmacol Ther, 2011. **130**(3): p. 248-82.
84. French, S.L. and J.R. Hamilton, *Protease-activated receptor 4: from structure to function and back again.* Br J Pharmacol, 2016. **173**(20): p. 2952-65.
85. Jacques, S.L. and A. Kuliopulos, *Protease-activated receptor-4 uses dual prolines and an anionic retention motif for thrombin recognition and cleavage.* Biochem J, 2003. **376**(Pt 3): p. 733-40.
86. Nieman, M.T., *Protease-activated receptor 4 uses anionic residues to interact with alpha-thrombin in the absence or presence of protease-activated receptor 1.* Biochemistry, 2008. **47**(50): p. 13279-86.
87. Ramachandran, R., et al., *Targeting proteinase-activated receptors: therapeutic potential and challenges.* Nat Rev Drug Discov, 2012. **11**(1): p. 69-86.
88. Coughlin, S.R., *Thrombin signalling and protease-activated receptors.* Nature, 2000. **407**(6801): p. 258-64.
89. Vergnolle, N., et al., *Characterization of thrombin-induced leukocyte rolling and adherence: a potential proinflammatory role for proteinase-activated receptor-4.* J Immunol, 2002. **169**(3): p. 1467-73.
90. Kataoka, H., et al., *Protease-activated receptors 1 and 4 mediate thrombin signaling in endothelial cells.* Blood, 2003. **102**(9): p. 3224-31.
91. Hamilton, J.R., A.G. Frauman, and T.M. Cocks, *Increased expression of protease-activated receptor-2 (PAR2) and PAR4 in human coronary artery by inflammatory stimuli unveils endothelium-dependent relaxations to PAR2 and PAR4 agonists.* Circ Res, 2001. **89**(1): p. 92-8.
92. Chen, D., et al., *Capsaicin up-regulates protease-activated receptor-4 mRNA and protein in primary cultured dorsal root ganglion neurons.* Cell Mol Neurobiol, 2013. **33**(3): p. 337-46.
93. Mahajan-Thakur, S., et al., *Sphingosine-1-phosphate induces thrombin receptor PAR-4 expression to enhance cell migration and COX-2 formation in human monocytes.* J Leukoc Biol, 2014. **96**(4): p. 611-8.
94. Pavic, G., et al., *Thrombin receptor protease-activated receptor 4 is a key regulator of exaggerated intimal thickening in diabetes mellitus.* Circulation, 2014. **130**(19): p. 1700-11.
95. Jiang, P., et al., *Down-regulation of protease-activated receptor 4 in lung adenocarcinoma is associated with a more aggressive phenotype.* Asian Pac J Cancer Prev, 2013. **14**(6): p. 3793-8.

96. Li, S.M., et al., *Protease-activated receptor (PAR)1, PAR2 and PAR4 expressions in esophageal squamous cell carcinoma.* Dongwuxue Yanjiu, 2014. **35**(5): p. 420-5.
97. Coughlin, S.R., *Protease-activated receptors in hemostasis, thrombosis and vascular biology.* J Thromb Haemost, 2005. **3**(8): p. 1800-14.
98. Kaplan, Z.S., et al., *Thrombin-dependent intravascular leukocyte trafficking regulated by fibrin and the platelet receptors GPIb and PAR4.* Nat Commun, 2015. **6**: p. 7835.
99. Camerer, E., W. Huang, and S.R. Coughlin, *Tissue factor- and factor X-dependent activation of protease-activated receptor 2 by factor VIIa.* Proc Natl Acad Sci U S A, 2000. **97**(10): p. 5255-60.
100. Kang, O.H., et al., *Trypsin induces tumour necrosis factor-alpha secretion from a human leukemic mast cell line.* Cell Biochem Funct, 2003. **21**(2): p. 161-7.
101. Hollenberg, M.D. and M. Saifeddine, *Proteinase-activated receptor 4 (PAR4): activation and inhibition of rat platelet aggregation by PAR4-derived peptides.* Can J Physiol Pharmacol, 2001. **79**(5): p. 439-42.
102. Faruqi, T.R., et al., *Structure-function analysis of protease-activated receptor 4 tethered ligand peptides. Determinants of specificity and utility in assays of receptor function.* J Biol Chem, 2000. **275**(26): p. 19728-34.
103. Connolly, A.J., et al., *Role of the thrombin receptor in development and evidence for a second receptor.* Nature, 1996. **381**(6582): p. 516-9.
104. Kinlough-Rathbone, R.L., M.L. Rand, and M.A. Packham, *Rabbit and rat platelets do not respond to thrombin receptor peptides that activate human platelets.* Blood, 1993. **82**(1): p. 103-6.
105. Nakanishi-Matsui, M., et al., *PAR3 is a cofactor for PAR4 activation by thrombin.* Nature, 2000. **404**(6778): p. 609-13.
106. Sambrano, G.R., et al., *Role of thrombin signalling in platelets in haemostasis and thrombosis.* Nature, 2001. **413**(6851): p. 74-8.
107. Covic, L., et al., *Pepducin-based intervention of thrombin-receptor signaling and systemic platelet activation.* Nat Med, 2002. **8**(10): p. 1161-5.
108. Hamilton, J.R., I. Cornelissen, and S.R. Coughlin, *Impaired hemostasis and protection against thrombosis in protease-activated receptor 4-deficient mice is due to lack of thrombin signaling in platelets.* J Thromb Haemost, 2004. **2**(8): p. 1429-35.
109. Lee, H., et al., *Safety and efficacy of targeting platelet proteinase-activated receptors in combination with existing anti-platelet drugs as antithrombotics in mice.* Br J Pharmacol, 2012. **166**(7): p. 2188-97.
110. Busso, N., et al., *Essential role of platelet activation via protease activated receptor 4 in tissue factor-initiated inflammation.* Arthritis Res Ther, 2008. **10**(2): p. R42.
111. Mao, Y., et al., *Deficiency of PAR4 attenuates cerebral ischemia/reperfusion injury in mice.* J Cereb Blood Flow Metab, 2010. **30**(5): p. 1044-52.
112. Houle, S., et al., *Neutrophils and the kallikrein-kinin system in proteinase-activated receptor 4-mediated inflammation in rodents.* Br J Pharmacol, 2005. **146**(5): p. 670-8.
113. Deibel, R., T.D. Flanagan, and V. Smith, *Central nervous system infections in New York State. Etiologic and epidemiologic observations, 1974.* N Y State J Med, 1975. **75**(13): p. 2337-42.
114. Owen, C.A., et al., *Cell surface-bound elastase and cathepsin G on human neutrophils: a novel, non-oxidative mechanism by which neutrophils focus and preserve catalytic activity of serine proteinases.* J Cell Biol, 1995. **131**(3): p. 775-89.

115. Hohn, P.A., et al., *Genomic organization and chromosomal localization of the human cathepsin G gene.* J Biol Chem, 1989. **264**(23): p. 13412-9.
116. Heusel, J.W., et al., *Molecular cloning, chromosomal location, and tissue-specific expression of the murine cathepsin G gene.* Blood, 1993. **81**(6): p. 1614-23.
117. MacIvor, D.M., et al., *Normal neutrophil function in cathepsin G-deficient mice.* Blood, 1999. **94**(12): p. 4282-93.
118. Tanaka, T., et al., *Human leukocyte cathepsin G. Subsite mapping with 4-nitroanilides, chemical modification, and effect of possible cofactors.* Biochemistry, 1985. **24**(8): p. 2040-7.
119. Gramse, M., et al., *Degradation products of fibrinogen by elastase-like neutral protease from human granulocytes. Characterization and effects on blood coagulation in vitro.* J Clin Invest, 1978. **61**(4): p. 1027-33.
120. Turkington, P.T., N.L. Blumsom, and D.T. Elmore, *The degradation of bovine and human prothrombin by human polymorphonuclear leukocyte cathepsin G.* Thromb Res, 1986. **44**(3): p. 339-45.
121. Anderssen, T., et al., *Human leukocyte elastase and cathepsin G inactivate factor VII by limited proteolysis.* Thromb Haemost, 1993. **70**(3): p. 414-7.
122. Allen, D.H. and P.B. Tracy, *Human coagulation factor V is activated to the functional cofactor by elastase and cathepsin G expressed at the monocyte surface.* J Biol Chem, 1995. **270**(3): p. 1408-15.
123. Turkington, P.T., *Cathepsin G, a regulator of human vitamin K, dependent clotting factors and inhibitors.* Thromb Res, 1992. **67**(2): p. 147-55.
124. Perrin, J., et al., *In vitro effects of human neutrophil cathepsin G on thrombin generation: Both acceleration and decreased potential.* Thromb Haemost, 2010. **104**(3): p. 514-22.
125. Weksler, B.B., et al., *Human leukocyte cathepsin G and elastase specifically suppress thrombin-induced prostacyclin production in human endothelial cells.* Blood, 1989. **74**(5): p. 1627-34.
126. Molino, M., et al., *Proteolysis of the human platelet and endothelial cell thrombin receptor by neutrophil-derived cathepsin G.* J Biol Chem, 1995. **270**(19): p. 11168-75.
127. Renesto, P. and M. Chignard, *Enhancement of cathepsin G-induced platelet activation by leukocyte elastase: consequence for the neutrophil-mediated platelet activation.* Blood, 1993. **82**(1): p. 139-44.
128. Selak, M.A., M. Chignard, and J.B. Smith, *Cathepsin G is a strong platelet agonist released by neutrophils.* Biochem J, 1988. **251**(1): p. 293-9.
129. Selak, M.A. and J.B. Smith, *Cathepsin G binding to human platelets. Evidence for a specific receptor.* Biochem J, 1990. **266**(1): p. 55-62.
130. Ferrer-Lopez, P., et al., *Activation of human platelets by C5a-stimulated neutrophils: a role for cathepsin G.* Am J Physiol, 1990. **258**(6 Pt 1): p. C1100-7.
131. Evangelista, V., et al., *Platelet activation by fMLP-stimulated polymorphonuclear leukocytes: the activity of cathepsin G is not prevented by antiproteinases.* Blood, 1991. **77**(11): p. 2379-88.
132. Evangelista, V., et al., *Cathepsin G-dependent platelet stimulation by activated polymorphonuclear leukocytes and its inhibition by antiproteinases: role of P-selectin-mediated cell-cell adhesion.* Blood, 1993. **81**(11): p. 2947-57.
133. LaRosa, C.A., et al., *Human neutrophil cathepsin G is a potent platelet activator.* J Vasc Surg, 1994. **19**(2): p. 306-18; discussion 318-9.

134. Si-Tahar, M., et al., *The phospholipase C/protein kinase C pathway is involved in cathepsin G-induced human platelet activation: comparison with thrombin.* Biochem J, 1996. **313 (Pt 2)**: p. 401-8.
135. Faraday, N., et al., *Cathepsin G-dependent modulation of platelet thrombus formation in vivo by blood neutrophils.* PLoS One, 2013. **8**(8): p. e71447.
136. Pham, C.T., *Neutrophil serine proteases: specific regulators of inflammation.* Nat Rev Immunol, 2006. **6**(7): p. 541-50.
137. Raptis, S.Z., et al., *Serine protease cathepsin G regulates adhesion-dependent neutrophil effector functions by modulating integrin clustering.* Immunity, 2005. **22**(6): p. 679-91.
138. Adkison, A.M., et al., *Dipeptidyl peptidase I activates neutrophil-derived serine proteases and regulates the development of acute experimental arthritis.* J Clin Invest, 2002. **109**(3): p. 363-71.
139. Hara, T., et al., *Platelets control leukocyte recruitment in a murine model of cutaneous arthus reaction.* Am J Pathol, 2010. **176**(1): p. 259-69.
140. Hillgruber, C., et al., *Blocking neutrophil diapedesis prevents hemorrhage during thrombocytopenia.* J Exp Med, 2015. **212**(8): p. 1255-66.
141. Cai, Y., C. Fleming, and J. Yan, *New insights of T cells in the pathogenesis of psoriasis.* Cell Mol Immunol, 2012. **9**(4): p. 302-9.
142. Clark, R.A. and T.S. Kupper, *Misbehaving macrophages in the pathogenesis of psoriasis.* J Clin Invest, 2006. **116**(8): p. 2084-7.
143. Bieber, T., *Atopic dermatitis.* N Engl J Med, 2008. **358**(14): p. 1483-94.
144. Eyerich, K. and N. Novak, *Immunology of atopic eczema: overcoming the Th1/Th2 paradigm.* Allergy, 2013. **68**(8): p. 974-82.
145. Kasraie, S. and T. Werfel, *Role of macrophages in the pathogenesis of atopic dermatitis.* Mediators Inflamm, 2013. **2013**: p. 942375.
146. Wang, H., et al., *Activated macrophages are essential in a murine model for T cell-mediated chronic psoriasiform skin inflammation.* J Clin Invest, 2006. **116**(8): p. 2105-14.
147. Stratis, A., et al., *Pathogenic role for skin macrophages in a mouse model of keratinocyte-induced psoriasis-like skin inflammation.* J Clin Invest, 2006. **116**(8): p. 2094-104.
148. Vestergaard, C., et al., *Expression of CCR2 on monocytes and macrophages in chronically inflamed skin in atopic dermatitis and psoriasis.* Acta Derm Venereol, 2004. **84**(5): p. 353-8.
149. Kryczek, I., et al., *Induction of IL-17+ T cell trafficking and development by IFN-gamma: mechanism and pathological relevance in psoriasis.* J Immunol, 2008. **181**(7): p. 4733-41.
150. Ortega, C., et al., *IL-17-producing CD8+ T lymphocytes from psoriasis skin plaques are cytotoxic effector cells that secrete Th17-related cytokines.* J Leukoc Biol, 2009. **86**(2): p. 435-43.
151. Hijnen, D., et al., *CD8(+) T cells in the lesional skin of atopic dermatitis and psoriasis patients are an important source of IFN-gamma, IL-13, IL-17, and IL-22.* J Invest Dermatol, 2013. **133**(4): p. 973-9.
152. Alberts B, J.A., Lewis J,, *Lymphocytes and the Cellular Basis of Adaptive Immunity*, in *Molecular Biology of the Cell. 4th edition.* 2002, Garland Science.

153. Jung, S.M. and M. Moroi, *Platelet glycoprotein VI.* Adv Exp Med Biol, 2008. **640**: p. 53-63.
154. Stenberg, P.E., et al., *A platelet alpha-granule membrane protein (GMP-140) is expressed on the plasma membrane after activation.* J Cell Biol, 1985. **101**(3): p. 880-6.
155. Berman, C.L., et al., *A platelet alpha granule membrane protein that is associated with the plasma membrane after activation. Characterization and subcellular localization of platelet activation-dependent granule-external membrane protein.* J Clin Invest, 1986. **78**(1): p. 130-7.
156. Yuan, Y., et al., *Identification of a novel 14-3-3zeta binding site within the cytoplasmic domain of platelet glycoprotein Ibalpha that plays a key role in regulating the von Willebrand factor binding function of glycoprotein Ib-IX.* Circ Res, 2009. **105**(12): p. 1177-85.
157. Einhorn, J. and J.T. Levis, *Dermatologic Diagnosis: Leukocytoclastic Vasculitis.* Perm J, 2015. **19**(3): p. 77-8.
158. Broos, K., et al., *Platelets at work in primary hemostasis.* Blood Rev, 2011. **25**(4): p. 155-67.
159. Stegner, D., E.J. Haining, and B. Nieswandt, *Targeting glycoprotein VI and the immunoreceptor tyrosine-based activation motif signaling pathway.* Arterioscler Thromb Vasc Biol, 2014. **34**(8): p. 1615-20.
160. Rossaint, J. and A. Zarbock, *Platelets in leucocyte recruitment and function.* Cardiovasc Res, 2015. **107**(3): p. 386-95.
161. Nobis, U., et al., *Radial distribution of white cells during blood flow in small tubes.* Microvasc Res, 1985. **29**(3): p. 295-304.
162. Pitchford, S., D. Pan, and H.C. Welch, *Platelets in neutrophil recruitment to sites of inflammation.* Curr Opin Hematol, 2016.
163. Slaba, I., et al., *Imaging the dynamic platelet-neutrophil response in sterile liver injury and repair in mice.* Hepatology, 2015. **62**(5): p. 1593-605.
164. Rahman, M., et al., *Metalloproteinases regulate CD40L shedding from platelets and pulmonary recruitment of neutrophils in abdominal sepsis.* Inflamm Res, 2012. **61**(6): p. 571-9.
165. Duerschmied, D., et al., *Platelet serotonin promotes the recruitment of neutrophils to sites of acute inflammation in mice.* Blood, 2013. **121**(6): p. 1008-15.
166. Mocsai, A., B. Walzog, and C.A. Lowell, *Intracellular signalling during neutrophil recruitment.* Cardiovasc Res, 2015. **107**(3): p. 373-85.
167. Middleton, J., et al., *Leukocyte extravasation: chemokine transport and presentation by the endothelium.* Blood, 2002. **100**(12): p. 3853-60.
168. Page, C. and S. Pitchford, *Neutrophil and platelet complexes and their relevance to neutrophil recruitment and activation.* Int Immunopharmacol, 2013. **17**(4): p. 1176-84.
169. Walz, A., et al., *Effects of the neutrophil-activating peptide NAP-2, platelet basic protein, connective tissue-activating peptide III and platelet factor 4 on human neutrophils.* J Exp Med, 1989. **170**(5): p. 1745-50.
170. Hamburger, S.A. and R.P. McEver, *GMP-140 mediates adhesion of stimulated platelets to neutrophils.* Blood, 1990. **75**(3): p. 550-4.

171. Zarbock, A., K. Singbartl, and K. Ley, *Complete reversal of acid-induced acute lung injury by blocking of platelet-neutrophil aggregation.* J Clin Invest, 2006. **116**(12): p. 3211-9.
172. Ortega-Gomez, A., et al., *Cathepsin G Controls Arterial But Not Venular Myeloid Cell Recruitment.* Circulation, 2016. **134**(16): p. 1176-1188.
173. Guyot, N., et al., *Unopposed cathepsin G, neutrophil elastase, and proteinase 3 cause severe lung damage and emphysema.* Am J Pathol, 2014. **184**(8): p. 2197-210.
174. Twigg, M.S., et al., *The Role of Serine Proteases and Antiproteases in the Cystic Fibrosis Lung.* Mediators Inflamm, 2015. **2015**: p. 293053.
175. Korkmaz, B., T. Moreau, and F. Gauthier, *Neutrophil elastase, proteinase 3 and cathepsin G: physicochemical properties, activity and physiopathological functions.* Biochimie, 2008. **90**(2): p. 227-42.
176. Jerke, U., et al., *Neutrophil serine proteases exert proteolytic activity on endothelial cells.* Kidney Int, 2015. **88**(4): p. 764-75.
177. Terui, T., M. Ozawa, and H. Tagami, *Role of neutrophils in induction of acute inflammation in T-cell-mediated immune dermatosis, psoriasis: a neutrophil-associated inflammation-boosting loop.* Exp Dermatol, 2000. **9**(1): p. 1-10.
178. Murphy, M., P. Kerr, and J.M. Grant-Kels, *The histopathologic spectrum of psoriasis.* Clin Dermatol, 2007. **25**(6): p. 524-8.
179. Amulic, B., et al., *Neutrophil function: from mechanisms to disease.* Annu Rev Immunol, 2012. **30**: p. 459-89.
180. Ikeda, S., et al., *Therapeutic depletion of myeloid lineage leukocytes in patients with generalized pustular psoriasis indicates a major role for neutrophils in the immunopathogenesis of psoriasis.* J Am Acad Dermatol, 2013. **68**(4): p. 609-17.
181. Henry, C.M., et al., *Neutrophil-Derived Proteases Escalate Inflammation through Activation of IL-36 Family Cytokines.* Cell Rep, 2016. **14**(4): p. 708-22.
182. Schonthaler, H.B., et al., *S100A8-S100A9 protein complex mediates psoriasis by regulating the expression of complement factor C3.* Immunity, 2013. **39**(6): p. 1171-81.
183. Johnston, A., et al., *IL-1F5, -F6, -F8, and -F9: a novel IL-1 family signaling system that is active in psoriasis and promotes keratinocyte antimicrobial peptide expression.* J Immunol, 2011. **186**(4): p. 2613-22.
184. Ramirez-Carrozzi, V., et al., *IL-17C regulates the innate immune function of epithelial cells in an autocrine manner.* Nat Immunol, 2011. **12**(12): p. 1159-66.
185. Lefrancais, E., et al., *IL-33 is processed into mature bioactive forms by neutrophil elastase and cathepsin G.* Proc Natl Acad Sci U S A, 2012. **109**(5): p. 1673-8.
186. Dinarello, C.A., *Immunological and inflammatory functions of the interleukin-1 family.* Annu Rev Immunol, 2009. **27**: p. 519-50.
187. Dinarello, C.A., *Interleukin-1 in the pathogenesis and treatment of inflammatory diseases.* Blood, 2011. **117**(14): p. 3720-32.
188. Sims, J.E. and D.E. Smith, *The IL-1 family: regulators of immunity.* Nat Rev Immunol, 2010. **10**(2): p. 89-102.
189. Gomides, L.F., et al., *Blockade of proteinase-activated receptor 4 inhibits neutrophil recruitment in experimental inflammation in mice.* Inflamm Res, 2014. **63**(11): p. 935-41.
190. Hillgruber, C., et al., *Blocking von Willebrand factor for treatment of cutaneous inflammation.* J Invest Dermatol, 2014. **134**(1): p. 77-86.

191. Murphy, H.S., *Chapter 2: Inflammation*, in *Rubin's Pathology - Clinicopathologic Foundations of Medicine - 5th Edition*, D.S.S. Raphael Rubin, Editor. 2008, Wolters Kluwer Lippincott Williams & Wilkins.
192. Goerge, T., et al., *Inflammation induces hemorrhage in thrombocytopenia.* Blood, 2008. **111**(10): p. 4958-64.
193. Boulaftali, Y., et al., *Platelet ITAM signaling is critical for vascular integrity in inflammation.* J Clin Invest, 2013. **123**(2): p. 908-16.
194. Ley, K., et al., *Sequential contribution of L- and P-selectin to leukocyte rolling in vivo.* J Exp Med, 1995. **181**(2): p. 669-75.
195. Savoia, A., et al., *Spectrum of the mutations in Bernard-Soulier syndrome.* Hum Mutat, 2014. **35**(9): p. 1033-45.
196. Stangl, P.A. and S. Lewis, *Review of Currently Available GP IIb/IIIa Inhibitors and Their Role in Peripheral Vascular Interventions.* Semin Intervent Radiol, 2010. **27**(4): p. 412-21.

10 List of Abbreviations

Abbreviation	Description
A	
ADP	Adenosine diphosphate
ag	Agonist
ANCA	Anti-neutrophil cytoplasmic autoantibodies
anti-BSA-ab	Anti-BSA-antibody
AP	Activating peptide
B	
BSA	Bovine serum albumine
C	
CatG	Cathepsin G
CD	Cluster of Differentiation
CGRP	Calcitonine gene related peptide
CRP	Collagen related peptide
Ctrl	Control
D	
DAPI	4‘,6-diamidino-2-phenylindole
DIF	Direct immunofluorescence
DMSO	Dimethylsulfoxid
DRG	Dorsal root ganglia
dT	Deoxythymidine
DTT	Dithiothreitol
E	
EDTA	Ethylenediaminetetraacetic acid
FACS	Fluorescence-activated cell sorting
F	
FBS	Fetal bovine serum
FcγR	Fc gamma receptor

fMLP	N-Formylmethionyl-leucyl-phenylalanine
G	
GPCRs	G-protein coupled receptors
GPIbα	Glycoprotein Ibα
GPIIbIIIa	Glycoprotein IIbIIIa
GPIII-β	Glycoprotein III-β
GPVI	Glycoprotein VI
H	
H&E	Hematoxylin and eosin
His	Histamine
HTAB	Hexadecyltrimethylammonium bromide
I	
IC	Immune complex
IHC	Immunohistochemistry
IF	Immunofluorescence
IL-1α	Interleukin-1 alpha
IL-1β	Interleukin-1 beta
ITAM	Immunoreceptor tyrosine-based activation motif
L	
LcV	Leukocytoclastic Vasculitis
LPS	Lipopolysaccharide
M	
Mac-1	Membrane-activated complex-1
Mac-2	Membrane-activated complex-2
MIP-2α	macrophage inflammatory protein 2 α
MCP-1	Monocyte chemoattractant protein-1
MFI	Mean fluorescent intensity
MPO	Myeloperoxidase
MRSA	Methicillin-resistant *Staphylococcus aureus*
N	
NK_xR (e.g. NK_1R)	Neurokinine-X receptor

NE	Neutrophil elastase
NFκB	Nuclear factor-κ B
NPA	Neutrophil-platelet aggregation
P	
PAR	Proteinase-activated receptor
PBS	Phosphate buffered saline
PCR	Polymerase chain reaction
PFA	Paraformaldehyde
PR3	Proteinase 3
PSGL-1	P-selectin glycoprotein ligand 1
R	
ROS	Reactive oxygen species
RPA	Reverse passive Arthus reaction
RT	Reverse Transcriptase
S	
sCD40L	soluble CD40L
SMCs	Smooth muscle cells
Substance P	SP
T	
TF	Tissue factor
TGF-β	Tumor growth factor beta
TNF-α	Tumor necrosis factor alpha
TMB	3,3',5,5'-Tetramethylbenzidine
TRAP	Thrombin receptor-activating protein
V	
VEGF	Vascular endothelial growth factor
vWF	von Willebrand factor

11 Conferences & Publications

11.1 Presentations at national conferences and symposia

Poster presentations

- 2nd ADF („Arbeitsgemeinschaft für Dermatologische Forschung“) Round Table, Bad Sassendorf, Germany

  Plesser K, Feld M, Smit F, Buddenkotte J, Fastrich M, Spelleken M, Hillgruber C, Elvers M, Homey B *The role of protease/PAR-axis on the regulation of neutrophil-platelet interactions*
- 5th ADF Winter School, Zugspitze, Germany

  Plesser K, Feld M, Smit F, Buddenkotte J, Fastrich M, Spelleken M, Hillgruber C, Elvers M, Homey B *The role of protease/PAR-axis on the regulation of neutrophil-platelet interactions*
- 43rd Annual Meeting of the Arbeitsgemeinschaft Dermatologische Forschung (ADF), Vienna, Austra

  Plesser K, Feld M, Smit F, Buddenkotte J, Fastrich M, Spelleken M, Hillgruber C, Elvers M, Homey B *The role of PAR4/ Cathepsin G (CatG)-axis on the regulation of neutrophil-platelet interactions (NPAs)*. (**Poster chosen for the poster walk**)
- 43rd Annual Meeting of the Arbeitsgemeinschaft Dermatologische Forschung (ADF), Vienna, Austra

  IL-31 poster (**Poster prize**)

Oral Presentations

- 2nd ADF („Arbeitsgemeinschaft für Dermatologische Forschung“) Round Table, Bad Sassendorf, Germany

  Plesser K, Feld M, Smit F, Buddenkotte J, Fastrich M, Spelleken M, Hillgruber C, Elvers M, Homey B *The role of protease/PAR-axis on the regulation of neutrophil-platelet interactions*

- 60th Annual Meeting of the Society of Thrombosis and Haemostasis Research (GTH), Muenster, Germany

  Plesser K, Feld M, Smit F, Buddenkotte J, Fastrich M, Spelleken M, Hillgruber C, Elvers M, Homey B. *The role of PAR4/ Cathepsin G (CatG)-axis on the regulation of neutrophil-platelet interactions (NPAs)*. (**Abstract selected for oral presentation**)

11.2 Publication in peer-reviewed journals

- ADF Winter School-An exciting concept of the Arbeitsgemeinschaft Dermatologische Forschung to connect young scientists and clinician scientists in Dermatology at the top of Germany. *Exp Dermatol. 2016*

  Yazdi AS, Barlin M, Böhm K, Gendrisch F, Ghorbanalipoor S, Häberle S, Hamel A, Hüning S, Hüttner C, Iwanova I, Kanaki T, Kimeswenger S, Lohmann N, Munir S, Muzumdar S, Pereira MP, Peking P, **Plesser** K, Rendon A, Rentschler M, Schlumprecht C, Smorodchenko A, Stock M, Tillmanns J, Uslu U, Ghoreschi K, Glatz M, Grabbe S, Kunz M, Ludwig R, Scharffetter-Kochanek K, Loser K.

- The pruritus- and T_H2-associated cytokine Interleukin-31 promotes growth of sensory nerves. *J Allergy Clin Immunol 2016*

  Feld M, PhD, Garcia R, Buddenkotte J, Katayama S, Lewis K, Muirhead G, Hevezi P, **Plesser K**, Schrumpf H, Krjutshkov K, Sergeeva O, Müller HW, PhD, Sophia Tsoka S, Kere J, Dillon S, Steinhoff M, Homey B.

- Round Table – new concept of the *Arbeitsgemeinschaft Dermatologische Forschung* to foster regional exchange between young clinician scientists in dermatology. *Exp Dermatol. 2016*

  Ali N, Baumann C, Castro-Kroner J, Do N, Friedrich H, Haas K, Kläschen S, Pfaff C, **Plesser K**, Pollet M, Schmidt J, Schneeweiss M, Siewert M, Stock M, Sucker S, Üstün Y, Vollmer V, Wachsmuth E, Jing Wang J, Schilling B, Fabri M, Loser K & Eming S.

Publication in process

- Protease activated receptor 4 mediates inflammation-associated neutrophil-platelet aggregation

  Plesser K, Feld M, Buddenkotte J, Carina Hillgruber C, Flora Smits F, Fastrich M, Spelleken M, Fender A, Goerge T, Elvers M, Steinhoff M, Homey B

12 Acknowledgement

I would like to thank Univ.-Prof. Dr. med. Bernhard Homey for making this thesis here, at the Department of Dermatology in Duesseldorf, possible and for his constant interest and support in my research project. I am very thankful that Univ.-Prof. Dr. med. Bernard Homey gave me the opportunity to join his young ambitious research team as a PhD student and gave me access to the laboratory and research facilities. I would also like to thank Prof. Dr. Dieter Willbold for the supervision of my PhD thesis and his valuable scientific feedback to improve my work.

I would express my sincere gratitude to my two supervisors Dr. Micha Feld and Dr. Jörg Buddenkotte for their continual guidance, enthusiasm and unrelenting support throughout this process, but also for the encouraging of scientific discussions that certainly were essential to successfully further my project. I am especially thankful that Micha and Jörg supported me to create my own ideas and solutions which helped me to become a better and more independent scientist. Furthermore, I am very grateful to Prof. Dr. Dr. med. Martin Steinhoff from the UCD Charles Institute of Dermatology in University College Dublin for his encouragement, scientific expertise and financial support during my PhD study and related research.

I further acknowledge Dr. Carina Hillgruber from the working group of Prof. Dr. med. Tobias George of the Department of Dermatology in Münster. I would like to thank Carina for teaching me the *in vivo* inflammatory model and for helping me out with valuable tips, material and support at any time.

I am also very thankful to Prof. Dr. Margitta Elvers and Martina Spelleken from the Molecular Hemostasis Institute for Hemostasis, Hemotherapy and Transfusion Medicine in Duesseldorf for their support and encouragement to successfully further my research project.

A special thank you goes to Dr. Anke Fender from the working group of Prof. Dr. Jens Fischer of the Institute for Pharmacology and Clinical Pharmacology for providing the *Par4*$^{-/-}$ mice

line and for valuable scientific advices especially during the final stages of my PhD. I would also like to thank Anne Petz from the same institute for her support during the last experiments of my PhD thesis.

Further, I would like to acknowledge the “Forschungskommission” of the Heinrich Heine University in Duesseldorf for their financial support of my PhD thesis.

My sincere thanks goes to my friend and the graphic and communications designer**,** Julia Schröder who’s expertise was essential to create a convincing graphic to illustrate my scientific research question in a confident way.

I sincerely thank my fellow labmates, Flora Smits, Heike Hawerkamp, Andreas Kislat, Holger Schrumpf, Juliane Noffke, Stefanie Müller, Michaela Fastrich and Sabine Kellerman for the stimulating discussions and for being part of an ambitious young research team. I further appreciate the funny times we had not only inside the lab. Furthermore, I would like to thank Ulrike Wiesner and Erich Bünemann who helped me with the answering of unsetting questions at all times.

I further thank my friends in Cologne Christine, Lukas, Ruth, Anna, Josch, Fred etc. for their motivation and mental support during the last three years. A special thank you goes to Elena and Niklas from Münster. Thank you for the friendly and warm welcome at any time, when I needed to come to Münster to perform experiments.

I would like to dedicate this work to my loving family, especially to my mother Claudia Matthias-Plesser, my father Klaus Plesser, my sister Evelyn Plesser and in particular my grandmother Elfriede Matthias who sadly died before this thesis was finished. I thank you for supporting me with love, listening and input during my whole education.

Last but not least I would like to thank my boyfriend Paul for his love, belief and motivation throughout my study and the three years of this thesis.

aus dem Institut für
der Heinrich-Heine-Universität Düsseldorf

Gedruckt mit der Genehmigung der
Mathematisch-Naturwissenschaftlichen Fakultät der
Heinrich-Heine-Universität Düsseldorf

Berichterstatter:

1. Prof. Dr. med. Bernhard Homey

2. Prof. Dr. Dieter Willbold

Tag der mündlichen Prüfung:
17.08.2017